RAM PIPE REQUAL
Pipeline Requalification Guidelines Project
Report 3

Risk Assessment and Management (RAM) Based Guidelines for Requalification of Marine Pipelines

To

Petroleos Mexicanos (PEMEX)

Instituto Mexicano de Petroleo (IMP)

Minerals Management Service (MMS)

By
Professor Robert Bea

Dr. Tao Xu

Marine Technology & Management Group
University of California at Berkeley

Dr. Wally Orisamolu
United Technologies Research Center
&
Professor Ahsan Kareem

Postdoctoral Research Associate Xinzhong Chen

Department of Civil Engineering and Geological Sciences
University of Notre Dame

December 15, 1999
MMS Order No. 1435-01-98-PO-15219
PEMEX Contrato No. 7TRDIN022798

RAM PIPE REQUAL Project

Report 3

Risk Assessment and Management (RAM) Based Requalification Guidelines for Marine Pipelines

By

Professor Robert Bea

Dr. Tao Xu

Marine Technology & Management Group

University of California at Berkeley

Dr. Wally Orisamolu

United Technologies Research Center

And

Professor Ahsan Kareem

Postdoctoral Research Associate Xinzhong Chen

University of Notre Dame

MMS Order No. 1435-01-98-PO-15219

PEMEX Contrato No. 7TRDIN022798

Table of Contents

List of Symbols

Abbreviations

API	- American Petroleum Institute
ASME	- American Society of Mechanical Engineers
ASTM	- American Society of Testing Material
AGA	- American Gas Association
AISC	- American Institute of Steel Construction, Inc.
BSI	- British Standard Institute
DNV	- Det Norske Veritas
IMP	- Instituto Mexicano de Petroleo
ISO	- International Standard Organization
PEMEX	- Petroleos Mexicano
SUPERB	- Submarine Pipeline Probabilistic Based Design Project
ALS	- Accidental Limit States
ASD	- Allowable Stress Design
CTOD	- Critical Tip Opening Displacement
FEA	- Finite Element Analysis
LRFD	- Load Resistance Factor Design
MOP	- Maximum operating pressure
OTC	- Offshore Technology Conference
OP	- Operating Pressure
FS	- Factor of Safety
SMYS	- Specified Minimum Yield Strength of pipe, in psi (N/mm^2)
SMTS	- Specified Minimum Ultimate Tensile Strength of pipe, in psi (N/mm^2)
WSD	- Working stress design
LRFD	- Load Resistance Factor Design
ULS	- Ultimate Limit State
SLS	- Serviceability Limit States
SCF	- Stress Concentration Factor
SNCF	- Strain Concentration Factor
COV	- Coefficient of Variation
X52	- Material grade, yield strength = 52 ksi=358 Mpa
X65	- Material grade, yield strength = 65 ksi=448 Mpa
X52	- Material grade, yield strength = 70 ksi=530 Mpa

Subscripts

0	- mean
d	- design
θ	- circumferential
r	- radial
res	- residual
co	- collapse
u	- ultimate capacity
p	- plastic capacity
g	- global
l	- local
F50	- Median

Superscripts

M	- Moment
P	- Pressure
T	- Tension
C	- Compression

Roman Symbols

General

B_{F50}	- Median bias factor
V	- Coefficient of Variation
γ	- Load Factor
φ	- Resistance Factor
S	- Demand
R	- Capacity
β	- Reliability Index

Design

A	- Cross sectional area of pipe steel, in inches^2 (mm^2)
A_i	- Internal cross sectional area of the pipe, in inches^2 (mm^2)
A_o	- External cross sectional area of the pipe
C_l	-Inelastic local buckling strength in stress units, pond per square inch (N / mm^2)
C_g	- Inelastic global buckling strength in stress units, pond per square inch (N / mm^2)
D	- Outside diameter of pipe (Equation dependent)
D_i	- Inside diameter of pipe, in inches (mm) = (D – 2t)
D_{max}	- Maximum diameter at any given cross section, in inches (mm)
D_{min}	- Minimum diameter at any given cross section, in inches (mm)
E	- Elastic modulus, in pounds per square inch (N / mm^2)
g(δ)	- Collapse reduction factor
K	- Effective length factor
L	- Pipe length, in inches (mm)
M	- Applied moment, pond-inch (Nmm)
M_p	- Plastic moment capacity, pond-inch (Nmm)

P - Applied pressure
P_b - Minimum burst pressure of pipe, in psi (N / mm^2)
P_c - Collapse pressure of the pipe, in psi (N / mm^2)
P_e - Elastic collapse pressure of the pipe, in psi (N / mm^2)
P_i - Internal pressure in the pipe, in psi (N / mm^2)
P_o - External hydrostatic pressure, in psi (N / mm^2)
P_p - Buckle propagation pressure, in psi (N / mm^2)
P_y - Yield pressure at collapse, in psi (N / mm^2)
r - Radius of gyration
t_{nom} - Nominal wall thickness of pipe, in inches (mm)
t_{min} - Minimum measured wall thickness, in inches (mm)
t - Pipe wall thickness, in inches (mm)
f_0 - The initial ovalization
n - The strain hardening parameter
S - The anisotropy parameter
T_a - Axial tension in the pipe, in pounds (N)
T_{eff} - Effective tension in pipe, in pounds (N)
T_y - Yield tension of the pipe, in pounds (N)
T_u - Tension Load Capacity
δ - Ovality
δ_c - the critical CTOD value
ε_0 - the yield strain
a_{max} - the equivalent through-thickness crack size.
ε_b - Bending strain in the pipe
ε_{cr} - Critical strain
ε_{bm} - The maximum bending strain
σ_a - The axial stress
σ_h - Hoop stress
σ_{he} - Effective hoop stress
σ_{res} - Residual stress
σ_θ - Circumferential stress
σ_{xkL} - The classic local elastic critical stress
σ_u - ultimate tensile stress
σ_y - yield stress
σ_0 - flow stress
λ - Slenderness parameter

Reassessment

A_d - effective cross sectional area of damaged (dent) section
A_0 - cross-sectional area of undamaged section
d - damage depth
ΔY - Primary out-of-straightness of a dented member
ΔY_0 - 0.001L

I_d - Effective moment of inertia of undamaged cross-section
K_0 - Effective length factor of undamaged member
K - Effective buckling length factor
λ_d - Slenderness parameter of a dented member $=(P_{ud} / P_{ed})^{0.5}$
M_u - Ultimate moment capacity
M_{cr} - Critical moment capacity (local buckling)
M_{ud} - Ultimate negative moment capacity of dent section
M_- - Negative moment of dent section
M_+ - Positive moment of dent section
M^* - Neutral moment of dent section
P_{crd} - Critical axial buckling capacity of a dented member ($\Delta / L > 0.001$)
P_{crd0} - Critical axial buckling capacity of a dented member ($\Delta / L = 0.001$)
P_E - Euler load of undamaged member
P_{crl} - Axial local buckling capacity
P_{cr} - Axial column buckling capacity
P_u - Axial compression capacity
P_{ud} - Axial compression capacity of a short dented member

1.0 Introduction

1.1 Objective

The objective of this joint United States - Mexico cooperative project is to develop and verify Risk Assessment and Management (RAM) based criteria and guidelines for **reassessment and requalification** of marine pipelines and risers. The project is identified as the **RAM PIPE REQUAL** project. This project was sponsored by the U. S. Minerals Management Service (MMS), Petroleos Mexicanos (PEMEX), and Instituto Mexicano del Petroleo (IMP).

1.2 Scope

The **RAM PIPE REQUAL** project addressed the following key aspects of criteria for requalification of conventional existing marine pipelines and risers:

- Development of Safety and Serviceability Classifications (SSC) for different types of marine pipelines and risers that reflect the different types of products transported, the volumes transported and their importance to maintenance of productivity, and their potential consequences given loss of containment,
- Definition of target reliabilities for different SSC of marine risers and pipelines,
- Guidelines for assessment of pressure containment given corrosion and local damage including guidelines for evaluation of corrosion of non-piggable pipelines,
- Guidelines for assessment of local, propagating, and global buckling of pipelines given corrosion and local damage,
- Guidelines for assessment of hydrodynamic stability in extreme condition hurricanes, and
- Guidelines for assessment of combined stresses during operations that reflect the effects of pressure testing and limitations in operating pressures.

Important additional parts of this project provided by PEMEX and IMP were:

- Conduct of workshops and meetings in Mexico and the United States to review progress and developments from this project and to exchange technologies regarding the design and requalification of marine pipelines,
- Provision of a scholarships to fund the work of graduate student researchers (GSR) that assisted in performing this project, and
- Provision of technical support, background, and field operations data to advance the objectives of the RAM PIPE REQUAL project.

1.3 Background

During the period 1996 - 1998, PEMEX (Petroleos Mexicanos) and IMP (Instituto Mexicanos del Petroleo) sponsored a project performed by the Marine Technology and Development Group of the University of California at Berkeley to help develop first-generation Reliability Assessment and Management (RAM) based guidelines for design of pipelines and risers in the Bay of Campeche. These guidelines were based on both Working Stress Design (WSD) and Load and Resistance Factor Design (LRFD) formats. The following guidelines were developed during this project:

- Serviceability and Safety Classifications (SSC) of pipelines and risers,
- Guidelines for analysis of in-place pipeline loadings (demands) and capacities (resistances), and

- Guidelines for analysis of on-bottom stability (hydrodynamic and geotechnical forces),

This work formed an important starting point for this project.

During the first phase of this project, PEMEX and IMP sponsored two international workshops that addressed the issues and challenges associated with development of criteria and guidelines for design and requalification of marine pipelines.

1.4 Approach

Very significant advances have been achieved in the requalification and reassessment of onshore pipelines. A very general strategy for the requalification of marine pipelines has been proposed by DNV and incorporated into the ISO guidelines for reliability-based limit state design of pipelines (Collberg, Cramer, Bjornoyl, 1996; ISO, 1997). This project is founded on these significant advances.

The fundamental approach used in this project is a Risk Assessment and Management (RAM) approach. This approach is founded on two fundamental strategies:

1) Assess the risks (likelihoods, consequences) associated with existing pipelines, and

- Manage the risks so as to produce acceptable and desirable quality in the pipeline operations.

It is recognized that some risks are knowable (can be foreseen) and can be managed to produce acceptable performance. Also, it is recognized that some risks are not knowable (can not be foreseen, and that management processes must be put in place to help manage such risks.

Applied to development of criteria for the requalification of pipelines, a RAM approach proceeds through the following steps:

- Based on an assessment of costs and benefits associated with a particular development and generic type of system, and regulatory - legal requirements, national requirements, define the target reliabilities for the system. These target reliabilities should address the four quality attributes of the system including serviceability, safety, durability, and compatibility.
- Characterize the environmental conditions (e.g. hurricane, nominal oceanographic, geologic) and the operating conditions (installation, production, maintenance) that can affect the pipeline during its life.
- Based on the unique characteristics of the pipeline system characterize the 'demands' (imposed loads, induced forces, displacements) associated with the environmental and operating conditions. These demands and the associated conditions should address each of the four quality attributes of interest (serviceability, safety, durability, compatibility).
- Evaluate the variabilities, uncertainties, and 'Biases' (differences between nominal and true values) associated with the demands. This evaluation must be consistent with the variabilities and uncertainties that were included in the decision process that determined the desirable and acceptable 'target' reliabilities for the system (Step #1).
- For the pipeline system define how the elements will be designed according to a proposed engineering process (procedures, analyses, strategies used to determine the structure element sizes), how these elements will be configured into a system, how the system will be constructed, operated, maintained, and decommissioned (including Quality Assurance - QA, and Quality Control - QC processes).
- Evaluate the variabilities, uncertainties, and 'Biases' (ratio of true or actual values to the predicted or nominal values) associated with the capacities of the pipeline elements and the

pipeline system for the anticipated environmental and operating conditions, construction, operations, and maintenance activities, and specified QA - QC programs). This evaluation must be consistent with the variabilities and uncertainties that were included in the decision process that determined the desirable and acceptable 'target' reliabilities for the system (Step #1).

- Based on the results from Steps #1, #4, and #6, and for a specified 'design format' (e.g. Working Stress Design - WSD, Load and Resistance Factor Design- LRFD, Limit States Design - LSD), determine the design format factors (e.g. factors-of-safety for WSD, load and resistance factors for LRFD, and design conditions return periods for LSD).

It is important to note that several of these steps are highly interactive. For some systems, the loadings induced in the system are strongly dependent on the details of the design of the system. Thus, there is a potential coupling or interaction between Steps #3, #4, and #5. The assessment of variabilities and uncertainties in Steps #3 and #5 must be closely coordinated with the variabilities and uncertainties that are included in Step #1. The QA - QC processes that are to be used throughout the life-cycle of the system influence the characterizations of variabilities, uncertainties, and Biases in the 'capacities' of the system elements and the system itself. This is particularly true for the proposed IMR (Inspection, Maintenance, Repair) programs that are to be implemented during the system's life cycle. Design criteria, QA - QC, and IMR programs are highly interactive and are very inter-related.

The RAM PIPE REQUAL guidelines are based on the following current criteria and guidelines:

- American Petroleum Institute (API RP 1111, 1996, 1998),
- Det Norske Veritas (DNV, 1981, 1996, 1998, 1999),
- American Gas Association (AGA, 1990, 1993),
- American Society of Mechanical Engineers (ASME B31),
- British Standards Institute (BSI 8010, PD 6493), and
- International Standards Institute (ISO, 1998).

1.5 Guideline Development Premises

The design criteria and guideline formulations developed during this project are conditional on the following key premises:

- The design and reassessment – requalification analytical models used in this project were based in so far as possible on analytical procedures that are founded on fundamental physics, materials, and mechanics theories.
- The design and reassessment – requalification analytical models used in this –project were founded on in so far as possible on analytical procedures that result in un-biased (the analytical result equals the median – expected true value) assessments of the pipeline demands and capacities.
- Physical test data and verified – calibrated analytical model data were used in so far as possible to characterize the uncertainties and variabilities associated with the pipeline demands and capacities.
- The uncertainties and variabilities associated with the pipeline demands and capacities will be concordant with the uncertainties and variabilities associated with the background used to define the pipeline reliability goals.

1.6 Pipeline Operating Premises

- The pipelines will be operated at a minimum pressure equal to the normal hydrostatic pressure exerted on the pipeline.
- The pipelines will be maintained to minimize corrosion damage through coatings, cathodic protection, use of inhibitors, and dehydration so as to produce moderate corrosion during the life of the pipeline. If more than moderate corrosion is developed, then the reassessment capacity factors are modified to reflect the greater uncertainties and variabilities associated with severe corrosion.
- The pipelines will be operated at a maximum pressure not to exceed the maximum design pressure. If pipelines are reassessed and requalified to a lower pressure than the maximum design pressure, they will be operated at the specified lower maximum operating pressure. Maximum incidental pressures will not exceed 10 % of the specified maximum operating pressures.

1.7 Schedule

This project will take two years to complete. The project was initiated in August 1998. The first phase of this project was completed on 1 July, 1999. RAMP PIPE REQUAL Report 1 (Part 1) and Report 2 (Part 2) document results from the first year study. The second phase of this project was initiated in August 1999 and will be completed during July 2000. This report, Report 3, documents the results of Part 3 of this study.

The schedule for each of the project tasks is summarized in Table 1.1.

Table 1.1 - Project Task Schedule

Task	Part 1, Year 1	Part 2, Year 1	Part 3, Year 2	Part 4, Year 2
1 Classifications	----------X			
2 Buckling	----------X			
3 Pressure	----------X			
4 Op. Pressures	----------X			
5 Pipe Char.		----------X		
6 Stability		----------X		
7 Buckling Gl.		----------X		
8 Press. Gl.		----------X		
9 Stab. Gl.			----------X	
10 Requal. Gl.			----------X	----------X
11 Workshops.	X X X	X	X	X
12 GSR	----------X	----------X	----------X	----------X
13 Review	X----------X	----------X	----------X	----------X

1.8 Project Reports

A report will document the developments from each of the four parts or phases of this project. The reports that will be issued at the end of each of the project phases are as follows:

- **Report 1** – Requalification Process and Objectives, Risk Assessment & Management Background, Pipeline and Riser Classifications and Targets, Templates for Requalification Guidelines, Pipeline Operating Pressures and Capacities (corrosion, denting, gouging – cracking).

- **Report 2** – Pipeline characteristics, Hydrodynamic Stability, Geotechnical Stability, Guidelines for Assessing Capacities of Defective and Damaged Pipelines.

- **Report 3** – Guidelines for Assessing Pipeline Stability (Hydrodynamic), System Reliability Considerations, More on Corrosion Effects, Preliminary Requalification Guidelines.

- **Report 4** – Guidelines for Requalifying and Reassessing Marine Pipelines.

2.0 RAM PIPE REQUAL

2.1 Attributes

Practicality is one of the most important attributes of an engineering approach. Industry experience indicates that a practical RAM PIPE REQUAL approach should embody the following attributes:

- **Simplicity** – ease of use and implementation,
- **Versatility** – the ability to handle a wide variety of real problems,
- **Compatibility** – readily integrated into common engineering and operations procedures,
- **Workability** – the information and data required for input is available or economically attainable, and the output is understandable and can be easily communicated,
- **Feasibility** – available engineering, inspection, instrumentation, and maintenance tools and techniques are sufficient for application of the approach, and
- **Consistency** – the approach can produce similar results for similar problems when used by different engineers.

2.2 Strategies

The RAM PIPE REQUAL approach is founded on the following key strategies:

- **Keep pipeline systems in service** by using preventative and remedial IMR (Inspection, Maintenance, Repair) techniques. RAM PIPE attempts to establish and maintain the integrity of a pipeline system at the least possible cost.
- RAM PIPE REQUAL procedures are intended to **lower risks to the minimum that is practically attainable**. Comprehensive solutions may not be possible. Funding and technology limitations may prevent implementation of ideally comprehensive solutions. Practicality implicates an **incremental investment in identifying and remedying pipeline system defects in the order of the hazards they represent**. This is a prioritized approach.
- RAM PIPE REQUAL should be one of **progressive and continued reduction of risks to tolerable levels.** The **investment of resources must be justified by the scope of the benefits achieved.** This is a repetitive, continuing process of improving understanding and practices. This is a process based on economics and benefits.

2.3 Approach

The fundamental steps of the RAM PIPE REQUAL approach are identified in Figure 2.1. The steps can be summarized as follows:

- **Identification** – this selection is based on an assessment of the likelihood of finding significant degradation in the quality (serviceability, safety, durability, compatibility) characteristics of a given pipeline system, and on an evaluation of the consequences that could be associated with the degradation in quality. The selection can be triggered by either a regulatory requirement or by an owner's initiative, following an unusual event, an accident, proposed upgrading of the operations, or a desire to significantly extend the life of the pipeline system beyond that originally intended. ISO (1997) has identified the following triggers for requalification of pipelines: extension of design life, observed damage, changes in operational and environmental conditions, discovery of errors made during design or installation, concerns for the safety of the pipeline for any reason including increased consequences of a possible failure.

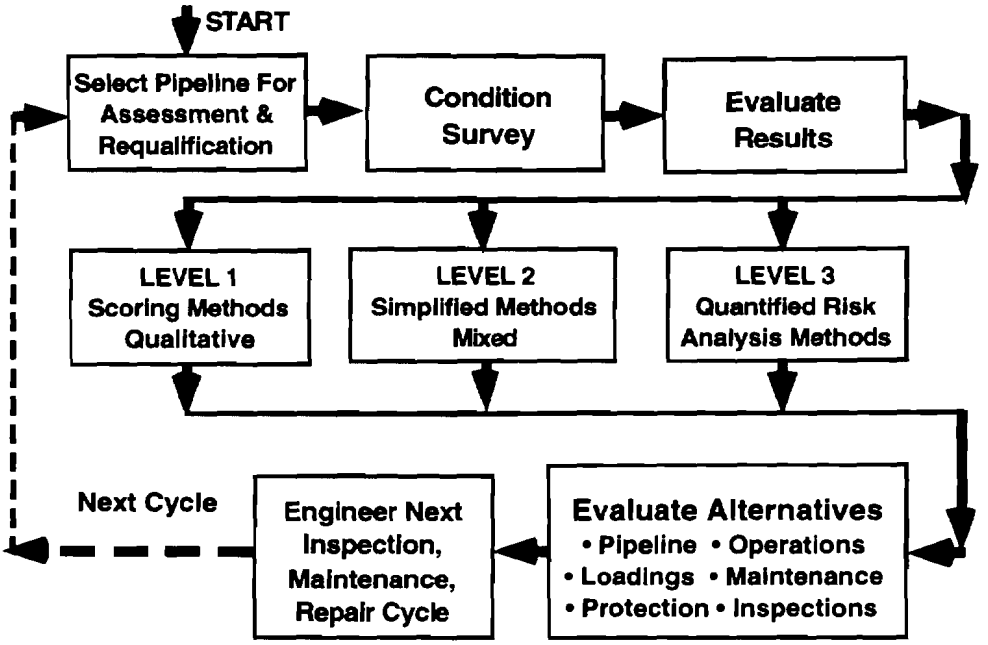

Figure 2.1 – RAM PIPE Approach

- **Condition survey** – this survey includes the formation of or continuance of a databank that contains all pertinent information the design, construction, operation, and maintenance of a pipeline system. Of particular importance are identification and recording of exceptional events or developments during the pipeline system history. Causes of damage or defects can provide important clues in determining what, where, how ,and when to inspect and/or instrument the pipeline system. This step is of critical importance because the RAM PIPE process can only be as effective as the information that is provided for the subsequent evaluations (garbage in, garbage out). Inspections can include external observations (eye, ROV) and measurements (ultrasonic, eddy current, caliper), and internal measurements utilizing in-line instrumentation (smart pigs: magnetic flux, ultrasonic, eddy current, caliper, inertia – geo).
- **Results assessment** – this effort is one of assessing or screening the pipeline system based on the presence or absence of any significant signs of degradation its quality characteristics. The defects can be those of design, construction, operations, or maintenance. If there appear to be no potentially significant defects, the procedure becomes concerned with engineering the next IMR cycle. If there appear to be potentially significant defects, the next step is to determine if mitigation of these defects is warranted. Three levels of assessment of increasing detail and difficulty can be applied: Level 1 – Qualitative (Scoring, Muhlbauer 1992; Kirkwood, Karam 1994), Level 2 – Simplified Qualitative – Quantitative (Bea, 1998), and Level 3 – Quantitative (Quantitative Risk Assessment, QRA, Nessim, Stephens 1995; Bai, Song 1998; Collberg, et al 1996). ISO guidelines (1997) have noted these levels as those of simple calculations, state of practice methods, and state of art methods, respectively.

  The basis for selection of one these levels is one that is intended to allow assessment of the pipeline with the simplest method. The level of assessment is intended to identify pipelines that are clearly fit for purpose as quickly and easily as is possible, and reserve more complex and intense analyses for those pipelines that warrant such evaluations. The engineer is able to choose the method that will facilitate and expedite the requalification process. There are more stringent Fitness for Purpose (FFP) criteria associated with the simpler methods because of the greater uncertainties associated with these methods, and because of the need to minimize the likelihood

of 'false positives' (pipelines identified to FFP that are not FFP).

- **Mitigation measures evaluation** – mitigation of defects refers to prioritizing the defects to remedied (first things first), and identifying practical alternative remedial actions. The need for the remedial actions depends on the hazard potential of a given pipeline system, i.e., the likelihood that the pipeline system would not perform adequately during the next RAM PIPE REQUAL cycle. If mitigation appears to be warranted, the next step is to evaluate the alternatives for mitigation.
- **Evaluating alternatives** – mitigation alternatives include those concerning the pipeline itself (patches, replacement of sections), its loadings (cover protection, tie-downs), supports, its operations (pressure de-rating, pressure controls, dehydration) maintenance (cathodic protection, corrosion inhibitors), protective measures (structures, procedures, personnel), and its information (instrumentation, data gathering). Economics based methods (Kulkarni, Conroy 1994; Nessim, Stephens 1995), historic precedents (data on the rates of compromises in pipeline quality), and current standards of practice (pipeline design codes and guidelines, and reassessment outcomes that represent decisions on acceptable pipeline quality) should be used as complimentary methods to evaluate the alternatives and the pipeline FFP. An important alternative is that of improving information and data on the pipeline system (information on the internal characteristics of the pipeline with instrumentation – 'smart pigs' and with sampling, information on the external characteristics of the pipeline using remote sensing methods and on-site inspections).
- **Implementing alternatives** – once the desirable mitigation alternative has been defined, the next step is to engineer that alternative and implement it. The results of this implementation should be incorporated into the pipeline system condition survey – inspection databank. The experiences associated with implementation of a given IMR program provide important feed-back to the RAM PIPE REQUAL process.
- **Engineering the next RAM PIPE REQUAL cycle** – the final step concluding a RAM PIPE REQUAL cycle is that of engineering and implementing the next IMR cycle. The length of the cycle will depend on the anticipated performance of the pipeline system, and the need for and benefits of improving knowledge, information and data on the pipeline condition and performance characteristics.

The ISO guidelines for requalification of pipelines (1997) cite the following essential aspects of an adequate requalifcation procedure – process:

- Account for all the governing factors for the pipeline, with emphasis on the factors initiating the requalification process
- Account for the differences between design of anew pipeline and the reassessment of an existing pipeline
- Apply a decision-theoretic framework and sound engineering judgement
- Utilize an approach in which the requalification process is refined in graduate steps
- Define a simple approach allowing most requalification problems to be solved using conventional methods.

The proposed RAM PIPE REQUAL process, guidelines, and criteria developed during this project are intended to fully satisfy these requirements. A Limit State format will be developed based on Risk Assessment and Management (RAM) background outlined in the next section of this report.

3.0 Pipeline Requalification Formulations & Criteria

The following tables summarize the pipeline requalification guidelines for determination of pipeline strength – capacity characteristics developed during the first phase of this project for in-place operating and accidental conditions. While the tables are not complete at this time, these tables will provide the format that will be used to compile requalification formulations and criteria developed as a result of this project. At this stage, one SSC has been identified for requalification strength criteria. This SSC represents the highest reliability requirements for pipelines and risers for the SSC evaluated during the first phase of this project. The SSC annual Safety Indices are summarized in Table 3.3.

Table 3.1 – Pipeline Capacities

Loading States (1)	Capacity Analysis Eqn. (2)	Data Bases (3)	Capacity Analysis Eqn. Median Bias (4)	Capacity Analysis Eqn. Coef. Var. (5)
Single				
Longitudinal • Tension - **Td**	**1**	**1.1**	1.0	0.25
• Compression -**Cd** local - **Cld**	**2**	**1.2**	1.0	0.25
• Compression global - **Cgd**	**3**	**1.3**	1.0	0.25
Transverse • Bending - **Mud**	**4**	**1.4**	1.0	0.25
Pressure • Burst - **Pbd**	**5**	**1.5**	1.2	0.25
• Collapse – **Pcd***	**6**	**1.6**	1.0	0.25
• Propagating–**Pp***	**7**	**1.7**	1.0	0.12
Combined				
T - Mu	**8**	**2.1**	1.0	0.25
T – Pc*	**9**	**2.2**	1.0	0.25
Mu – Pc*	**10**	**2.3**	1.0	0.25
T–Mu-Pc*	**11**	**2.4**	1.0	0.25
C–Mu–Pb	**12**	**2.5**	1.0	0.25
C–Mu-Pc*	**13**	**2.6**	1.0	0.25

*** Accidental Limit State (evaluated with 10-year return period conditions)**

Table 3.2 – Pipeline Loadings & Pressures Biases and Uncertainties

Loading States (1)	In-Place Loading Median Bias B_{F50} (2)	In-Place Loading Annual Coefficient of Variation V_F (3)
Single		
Longitudinal • Tension - **Td**	1.0	0.10
• Compression- **Cd** local - **Cld**	1.0	0.10
• Compression global - **Cgd**	1.0	0.10
Transverse • Bending - **Mud**	1.0	0.10
Pressure • Burst - **Pbd**	1.0	0.10
• Collapse – **Pcd***	0.98	0.02
• Propagating-**Pp***	0.98	0.02
Combined		
T - Mu	1.0	0.10
T – Pc*	0.98	0.02
Mu – Pc*	0.98	0.02
T – Mu – Pc*	0.98	0.02
C– Mu -Pb	1.0	0.10
C– Mu –Pc*	0.98	0.02

*** Accidental Limit State (evaluated with 10-year return period conditions)**

Table 3.3 – Pipeline Design and Reassessment Ultimate Limit State Annual Safety Indices

Loading States (1)	Annual Safety Index In-Place ULS Pipelines (2)	Annual Safety Index In-Place ULS Risers (3)
Single		
Longitudinal • Tension - **Td**	3.4	3.8
• Compression -**Cd** local - **Cld**	3.4	3.8
• Compression global - **Cgd**	3.4	3.8
Transverse • Bending - **Mud**	3.4	3.8
Pressure • Burst - **Pbd**	3.4	3.8
• Collapse – **Pcd***	1.7	1.7
• Propagating-**Pp***	1.7	1.7
Combined		
T - Mu	3.6	3.8
T – Pc*	2.0	2.0
Mu – Pc*	2.0	2.0
T – Mu – Pc*	2.0	2.0
C – Mu - Pb	3.6	3.6
C – Mu – Pc*	**2.0**	**2.0**

***Accidental Limit State (evaluated with 10-year return period conditions)**

Table 3.4 –In-Place Reassessment Working Stress Factors

WSD Single In-Place Loadings	Demand/ Capacity	Demand & Capacity	In-Place Pipelines	In-Place Risers
	Median Bias	Uncertainty V	ULS - f	ULS - f
Tension	1.00	0.27	0.40	0.36
Compression (local)	1.00	0.27	0.40	0.36
Compression (global)	1.00	0.27	0.40	0.36
Bending	1.00	0.27	0.40	0.36
Burst Pressure (no corrosion)	0.91	0.27	0.44	0.39
Burst Pressure (20 yr corrosion)	0.83	0.27	0.48	0.43
Collapse Pressure (high ovality)*	0.98	0.31	0.60	0.60
Collapse Pressure (low ovality)*	0.98	0.27	0.64	0.64
Propagating Buckling*	0.98	0.12	0.83	0.83
WSD Combined In-Place Loadings				
Tension-Bending-Collapse Pressure*	0.98	0.27	0.64	0.64
Compression-Bending-Collapse Pressure*	0.98	0.27	0.64	0.64
Compression-Bending-Burst Pressure	1.00	0.27	0.40	0.36
*accidental condition with 10-yr demands				

Table 3.5 – In-Place Reassessment Loading Factors

LRFD Single In-Place Loadings	Demand	Demand	In-Place Pipelines	In-Place Risers
	Median Bias	Uncertainty V	LRFD - γ	LRFD - γ
Tension	1.00	0.10	1.29	1.33
Compression (local)	1.00	0.10	1.29	1.33
Compression (global)	1.00	0.10	1.29	1.33
Bending	1.00	0.10	1.29	1.33
Burst Pressure (no corrosion)	1.00	0.10	1.29	1.33
Burst Pressure (20 yr corrosion)	1.00	0.10	1.29	1.33
Collapse Pressure (high ovality)*	0.98	0.02	1.01	1.01
Collapse Pressure (low ovality)*	0.98	0.02	1.01	1.01
Propagating Buckling*	0.98	0.02	1.01	1.01
LRFD Combined In-Place Loadings				
Tension-Bending-Collapse Pressure*	0.98	0.02	1.01	1.01
Compression-Bending-Collapse Pressure*	0.98	0.02	1.01	1.01
Compression-Bending-Burst Pressure	1.00	0.10	1.29	1.33
*accidental condition with 10-yr demands				

Table 3.6 – In-Place Reassessment Resistance Factors

LRFD Single In-Place Loadings	Capacity Median Bias	Capacity Uncertainty V	Pipelines LRFD - ϕ	Risers LRFD - ϕ
Tension	1.00	0.25	0.53	0.49
Compression (local)	1.00	0.25	0.53	0.49
Compression (global)	1.00	0.25	0.53	0.49
Bending	1.00	0.25	0.53	0.49
Burst Pressure (no corrosion)	1.10	0.25	0.58	0.54
Burst Pressure (20 yr corrosion)	1.20	0.25	0.63	0.59
Collapse Pressure (high ovality)*	1.00	0.25	0.73	0.73
Collapse Pressure (low ovality)*	1.00	0.25	0.73	0.73
Propagating Buckling*	1.00	0.12	0.86	0.86
LRFD Combined In-Place Loadings				
Tension-Bending-Collapse Pressure*	1.00	0.25	0.73	0.73
Compression-Bending-Collapse Pressure*	1.00	0.25	0.73	0.73
Compression-Bending-Burst Pressure	1.00	0.25	0.53	0.49
*accidental condition with 10 yr demands				

Table 3.7 –Analysis Equations References

Loading States (1)	Analysis Eqn. (2)	Capacity Analysis Equations References (3)
Single - Design		
Longitudinal • Tension -**T**	**1**	Andersen, T.L., (1990), API RP 1111 (1997), DNV96 (1996), ISO (1996), Crentsil, et al (1990)
• Compression -**C** • local - **Cl**	**2**	API RP 2A (1993), Tvergaard, V., (1976), Hobbs, R. E., (1984)
• Compression • global - **Cg**	**3**	API RP 2A (1993), Tvergaard, V., (1976), Hobbs, R. E., (1984)
Transverse • Bending - **Mp**	**4**	BSI 8010 (1993), DNV 96 (1996), API RP 1111 (1997), Bai, Y. et al (1993), Bai, Y. et al (1997a), Sherman, D.R., (1983), Sherman, D.R., (1984), Kyriakides, S. et al (1987), Gresnigt, A.M., et al (1998)
Pressure • Burst - **Pb**	**5**	Bea, R. G. (1997), Jiao, et al (1996), Sewart, G., (1994), ANSI/ASME B31G (1991), API RP 1111 (1997), DNV 96 (1996), BSI 8010 (1993)
• Collapse - **Pc**	**6**	Timoshenko,S.P., (1961), Bai, Y., et al (1997a), Bai, Y., et al (1997b), Bai, Y., et al (1998), Mork, K., (1997), DNV 96 (1996), BSI 8010 (1993), API RP 1111 (1997), ISO (1996), Fowler, J.R., (1990)
Single - Reassessment		
Longitudinal • Tension - **Td**	**7**	Andersen, T.L., (1990)
•Compression -**Cd** • local - **Cld**	**8**	Loh, J. T., (1993), Ricles, J. M., et al (1992), Taby, J., et al (1980), Smith, C. S., et al (1979)
• Compression • global - **Cgd**	**9**	Loh, J. T., (1993), Ricles, J. M., et al (1992), Taby, J., et al (1980), Smith, C.S., et al (1979)
Transverse • Bending - **Mpd**	**10**	Loh, J. T., (1993), Ricles, J. M., et al (1992), Taby, J., et al (1980), Smith, C. S., et al (1979)
Pressure • Burst - **Pbd**	**11**	Kiefner, J. F., (1974), Kiefner, et al (1989), Chouchaoui et al (1992), Bea, R. G., (1997), Bai, et al (1997c), ASME B31G (1991), Klever, F. J., (1992), Jones, D. G., (1992), Gresnigt, A.M. et al (1996)
• Collapse - **Pcd**	**12**	Bai, et al (1998)
•Propagating–**Pp***	**13**	Estefen, et al (1995), Melosh, R. , et al (1976), Palmer, A.C., et al (1979), Kyridkides, et al (1981), Kyriakides, S. et al (1992), Chater, E., (1984), Kyriakides, S. (1991)
Combined -Design		
T - Mp	**14**	Bai, Y., et al (1993), Bai, Y., et al (1994), Bai, Y., (1997), Mork, K et al (1997), DNV 96 (1996), Yeh, M.K., et al (1986), Yeh, M.K., et al (1988), Murphey, C.E., et al (1984)
T - Pc	**15**	Kyogoku, T., et al (1981), Tamano, et al (1982)
B - Pc	**16**	Ju, G. T., et al (1991), Kyriakides, S., et al (1987), Bai, Y., et al (1993), Bai, Y., et al (1994), Bai, Y., et al (1993), Corona, E., et al (1988), DNV96 (1996), BSI 8010 (1993), API RP 1111 (1997), Estefen, S. F. et al (1995)
T – Mp - Pc	**17**	Li, R., et al (1995), DNV 96 (1996), Bai et al (1993), Bai, Y. et al (1994), Bai, Y. et al (1997), Kyriakides, et al (1989)
C – Mp - Pb	**18**	DNV 96 (1996), Bruschi, R., et al (1995), Mohareb, M. E. et al (1994)
C – Mp - Pc	**19**	Kim, H. O., (1992), Bruschi, R., et al (1995), Popv E. P., et al (1974),

Table 3.8 – Capacity Database References

Loading States (1)	Database	Capacity Analysis Equations References (3)
Single - Design		
Longitudinal • Tension -**T**	**1.1**	Fowler, J. R., (1990)
• Compression -**C** • local - **Cl**	**1.2**	Ostapenko, A. et al (1979)
• Compression • global - **Cg**	**1.3**	Chen, W.F., et al (1978),
Transverse • Bending - **Mp**	**1.4**	Schilling, G. S. (1965), Jirsa, J. O., et al (1972), Korol, R. M., et al (1979), Sherman, D.R., (1984), Steinmann, S.L., et al (1989), Fowler, J. R., (1990), KyRiakides, S., et al (1985), Johns, T. G., et al (1983)
Pressure • Burst - **Pb**	**1.5**	Sewart, G., et al (1994)
• Collapse - **Pc**	**1.6**	Kyriakides, et al (1984), Kyriakides, et al (1987), Fowler, J. R., (1990), Johns, T. G., et al (1983)
Single - Reassessment		
Longitudinal • Tension - **Td**	**2.1**	Taby, J., et al (1981)
• Compression -**Cd** • local - **Cld**	**2.2**	Loh, J.T., (1993), Ricles, J. M., et al (1992), Taby, J., et al (1981)
• Compression • global - **Cgd**	**2.3**	Loh, J.T., (1993), Ricles, J. M., et al (1992), Smith, C.S., et al (1979)
Transverse • Bending - **Mp d**	**2.4**	Loh, J.T., (1993), Ricles, J. M., et al (1992), Taby, J., et al (1981)
Pressure • Burst - **Pbd**	**2.5**	DNV (93-3637)
• Collapse - **Pcd**	**2.6**	
• Propagating–**Pp***	**2.7**	Kyriakides, S., (1984), Estefen S. F., et al (1995), Mesloh, et al (1976)
Combined -Design		
T - Mp	**3.1**	Dyau, J.Y., (1991), Wilhoit, Jr. J.C., et al (1973)
T - Pc	**3.2**	Edwards, S.H., et al (1939), Kyogoku, T., et al (1981), Tamano, T., et al (1982), Kyriakides, S., et al (1987), Fowler, J. R., (1990)
B - Pc	**3.3**	Kyriakides, S., et al (1987), Fowler, J. R., (1990), Winter, P. E., (1985), Johns, T. G., (1983)
T – Mp - Pc	**3.4**	Walker, G.E., et al (1971), Langner, C.G., (1974)
C – Mp - Pb	**3.5**	Walker, G.E., et al (1971), Langner, C.G., (1974)

Table 3.9 – Formulations for Single Loading States

Loading States (1)	Formulation (2)	Formulation Factors (3)
Longitudinal • Tension - **Td**	$Td = 1.1SMYS(A - \Delta)$	
• Compression- **Cd** local - **Cld**	$Cl = 1.1 \bullet SMYS\left(2.0 - 0.28(D/t_{\min})^{1/4}\right) \bullet A \bullet Kd$	Kd = 1 + 3 fd (D / t)
• Compression global - **Cgd**	$Cg = 1.1SMYS\left(1.2 - 0.25\lambda^2\right) \bullet A$ $\lambda = \frac{KL}{\pi r}\left[\frac{SMYS}{E}\right]^{0.5}$	$\frac{P_{crd}}{P_{crdo}} + \frac{P_{crd}\Delta Y}{\left(1 - \frac{P_{crd}}{P_{Ed}}\right)M_{ud}} \le 1.0$ $\lambda_d = \left(P_{ud}/P_{ed}\right)^{0.5}$ $P_{ud} = P_u\frac{A_d}{A_o} = P_u \exp\left(-0.08\frac{\Delta}{t}\right)$
Transverse • Bending - **Mud**	$\frac{M_d}{M_u} = \exp\left(-0.06\frac{\Delta}{t}\right)$	
Pressure **Burst – Pbd** **Corroded** **Dented** **Gouged** **Dented & Gouged**	$P_{bC} = \frac{2.2 \bullet t \bullet SMTS}{(D-t) \bullet SCFc}$ $Pb_D = \frac{2t\sigma_u}{(D-t) \bullet SCF_D}$ $Pb_G = \frac{2t\sigma_u}{(D-t) \bullet SCF_G}$ $Pb_{DG} = \frac{2t\sigma_u}{(D-t) \bullet SCF_{DG}}$	$SCFc = 1 + 2\ (d/R)^{0.5}$ $SCF_D = 1 + 0.2\ (H/t)^3$ $SCF_G = 1 + 2\ (h/r)^{0.5}$ $SCF_{DG} = [1\text{-}d/t\text{-}(16H/D)(1\text{-}d/t)]^{-1}$
• **Collapse – Pcd** **High Ovality Pipe* ($f_{so} = 1$ %)** **Low Ovality Pipe* ($f_{so} = 0.1$ %)**	$P_c = 0.5\left\{P_{ud}' + P_{ed}K_d - \left[\left(P_{ud}' + P_{ed}K_d\right)^2 - 4P_{ud}'P_{ed}K_d\right]^{0.5}\right\}$ $P_c = 0.5\left\{P_{ud} + P_{ed}K_d - \left[\left(P_{ud} + P_{ed}K_d\right)^2 - 4P_{ud}P_{ed}K_d\right]^{0.5}\right\}$	$P_u' = 5.1\frac{\sigma_u t_d}{D_0}$ $P_E = \frac{2E}{1-\nu^2}\left(\frac{t_d}{D_0}\right)^3$ $K = 1 + 3f\left(\frac{D_0}{t_{nom}}\right)$ $P_{ud} = \frac{2SMTSt_{min}}{D_0}$
• Propagating-**Pp***	$Pp = 34 \bullet SMYS\left(\frac{t_{nom}}{D_0}\right)^{2.5}$	

*** Accidental Limit State (evaluated with 10-year return period conditions)**

Table 3.10 – Formulations for Combined Loading States

Loading States (1)	Formulation (2)	Formulation Factors (3)
T - Mu	$\left[\left(\frac{M}{Mu}\right)^2+\left(\frac{T}{Tu}\right)^2\right]^{0.5}=1.0$	
T - Pc	$\frac{P}{Pc}+\frac{T}{Tu}=1.0$	
Mu - Pc	$\frac{P}{Pc}+\frac{M}{Mu}=1.0$ *(load controlled)* $\left(\frac{P}{Pc}\right)^2+\left(\frac{M}{Mu}\right)^2=1.0$ *(displacement cont.)*	
T – Mu - Pc	$\left[\left(\frac{M}{M_u}\right)^2+\left(\frac{P}{P_c}\right)^2+\left(\frac{T}{Tu}\right)^2\right]^{0.5}\le 1$	
C– Mu -Pb	$M_c=M_p f_M$ $M_p=SMYS\bullet D^2 t\left(1-0.001\frac{D}{t}\right)$ $\left[\left(\frac{P}{P_{co}}\right)^2+\left(\frac{M}{M_u}\right)^2+\left(\frac{C}{C_g}\right)^2-2\mu\left(\frac{P}{P_{co}}\bullet\frac{M}{M_u}+\frac{M}{M_u}\bullet\frac{C}{C_g}+\frac{P}{P_{co}}\bullet\frac{C}{C_g}\right)\right]^{-0.5}\le 1$	$f_M=k_1\cos\left[\frac{\frac{\pi}{2}\left(k_2-\frac{1}{2}\frac{\sigma_{he}}{SMTS}\right)}{k_1}\right]$ $k_1=\sqrt{1-\frac{3}{4}\left(\frac{\sigma_{he}}{SMTS}\right)^2}$ $k_2=\frac{C}{\pi\bullet SMTS\bullet Dt}$
C– Mu -Pc	$\left(\frac{M}{M_{co}}\right)^2+\left(\frac{P}{P_{co}}\right)^2\le 1$ $\left[\left(\frac{P}{P_{co}}\right)^2+\left(\frac{M}{M_u}\right)^2+\left(\frac{C}{C_g}\right)^2-2\mu\left(\frac{P}{P_{co}}\bullet\frac{M}{M_u}+\frac{M}{M_u}\bullet\frac{C}{C_g}+\frac{P}{P_{co}}\bullet\frac{C}{C_g}\right)\right]^{0.5}\le 1$	$M_{co}=M_p\cos\left(\frac{\pi}{2}\frac{T}{T_u}\right)$ $M_p=SMYS\bullet D_0^2 t_{nom}\left(1-0.001\frac{D_0}{t_{nom}}\right)$ P_{co} : Timoshenko Ultimate or Elastic equation

Table 3.11 – Formulations for Hydrodynamic Loadings

Formulation (1)	Factors (2)
$F_D = C_D (\rho / 2) D' (Uw + Uc)^2$ $F_L = C_L (\rho / 2) D (Uw + Uc)^2$ $F_I = C_M \rho V' Aw$ $F_T = F_D + F_I$ $Ru \geq F_T \times FS$ $W \geq F_L \times FS$	See Fig. 3.1 $C_D = 1.0$ $C_L = 0.5$ $C_M = 2.5$ $FS = 1.0$
D' = vertical effective (unburied) height of pipe D = pipe diameter V = vertical effective (unburied) volume (per unit length) of pipe Ru = lateral soil – pipeline sliding resistance W = vertical effective weight of pipeline FS = factor of safety for 100-year conditions	Uw = maximum wave velocity normal to pipe axis Uc = maximum current velocity normal to pipe axis Aw = maximum wave acceleration normal to pipe axis

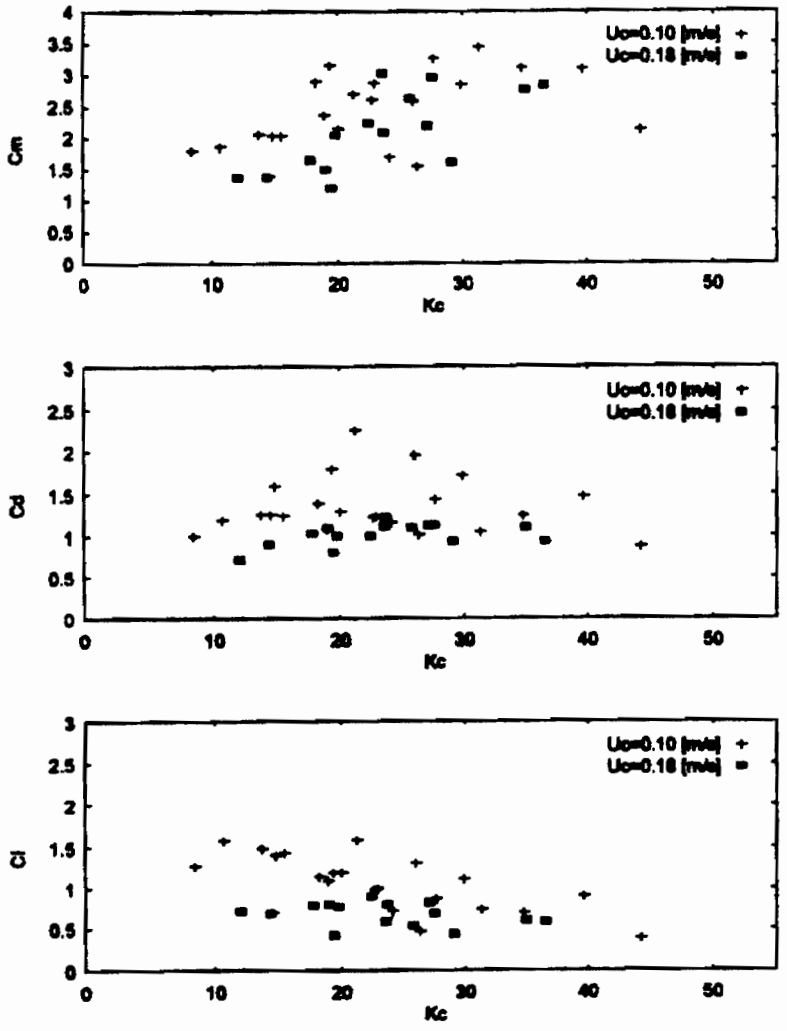

Figure 3.1 – Pipeline hydrodynamic loading coefficients (Neill and Hinwood, 1998)

4.0 Hydrodynamic Loadings

Wave forces on a fixed horizontal pipeline segment under the combined action of directionally spreading waves and currents are estimated utilizing a directional wave spectrum. The analysis includes the effects of reduction in forces due to three-dimensional seas, associated spatio-temporal correlation of water particle velocity field and the orientation of pipeline segment. These results are expressed in terms of biases for design applications. The final product includes biases for the hydrodynamic drag and inertial forces that result from the pipeline orientation and spatio-temporal correlation of directionally spreading seas. The analysis presented here can be applied to directionally spreading wave conditions experienced during hurricanes in the Gulf of Mexico and Bay of Campeche. A follow-up study will focus on developing simplified close-form expressions for codification and improved hydrodynamic loading models for drag and lift in the presence of pipeline movement in surrounding water-soil medium that results from bedload sediment transport under wave action.

4.1 Introduction

In the Gulf of Mexico and the Bay of Campeche, the integrity of thousands of miles of pipeline is threatened each year by the potential of hurricane activity in the region. The performance of pipeline is not only judged by its capacity to withstand pressure and impact of corrosion, but also by its ability to withstand movements of sea floor soils. The soft sea floor soils are known to develop significant motions during the passage of hurricanes. The wave and current induced hydrodynamic loads and movement of the sea floor influence the stability of the pipeline. Hurricane Roxanne, the most severe hurricane to affect the Bay of Campeche during this century inflicted major damage to offshore pipelines in the region (Valdex et al., 1997; Bea et al., 1998a; Cardone et al., 1998). Morris et al. (1988) and Bea et al. (1998a) have reported risk assessment and management (RAM) based criteria for the design and requalification of pipelines and risers in the Bay of Campeche. Their paper summarizes various possible loading scenarios on the pipeline, based on the specifications laid down by Instituto Mexicano del Petroleo (IMP) and guidelines developed by American Gas Association (AGA, 1993).

It is noted by Bea et al. (1998a) that the specified design loads will generally result in a significant conservative bias in the computed design loads. The bias is defined in terms of the ratio between the expected maximum loading and the design maximum loading. Based on the orientation of the pipeline, Bea et al. (1998a) developed biases in terms of the ratio between the current and wave induced particle velocities. Bea et al. (1998a) correctly pointed out another bias introduced by the space-time variation in the wave kinematics, associated hydrodynamic loads, and the transient nature of these loads. The spatial variation in hydrodynamic loads may not only reduce the effective loading on a section of pipeline, but may also influence the support conditions of the pipeline by shifting the soil support, thus limiting the displacements or deformations experienced by the pipeline.

It is noted in this discussion that the space-time variability of wave kinematics and variations in the currents can have a major influence on the design and performance of a pipeline. Several studies in the literature have addressed this topic at different levels of detail and modeling sophistication (Grace and Zee, 1981; Lambrakos, 1982; Zimmerman et al., 1986; Jacobsen et al., 1989; Lambrakos et al., 1987; Lammaert et al., 1989; Borgman and Hudspeth, 1992; Collins et al., 1995; Hale et al., 1989; Soedigdo et al., 1999). In light of the importance of the problem and a lack of unified

information on the hydrodynamic load effects, accurate assessment of these effects for risk based design standards and guidelines are needed.

This study examines the space-time variation of hydrodynamic loads acting on pipelines for a range of orientations with respect to the local bathymetry. The coherence modeling plays a central role in the analysis of structures exposed to wind, wave or seismic load effects (Kareem et al., 1997). A single point representation of the stochastic field concerning wind, wave, or seismic effects may be employed for structures smaller than a typical scale. However, partial correlation over larger or longer structures such as pipelines necessitates the use of multipoint stochastic field statistics to accurately ascertain dynamic load effects. The level of correlation is generally expressed in terms of a coherence function whose form depends on the characteristics of the stochastic field under consideration (Mitwally and Novak, 1989; Kareem and Song, 1998). Although the importance of directional distribution of ocean waves has been acknowledged in offshore engineering (Borgman, 1990), the directional wave spectra is not widely used in design practice due to its complexity and added computations.

The main feature of a directional wave system is that the total first order wave force on a structure is less than that of a unidirectional wave system having the same total energy. The lack of correlation may be accounted for by using a coherence function and cross-spectrum of the wave height and water particle velocity fluctuations between locations of interest. Therefore, associated hydrodynamic loads can be expressed in terms of this coherence function. This coherence function can be expressed in terms of spreading function. Once loads are expressed in terms of the coherence, several simplifications in the load description can be introduced. These simplifications are similar to those for wind effects, which are very attractive for inclusion in design specifications or other guidelines.

In this study, wave forces on a horizontal pipeline segment under the combined action of directionally spreading waves and currents are investigated using a directional spectrum. The effects of directional spreading are manifested in terms of an overall reduction of energy in the direction of wave propagation and lack of spatio-temporal correlation in the wave surface field. They have a direct influence on the water particle kinematics. The biases in the hydrodynamic drag and inertial forces due to pipeline orientation and spatial correlation are studied.

4.2 Water Particle Velocity

In this study, a Cartesian coordinate system is used with the origin at the mean water level (Fig. 4.1). The water depth, h, is assumed to be constant. The sea surface is denoted as $z = \xi(x, y, t)$, in which t is time, and can be treated as a stationary stochastic field.

Assuming that sea water is an incompressible, inviscid fluid and that the wave motion is irrotational, the velocity potential $\Phi(x, y, z)$ can be represented in the form of the Fourier-Stieltjes integral which leads to the surface elevation $\xi(x, y, t)$

$$\Phi(x,y,z,t) = -ig\int_{-\infty}^{\infty}\int_{-\pi}^{\pi}\frac{cosh[k(z+h)]}{\omega cosh(kh)}exp[ik(xcos\theta+ysin\theta)-i\omega t]dA(\omega,\theta) \tag{4.1}$$

$$\xi(x,y,t) = -\frac{1}{g}(\frac{\partial\Phi}{\partial t})_{z=0} = \int_{-\infty}^{\infty}\int_{-\pi}^{\pi}\exp[ik(x\cos\theta + y\sin\theta) - i\omega t]dA(\omega,\theta) \tag{4.2}$$

in which the wave number k is related to wave frequency ω by the dispersion relationship

$$\omega^2 = gk\tanh(kh) \tag{4.3}$$

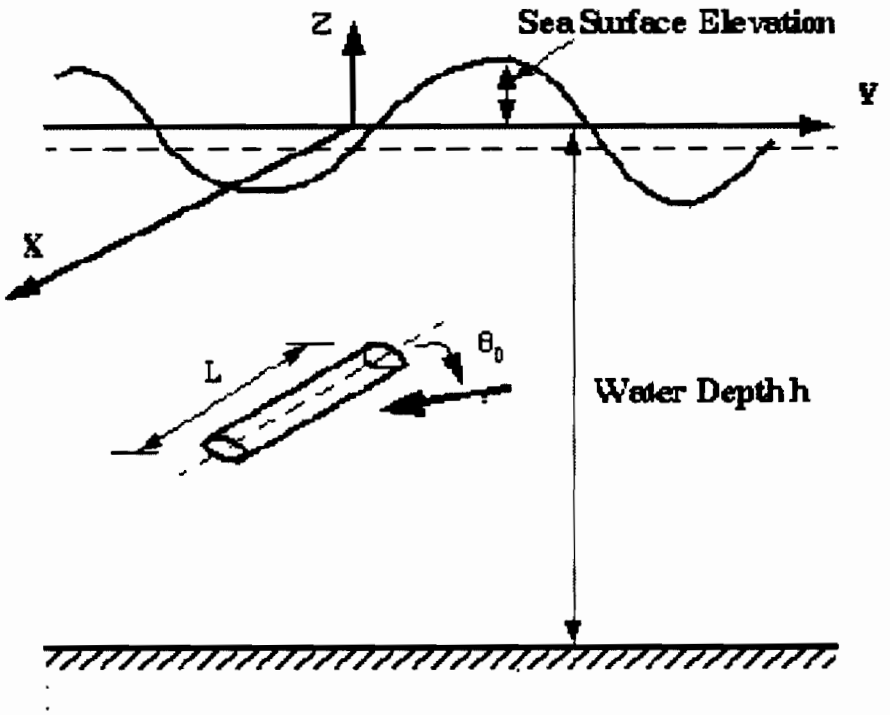

Fig. 4.1 Cartesian coordinate system

The angle θ denotes the direction of wave propagation of an elementary wave relative to the x-axis, $A(\omega,\theta)$ is the spectral amplitude, and is related to the two-dimensional energy spectrum (two-side) of the surface elevation $S_{\xi\xi}(\omega,\theta)$ as

$$< dA(\omega,\theta)dA^*(\omega_1,\theta_1) >= \bar{S}_{\xi\xi}(\omega,\theta)\delta(\omega-\omega_1)\delta(\theta-\theta_1)d\omega d\omega_1 d\theta d\theta_1 \tag{4.4}$$

in which $\delta(\ )$ is Dirac's delta function; * denotes the complex conjugate operator; and $< >$ represents the statistical averaging. The two-sided spectrum $S_{\xi\xi}(\omega,\theta)$ is related to the one side spectrum $S_{\xi\xi}(\omega,\theta)$ (extending from 0 to ∞) by

$$S_{\xi\xi}(\omega,\theta) = 2\bar{S}_{\xi\xi}(\omega,\theta) \tag{4.5}$$

The water particle velocity can be represented as

$$v(t) = \int_{-\infty}^{\infty}\int_{-\pi}^{\pi} \omega C(\theta)\frac{Hypb[k(z+h)]}{\sinh(kh)}\exp[ik(x\cos\theta+y\sin\theta)-i\omega t]dA(\omega,\theta) \tag{4.6}$$

in which $C(\theta)$ is given by

$$C(\theta) = \begin{cases} \cos\theta & for\ \ 1//X \\ \sin\theta & for\ \ 1//Y \\ 1 & for\ \ 1//Z \end{cases} \tag{4.7}$$

in which $1//X$ indicates the velocity component in the x-direction, with analogous definitions for $1//Y$ and $1//Z$; and

$$Hypb[k(z+h)] = \begin{cases} \cosh[k(z+h)] & for\ \ 1//X\ or\ 1//Y \\ -i\sinh[k(z+h)] & for\ \ 1//Z \end{cases} \tag{4.8}$$

4.3 Directional Wave Surface Spectrum

Within a storm-generation area, the sea surface elevation can be described by the directional spectrum in the form

$$S_{\xi\xi}(\omega,\theta) = S^u_{\xi\xi}(\omega)D(\omega,\theta) \tag{4.9}$$

in which $S_{\xi\xi}{}^u(\omega)$ is the unidirectional one side spectrum; and $D(\omega,\theta)$ is the directional spreading function which satisfies the condition

$$\int_{-\pi}^{\pi} D(\omega,\theta)d\theta = 1 \tag{4.10}$$

Various analytical expressions for the wave spectrum have been proposed. Some of them describe fully developed seas, while others depend on the fetch and duration. Without loss of generality, the Pierson-Moskowitz (1964) spectrum is used in this study, and it is given by

$$S^u_{\xi\xi}(\omega) = \frac{\alpha g^2}{\omega^5}\exp\left[-0.74(\frac{\bar{\omega}}{\omega})^4\right] \tag{4.11}$$

in which α=0.0081 is the Phillips constant; g is gravity acceleration; $\bar{\omega}=g/U$; and U is the mean wind velocity.
Alternatively, in terms of the peak frequency of the spectrum ω_p ($\omega_p=1.14\bar{\omega}$)

$$S^u_{\xi\xi}(\omega) = \frac{\alpha g^2}{\omega^5}\exp\left[-0.125(\frac{\omega_p}{\omega})^4\right] \tag{4.12}$$

The variance of the wave elevation is given by

$$\sigma^2_\xi = \int_0^\infty S^u_{\xi\xi}(\omega)d\omega = \frac{\alpha g^2}{5\omega_p^4} \tag{4.13}$$

Assuming that the wave height follows the Rayleigh distribution, the significant wave height H_s is related to the root-mean-square (RMS) surface elevation σ_ξ as

$$H_s = 4\sigma_\xi \tag{4.14}$$

The most probable maximum wave height (H_{max}) for a given number of wave cycles (N) in a record can be estimated from the significant wave height H_s as

$$H_{max} = \frac{1}{2}\left[\sqrt{2\ln N} + \frac{0.5772}{\sqrt{2\ln N}}\right]H_s \tag{4.15}$$

when N=1000, gives $H_{max}=1.86H_s$.
The wave spectrum describes only the mean square statistics of the surface elevation, whereas information about the directional waves (wave energy spreading) is described by the directional spreading function. If directionality is neglected, it implies that the total energy is traveling in one direction as in the case of a unidirectional wave system. Thus, directionality means spreading of

energy, with an apparent reduction in the along-wave force component and an increase in the lateral wave force component, which is normal to the mean direction of wave propagation.
The directional spreading function given by Donelan et al. (1985) is used in this study

$$D(\omega,\theta) = \frac{1}{2}\beta \cosh^{-2}[\beta(\theta-\theta_0)] \tag{4.16}$$

in which θ_0 is the mean direction of wave propagation.
Using high-frequency stereo photography, Banner (1990) proposed a formulation for β as

$$\beta = \begin{cases} 2.61(\omega/\omega_p)^{1.3} & for \quad 0.56 < \omega/\omega_p < 0.95 \\ 2.28(\omega/\omega_p)^{-1.3} & for \quad 0.95 < \omega/\omega_p < 1.60 \\ 10^{y} & for \quad \omega/\omega_p > 1.6 \end{cases} \tag{4.17}$$

in which

$$y = -0.4 + 0.8393\exp\left[-0.567\ln(\frac{\omega}{\omega_p})^2\right] \tag{4.18}$$

The preceding spreading function is a function of frequency to account for the fact that longer period waves (swell) are almost unidirectional, whereas the short period waves have directional features. However, the spreading function is often approximated by a frequency-independent format for storm waves. A wrapped normal distribution has also been used in this study for comparison

$$D(\omega,\theta) = \frac{1}{\sqrt{2\pi}\sigma_D}\exp\left[-\frac{(\theta-\theta_0)^2}{2\sigma_D^2}\right] \tag{4.19}$$

in which σ^2_D is the standard deviation of spreading.
The cross spectrum (one-side) of sea surface elevation at points 1 and 2 can be given as

$$S_{\xi_1\xi_2}(\omega) = S^u_{\xi\xi}(\omega)\int_{-\pi}^{\pi} D(\omega,\theta)\exp\{ik[(x_1-x_2)\cos\theta + (y_1-y_2)\sin\theta]\}d\theta \tag{4.20}$$

in which x_1, y_1 and z_1 and x_2, y_2 and z_2 are the Cartesian coordinates of points 1 and 2, respectively.
The coherence of sea surface elevation is

$$coh_\xi(\Delta x,\Delta y,\omega) = \int_{-\pi}^{\pi} D(\omega,\theta)\exp\{ik[(x_1-x_2)\cos\theta + (y_1-y_2)\sin\theta]\}d\theta \tag{4.21}$$

in which Δx=|x_1-x_2|, Δy=|y_1-y_2|.
For the unidirectional wave system, it is assumed that the total energy is traveling in the direction of wave propagation, i.e. the spreading function takes the form

$$D(\omega,\theta) = \delta(\theta-\theta_0) \tag{4.22}$$

Thus, the coherence of sea surface elevation for the unidirectional system is

$$coh^u_\xi(\Delta x,\Delta y,\omega) = \exp\{ik[(x_1-x_2)\cos\theta_0 + (y_1-y_2)\sin\theta_0]\} \tag{4.23}$$

The unidirectional sea elevation has spatial periodicity at a particular frequency and does not display loss of spatial correlation even for large values of separation. For separations that are across the wave front or along the water depth, the sea surface elevation is fully correlated even for large value of separation.

4.4 Power Spectra of Water Particle Velocity

To evaluate the resultant wave forces on a structure, the auto and cross spectral densities of the water particle velocity field are needed. After some manipulations, the power spectral density of the water particle velocity for the directional wave system, $S_{vv}(\omega)$, is obtained as

$$S_{vv}(\omega) = \omega^2 \frac{S^u_{\xi\xi}(\omega)}{\sinh^2(kh)} Hypb^2[k(z+h)] \int_{-\pi}^{\pi} D(\omega,\theta) C^2(\theta) d\theta \tag{4.24}$$

and the cross spectrum (one-side) of water particle velocities at points 1 and 2 can be expressed as

$$S_{v_1 v_2}(\omega) = \omega^2 \frac{S^u_{\xi\xi}(\omega)}{\sinh^2(kh)} Hypb_1[k(z_1+h)] Hypb_2[k(z_2+h)]$$

$$\int_{-\pi}^{\pi} D(\omega,\theta) C_1(\theta) C_2(\theta) \exp\{ik[(x_1-x_2)\cos\theta + (y_1-y_2)\sin\theta]\} d\theta \tag{4.25}$$

in which $C_1(\theta)$ and $C_2(\theta)$ are defined like $C(\theta)$ for the velocity components at points 1 and 2; $Hypb_1$ is defined like $Hypb$ for point 1 and $Hypb_2$ is defined as

$$Hypb_2[k(z_2+h)] = \begin{cases} \cosh[k(z_2+h)] & for\ \ 2//X\ or\ 2//Y \\ i\sinh[k(z_2+h)] & for\ \ 2//Z \end{cases} \tag{4.26}$$

The coherence function of the water particle velocity at two locations of interest is

$$coh(\Delta x, \Delta y, \omega) = S_{v_1 v_2}(\omega) / \sqrt{S_{v_1 v_1}(\omega) S_{v_2 v_2}(\omega)}$$

$$= \frac{\int_{-\pi}^{\pi} D(\omega,\theta) C_1(\theta) C_2(\theta) \exp\{ik[(x_1-x_2)\cos\theta + (y_1-y_2)\sin\theta]\} d\theta}{\int_{-\pi}^{\pi} D(\omega,\theta) C_1(\theta) C_2(\theta) d\theta} \tag{4.27}$$

For a unidirectional wave system propagating with an angle θ_0, the auto and cross spectra as well as coherence function of the water particle velocities can be given by

$$S^u_{vv}(\omega) = \omega^2 \frac{S^u_{\xi\xi}(\omega)}{sinh^2(kh)} C^2(\theta_0) Hypb^2[k(z+h)] \tag{4.28}$$

$$S^u_{v_1 v_2}(\omega) = \omega^2 \frac{S^u_{\xi\xi}(\omega)}{\sinh^2 kh} C_1(\theta_0) C_2(\theta_0) Hypb_1[k(z_1+h)] Hypb_2[k(z_2+h)]$$

$$\exp\{ik[(x_1-x_2)\cos\theta_0 + (y_1-y_2)\sin\theta_0]\} \tag{4.29}$$

$$coh^u(\Delta x, \Delta y, \omega) = \exp\{ik[(x_1-x_2)\cos\theta + (y_1-y_2)\sin\theta]\} \tag{4.30}$$

in which $C_1(\theta_0)$ and $C_2(\theta_0)$ are given in Eq. 4.7 with θ_0 substituted for θ.

4.5 Hydrodynamic Forces on a Horizontal Pipeline due to Combined Current and Wave Action

The hydrodynamic loads on a pipeline are derived from hurricane wave and current kinematics. The current velocity and water particle kinematics normal to the pipeline axis are of primary significance to these loads. In this study, for the sake of illustration the bias in the hydrodynamic forces due to

directional wave spreading effects, traditional Morison type formulation is utilized to estimate the drag and inertial forces. The lift force component is not addressed here.

4.5.1 Current and Water Particle Velocity and Acceleration near the Sea Bottom

Consider a fixed horizontal pipeline segment of length L which is parallel to the x-axis. For any two locations on the segment, y_1=y_2 and z_1=z_2, the power spectral density and the coherence functions of the water particle velocity and acceleration normal to the axis of the pipeline for directional seas near the bottom are

$$S_{vv}(\omega) = \omega^2 \frac{S^u_{\xi\xi}(\omega)}{\sinh^2(kh)} \int_{-\pi}^{\pi} D(\omega,\theta)\sin^2\theta d\theta \tag{4.31}$$

$$S_{\dot{v}\dot{v}}(\omega) = \omega^4 \frac{S^u_{\xi\xi}(\omega)}{\sinh^2(kh)} \int_{-\pi}^{\pi} D(\omega,\theta)\sin^2\theta d\theta \tag{4.32}$$

$$coh(\Delta x,\omega) = \frac{\int_{-\pi}^{\pi} D(\omega,\theta)\sin^2\theta \exp\{ik(x_1-x_2)\cos\theta\}d\theta}{\int_{-\pi}^{\pi} D(\omega,\theta)\sin^2\theta d\theta} \tag{4.33}$$

The transfer functions between the wave surface elevation and water particle velocity and acceleration near the sea bottom are given by

$$H_{v\xi}(\omega) = \frac{\omega}{\sinh(kh)}\sqrt{\int_{-\pi}^{\pi} D(\omega,\theta)\sin^2\theta d\theta} \tag{4.34}$$

$$H_{\dot{v}\xi}(\omega) = \frac{\omega^2}{\sinh(kh)}\sqrt{\int_{-\pi}^{\pi} D(\omega,\theta)\sin^2\theta d\theta} \tag{4.35}$$

Similarly, for the unidirectional seas, the preceding quantities are

$$S^u_{vv}(\omega) = \omega^2 \frac{S^u_{\xi\xi}(\omega)}{\sinh^2(kh)}\sin^2\theta_0 \tag{4.36}$$

$$S^u_{\dot{v}\dot{v}}(\omega) = \omega^4 \frac{S^u_{\xi\xi}(\omega)}{\sinh^2(kh)}\sin^2\theta_0 \tag{4.37}$$

$$coh_u(\Delta x,\omega) = \exp\{ik(x_1-x_2)\cos\theta_0\} \tag{4.38}$$

$$H^u_{v\xi}(\omega) = \frac{\omega}{\sinh(kh)}\sin\theta_0 \tag{4.39}$$

$$H^u_{\dot{v}\xi}(\omega) = \frac{\omega^2}{\sinh(kh)}\sin\theta_0 \tag{4.40}$$

Defining $R^2(\omega)$ as the ratio between the power spectra for unidirectional and directional seas as

$$R^2(\omega) = S_{vv}(\omega)/S^u_{vv}(\omega) = \int_{-\pi}^{\pi} D(\omega,\theta)\sin^2\theta d\theta / \sin^2\theta_0 \tag{4.41}$$

and defining the bias in the water particle velocity and acceleration due to wave directional spreading, B_v and $B\dot{v}$, as

$$B_v^2 = \sigma_v^2/\sigma_{v^u}^2 = \int_0^\infty S_{vv}(\omega)d\omega / \int_0^\infty S_{vv}^u(\omega)d\omega \tag{4.42}$$

$$B_{\dot{v}}^2 = \sigma_{\dot{v}}^2/\sigma_{\dot{v}^u}^2 = \int_0^\infty \omega^2 S_{vv}(\omega)d\omega / \int_0^\infty \omega^2 S_{vv}^u(\omega)d\omega \tag{4.43}$$

The relationship between the transfer functions for the directional and unidirectional wave systems is given by

$$H_{v\xi}(\omega) = H_{v\xi}^u(\omega)R(\omega); \quad H_{\dot{v}\xi}(\omega) = H_{\dot{v}\xi}^u(\omega)R(\omega) \tag{4.44}$$

It is obvious that the bias B_v and $B\dot{v}$ is generally dependent on spectrum of the water particle velocity and the spreading function. When the spreading function is approximated as frequency-independent function, the bias B_v and $B\dot{v}$ are identical and only dependent on the spreading function, and equals the frequency-independent coefficient R. For cosine spreading function, the reduction is approximately 10%, i.e. B_v is approximately 0.9, for relatively large spreading as given in the design guideline developed by American Gas Association (AGA, 1990).

Generally, in shallow water (less than 80 m) the principal direction of waves for extreme hurricane conditions will be approximately normal to the bathmetry. However, the principal direction of the near sea bottom currents is typical parallel to the bathymetry. Thus, the vectorial addition of water particle and current velocities should be used to take into account the lack of alignment between the principal direction of wave propagation and the near sea floor current direction relative to the pipeline axis (Bea et al., 1998a)
The design maximum horizontal current velocity (U_{cd}) relative to the design maximum water particle velocity (U_{wd}) near the sea bottom is defined as a ratio

$$\Psi = U_{cd}/U_{wd} \tag{4.45}$$

in which U_{wd} is given as

$$U_{wd} = g\sigma_{v^u}|_{\theta_0=90\ deg} = g\sqrt{\int_0^\infty \omega^2 \frac{S_{\xi\xi}^u(\omega)}{\sinh^2(kh)}d\omega} \tag{4.46}$$

and g is peak factor given as

$$g = \sqrt{2\ln N} + \frac{0.5772}{\sqrt{2\ln N}} \tag{4.47}$$

and for most probable maxima in 1000 wave cycles, g is 3.72.
It is assumed that the design of the pipeline has been based on the analysis that takes into account the orientation of the design water particle and current velocity relative to the pipeline axis. The current velocity and water particle velocity in the direction normal to the pipeline axis is given by

$$U_c = U_{cd}\cos\theta_0; \quad U_w = B_v U_{wd}\sin\theta_0 = g\sigma_v \tag{4.48}$$

Thus, the ratio between the current and the RMS water particle velocity normal to the pipeline axis is identified as

$$r = U_c/\sigma_v = g\Psi\cot\theta_0/B_v \tag{4.49}$$

For the unidirectional wave, it is

$$r_u = U_c/\sigma_{v^u} = g\Psi \cot\theta_0 \tag{4.50}$$

When the orientation of the current and water particle velocities relative to the pipeline axis is neglected

$$r_0 = gU_{cd}/U_{wd} = g\Psi \tag{4.51}$$

4.5.2 **Hydrodynamic Drag Force**

According to the Morison equation, the hydrodynamic drag force per unit length due to combined wave and current actions can be expressed as

$$f_D(x,t) = \frac{1}{2}\rho D C_D |U(x,t)| U(x,t) \tag{4.52}$$

in which ρ is the density of sea water; D is the diameter of the pipeline segment; C_D is the drag coefficient; and

$$U(x,t) = U_c + v(x,t) \tag{4.53}$$

in which U_c and $v(x,t)$ are current velocity and fluctuating water particle velocity components normal to the pipeline axis. The drag coefficient C_D is generally dependent on the Reynolds Number, Keulegan-Carpenter Number, the strength of currents relative to the wave velocities, the proximity of the pipeline to sea floor, and the roughness of the pipeline. In this study, emphasis will be placed only on the bias in hydrodynamic forces due to wave spreading, therefore, typical values of the drag coefficient will be used for simplification.

The term $U(x,t)$ in the hydrodynamic drag force is nonlinear. A statistical linearization of this term is required for pursuing spectral analysis, because it is based on a linear superposition over the frequencies described in the sea-state. Assuming that the water particle velocity is a stationary Gaussian process, the nonlinear drag forces can be linearized as (Kareem et al., 1995)

$$f_D(x,t) = \frac{1}{2}\rho D C_D[\alpha_0\sigma_v^2 + \alpha_1\sigma_v v(x,t)] \tag{4.54}$$

in which

$$\alpha_0 = 2(r^2 b_1 + r b_2 + b_1); \qquad \alpha_1 = 4(r b_1 + b_2) \tag{4.55}$$

and

$$b_1 = \frac{1}{\sqrt{2\pi}}\int_0^r exp(-\frac{y^2}{2})dy; \quad b_2 = \frac{1}{\sqrt{2\pi}}exp(-\frac{r^2}{2}); \quad r = \frac{U_c}{\sigma_v} \tag{4.56}$$

If the current velocity component normal to the pipeline axis is zero, i.e. $r=0$, yields $\alpha_0=0$ and $\alpha_1 = \sqrt{8/\pi}$.

The total drag force $F_D(t)$ on the pipeline segment of length L is given by

$$F_D(t) = \int_0^L f_D(x,t)dx \tag{4.57}$$

The mean value of total drag force is

$$\bar{F}_D = \frac{1}{2}\rho D C_D \alpha_0 \sigma_v^2 L \tag{4.58}$$

The power spectral density of total drag force, $S_{FD}(\omega)$, is expressed as

$$S_{F_D}(\omega) = (\frac{1}{2}\rho D C_D \alpha_1 \sigma_v L)^2 \int_0^\infty S_{vv}(\omega) J^2(\omega) d\omega \tag{4.59}$$

in which the J(ω) is the joint acceptance function and takes the form

$$J^2(\omega) = \frac{1}{L^2}\int_0^L \int_0^L coh(\Delta x, \omega) dx_1 dx_2$$

$$= \frac{2}{(kL)^2} \frac{\int_{-\pi}^{\pi} D(\omega,\theta)\tan^2\theta[1-\cos(kL\cos\theta)]d\theta}{\int_{-\pi}^{\pi} D(\omega,\theta)\sin^2\theta d\theta} \tag{4.60}$$

The joint acceptance function describes the hydrodynamic force reduction due to a lack of spatial correlation of water particle velocity. It can be readily confirmed that when the dimensionless length kL approaches zero, the joint acceptance function concomitantly reaches unity. When the spreading function is approximated as a frequency-independent function, the joint acceptance function is only a function of the dimensionless length kL.

Defining the bias (B_{vc}) in wave particle velocity due to spatial correlation for the spreading wave as

$$B_{vc}^2 = \int_0^\infty S_{vv}(\omega) J^2(\omega) d\omega / \int_0^\infty S_{vv}(\omega) d\omega \tag{4.61}$$

The RMS value of total force is then given as

$$F_{Drms} = \frac{1}{2}\rho D C_D \alpha_1 \sigma_v^2 B_{vc} L \tag{4.62}$$

The maximum value of the total drag force for the combined current and directional wave actions can be expressed as

$$F_{Dmax} = \bar{F}_D + gF_{Drms} = \frac{1}{2}\rho D C_D \sigma_v^2 L(\alpha_0 + g\alpha_1 B_{vc}) \tag{4.63}$$

Similarly, for the unidirectional wave system, and neglecting the spatial correlation of water particle velocities, the maximum drag force is given by

$$F_{Dmax}^u = \bar{F}_D^u + gF_{Drms}^u = \frac{1}{2}\rho D C_D \sigma_{vu}^2 L(\alpha_{0u} + g\alpha_{1u}) \tag{4.64}$$

in which α_{0u} and α_{1u} are given in Eq. 4.55 with r_u substituted for r.
The bias in the drag force between the directional and unidirectional system is

$$B_{F_D}^u = F_{Dmax}/F_{Dmax}^u = B_v^2 \frac{\alpha_0 + g\alpha_1 B_{vc}}{\alpha_{0u} + g\alpha_{1u}} \tag{4.65}$$

It is noted that the bias B_v also affects the linearization coefficients α_0 and α_1 , which in turn influences the bias in the drag force. When the steady current component is zero, it yields

$$B_{FD}{}^u = B_v{}^2 B_{vc} \tag{4.66}$$

Thus, the bias in the drag force can be separated into a component due to the overall reduction of energy and a component due to the spatio-temporal correlation of water particle velocity explicitly. It was specified by IMP that the analysis of hydrodynamic loadings for design of pipelines should be

based on the assumption that the currents are aligned with the waves and that these currents and wave kinematics are normal to the axis of the pipeline. In this design approach, the bias due to the orientation of design wave kinematics and current relative to the pipeline axis should be further included.
The design maximum drag force is given as

$$F_{Dmax}^{0} = \bar{F}_{D}^{0} + gF_{Drms}^{0} = \frac{1}{2}\rho D C_D \sigma_{v0}^{2}(\alpha_{00} + g\alpha_{10})L \tag{4.67}$$

in which α_{00} and α_{10} are given in Eq. 4.55 with r_0 substituted for r; and

$$\sigma_{v0}^{2} = \int_{0}^{\infty} \omega^2 \frac{S_{\xi\xi}^{u}(\omega)}{\sinh^2(kh)} d\omega = \sigma_{v^u}^{2} / \sin^2\theta_0 \tag{4.68}$$

Thus, the bias in the drag force is

$$B_{F_D}^{0} = F_{Dmax}/F_{Dmax}^{0} = B_v^2 \sin^2\theta_0 \frac{\alpha_0 + g\alpha_1 B_{vc}}{\alpha_{00} + g\alpha_{10}} \tag{4.69}$$

If the current is zero, it yields

$$B_{F_D}^{0} = B_v^2 B_{vc} \sin^2\theta_0 \tag{4.70}$$

4.5.3 **Hydrodynamic Inertial Force**

According to Morison equation, the hydrodynamic inertia force per unit length due to combined wave and current actions can be expressed as

$$f_I(x,t) = \frac{\pi}{4}\rho D^2 C_M \dot{v}(x,t) \tag{4.71}$$

in which C_M is the inertia force coefficient; and $\dot{v}(x,t)$ is the water particle acceleration normal to the pipeline axis.
The maximum inertia force is given by

$$F_{Imax} = gF_{Irms} = \frac{\pi}{4}\rho D^2 C_M \sigma_{\dot{v}} B_{\dot{v}c} g \tag{4.72}$$

in which $B_{\dot{v}c}$ is defined as the bias in the water particle acceleration due to spatial correlation of the directionally spreading wave

$$B_{\dot{v}c}^{2} = \int_{0}^{\infty} S_{\dot{v}\dot{v}}(\omega) J^2(\omega) d\omega / \int_{0}^{\infty} S_{\dot{v}\dot{v}}(\omega) d\omega \tag{4.73}$$

For the unidirectional wave system in which the spatial correlation of the water particle acceleration is generally neglected, it yields

$$F_{Imax}^{u} = gF_{Irms}^{u} = \frac{\pi}{4}\rho D^2 C_M \sigma_{\dot{v}^u} g \tag{4.74}$$

The bias in design inertia force between the directional and unidirectional wave systems is given by

$$B_{F_I}^{u} = F_{Imax}/F_{Imax}^{u} = B_{\dot{v}} B_{\dot{v}c} \tag{4.75}$$

If the orientation of the water particle acceleration relative to the pipeline axis has not been included in the design approach, the bias due to the orientation should be further included as

$$B_{F_i}^0 = B_{\dot{v}} B_{\dot{v}c} \sin\theta_0 \tag{4.76}$$

4.6 Numerical Results and Analysis

An example is presented to delineate the influence of different sea states characterized by water depths, significant wave heights, directional spreading features and current velocities on the pipeline loads. These are summarized in Table 4.1.

Table 4.1 Calculating conditions

Sea type	Type 1	Type 2	Type 3
Water depth h (m)	10-15	40-50	100
Significant wave height H_s (m)	6	8	9
Wave elevation spectrum	P-M	P-M	P-M
Current velocity U_{cd} (m/s)	0-1.05	0-7.0	0-0.35
Mean wave direction θ_0 (deg)	0-90	0-90	0-90
Length of pipeline segment L (m)	0-1000	0-1000	0-1000

The frequency dependent Donelan type spreading function and frequency-independent normally distributed spreading function are used to describe the wave spreading features. For the latter, two different values of the σ_D are assumed to be 30 deg and 40 deg for the sake of comparison. The Pierson-Moskowitz spectrum is used in this study. The mean direction of wave propagation relative to the axis of a pipeline segment (θ_0) is assumed to vary between 0 and 90 degrees. The length of the pipeline segment (L) is assumed to vary between 0 and 1000 m. The sea surface elevation spectra for different sea conditions are shown in Fig . 4.2.

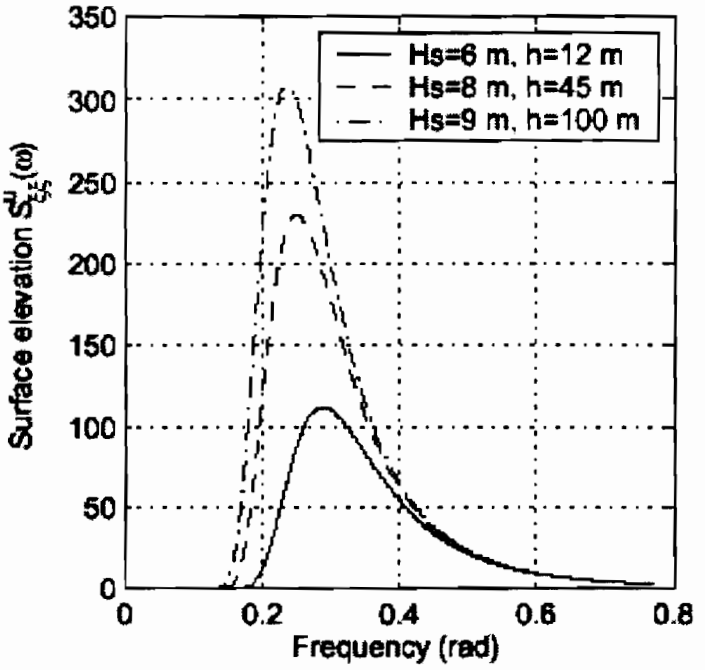

Fig. 4.2 Sea surface elevation spectra

Figure 4.3a demonstrates the frequency dependent Donelan type directional spreading function for θ_0= 90 deg and ω/ω_p=0.9, 1.0 and 1.1. Figure 4.3b shows the frequency-independent normally distributed spreading function for θ_0=90 deg, and σ_D=30 deg and 40 deg.

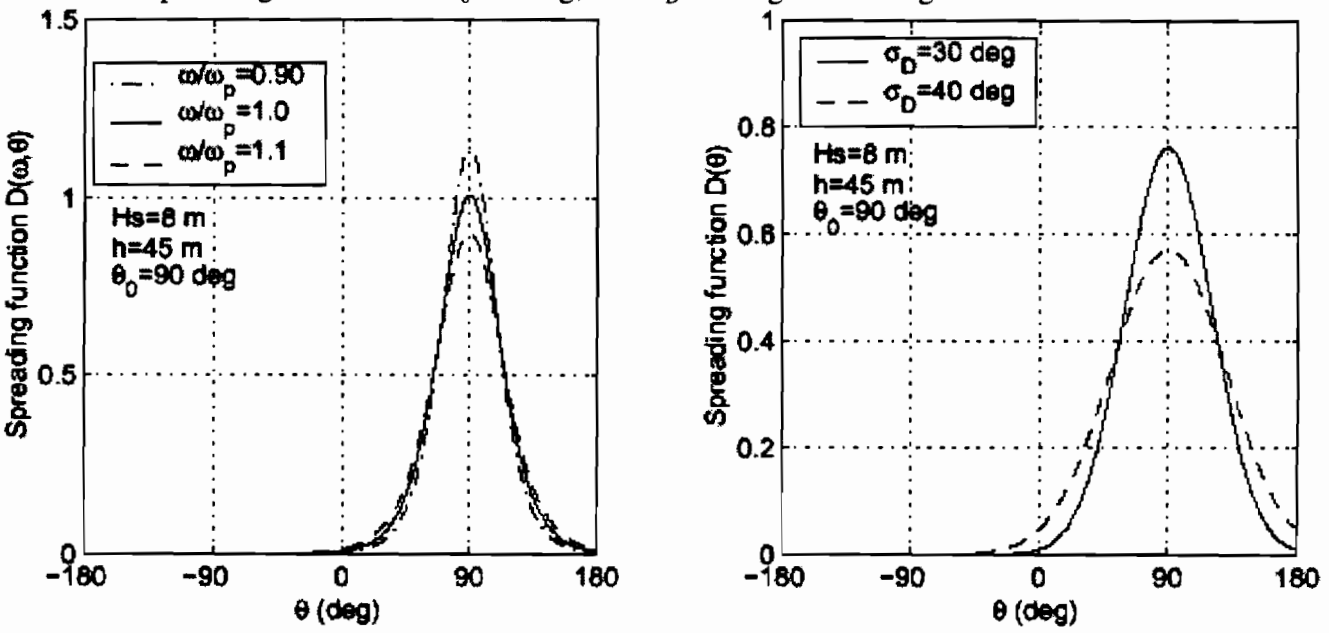

a) Frequency dependent, θ_0=90 deg

b) Frequency independent, θ_0=90 deg

Fig. 4.3 Directional wave spreading function

The power spectra of water particle velocity components normal to the pipeline segment in unidirectional and directional wave systems at different mean directions of wave propagation are shown in Figs. 4.4 and 4.5. The RMS water particle velocities and accelerations are presented in Figs. 4.6 and 4.7. The near bottom water particle kinematics decrease with the increase in the water depth. For the unidirectional wave system, the variation in the water particle kinematics corresponding to the changes in the mean wave direction follow the sine law. For the directional wave system, due to the directional spreading of energy, the loss of energy is identified, when the mean wave direction is close to the direction normal to the pipeline segment (θ_0=90 deg). On the contrary, the increase in energy in comparison with unidirectional case is significant when the mean wave direction nears the pipeline axis (θ_0=0 deg).

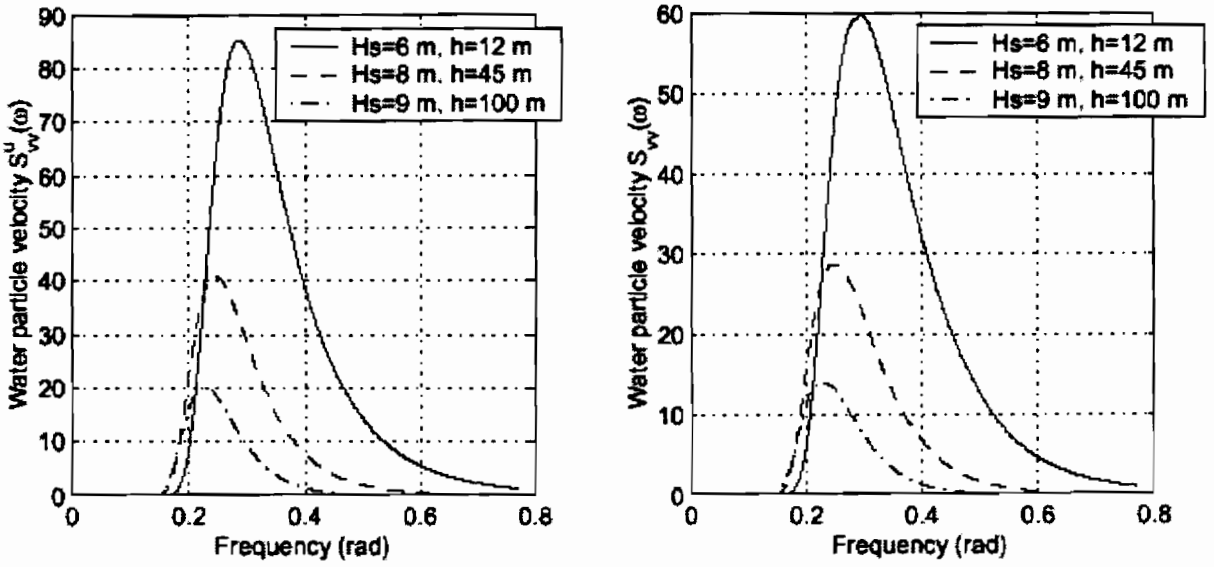

a) Unidirectional wave, θ_0=90 deg b) Directional wave, θ_0=90 deg

Fig. 4.4 Wave particle velocity spectra

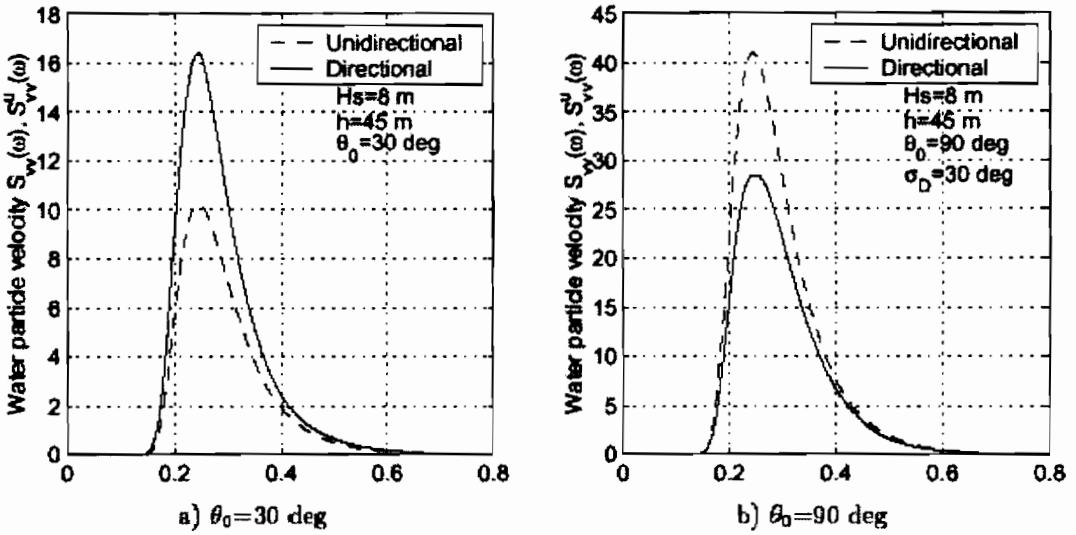

a) θ_0=30 deg b) θ_0=90 deg

Fig. 4.5 Comparison of water particle velocity spectra between unidirectional wave and directional spreading wave

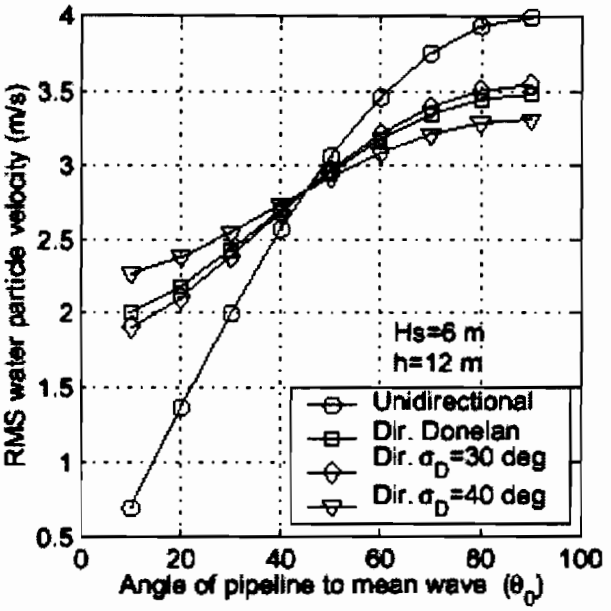

a) H_s=6 m, h=12 m

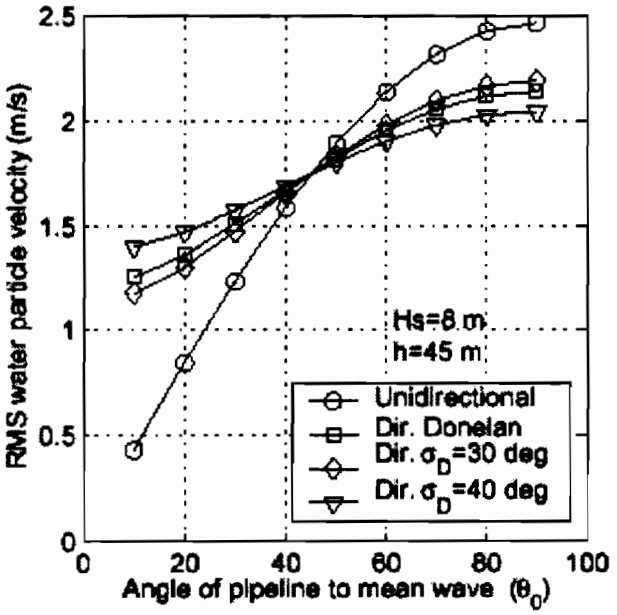

b) H_s=8 m, h=45 m

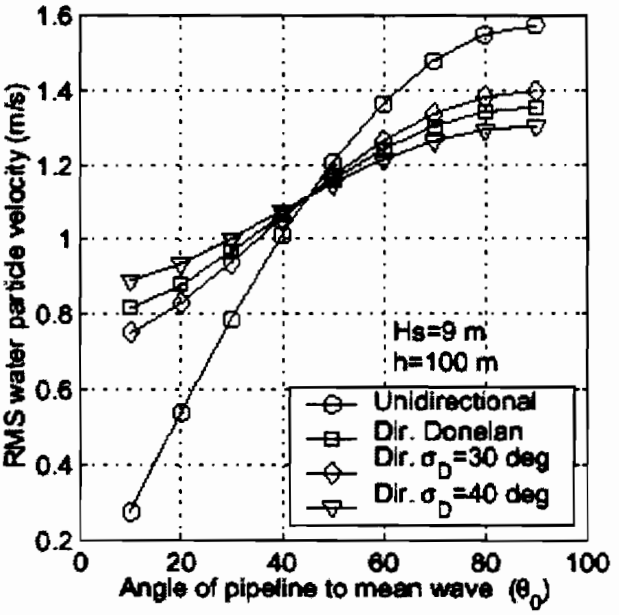

c) H_s=9 m, h=100 m

Fig. 4.6 RMS values of water particle velocities

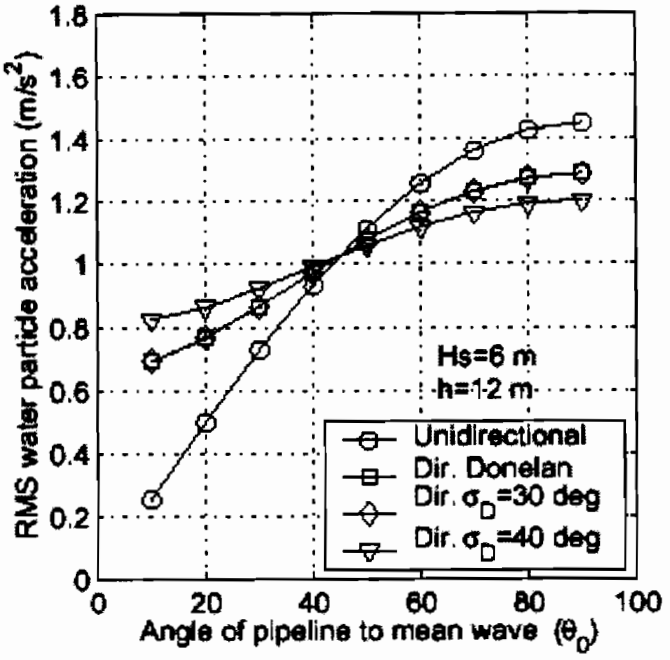

a) H_s=6 m, h=12 m

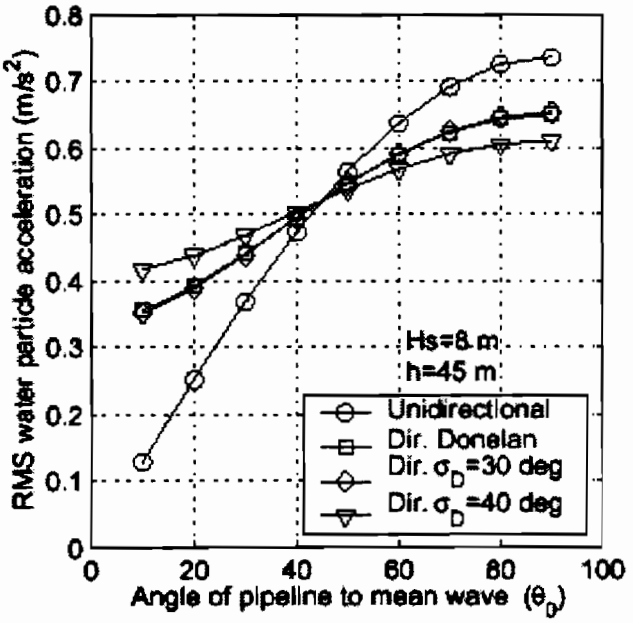

b) H_s=8 m, h=45 m

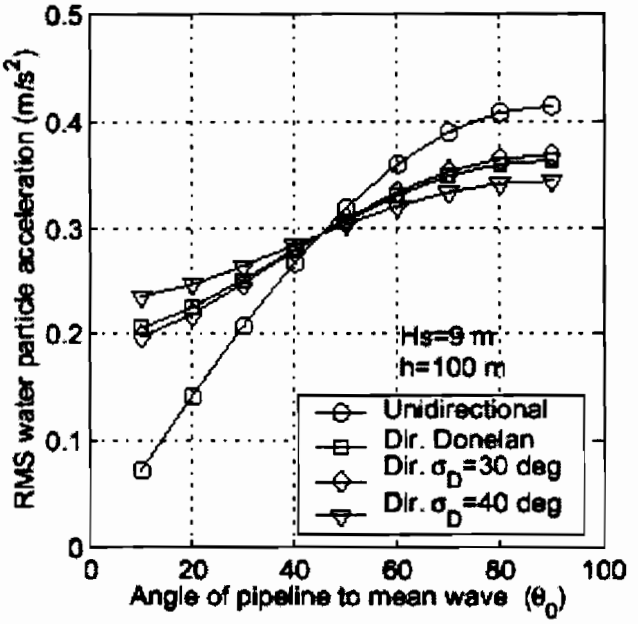

c) H_s=9 m, h=100 m

Fig. 4.7 RMS values of water particle accelerations

Figures 4.8 and 4.9 show the bias in the water particle velocity and acceleration normal to the pipeline axis due to wave spreading (Eqs. 4.42 and 4.43). $B_v \sin\theta_0$ and $B_{\dot{v}} \sin\theta_0$ represent the ratios of water particle kinematics relative to the maximum derived from the unidirectional wave, thus they always have a value less than unity. For the frequency-independent spreading functions, the bias in the water particle velocity and acceleration B_v and $B_{\dot{v}}$ are identical, and only dependent on the spreading function used. Results indicate that even using the frequency dependent spreading

function, due to the narrow-banded property of the random water particle kinematics, B_v and $B_{\dot{v}}$ are very close and can be assumed to be the same. It is noted that the bias in the water particle velocity, $B_v \sin\theta_0$, is between 0.45 to 0.9 depending on the spreading function and the orientation of the pipeline segment. Accordingly, the bias in the maximum water particle velocity is between 0.8 to 0.9 depending on the spreading function. Water depth and wave height have insignificant influence on these biases since these biases are strongly influenced by the spreading function. It is emphasized that the bias in the water particle kinematics is significantly dependent on the orientation of the pipeline segment.

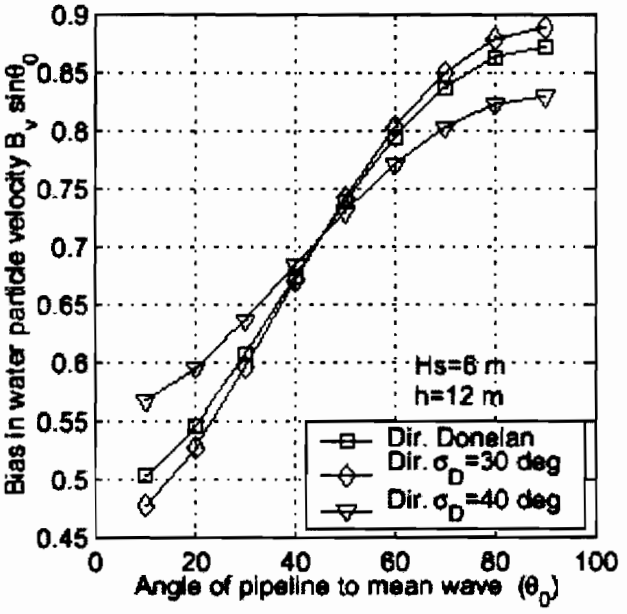

a) H_s=6 m, h=12 m

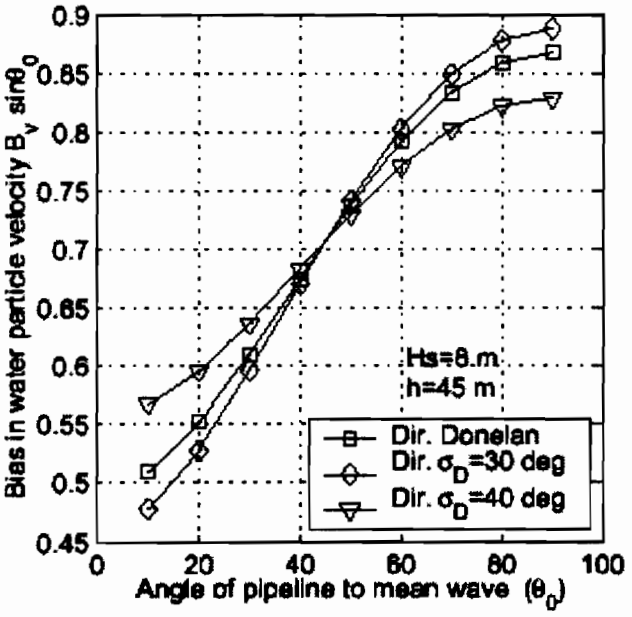

b) H_s=8 m, h=45 m

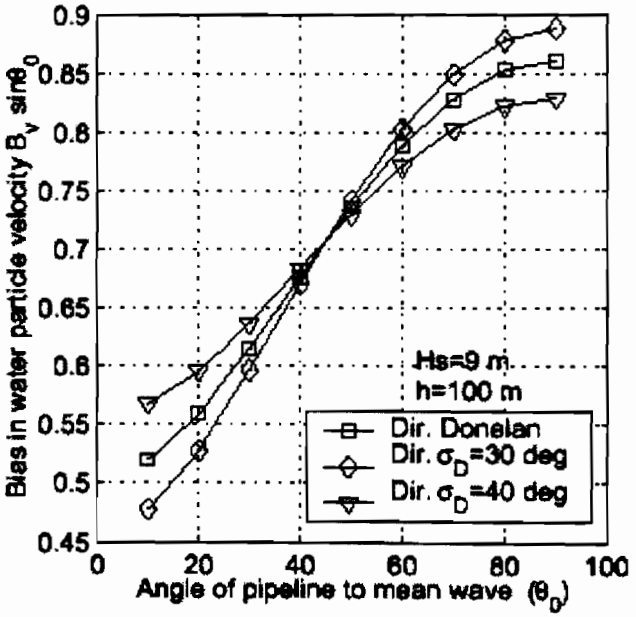

c) H_s=9 m, h=100 m

Fig. 4.8 Bias in water particle velocity due to wave spreading

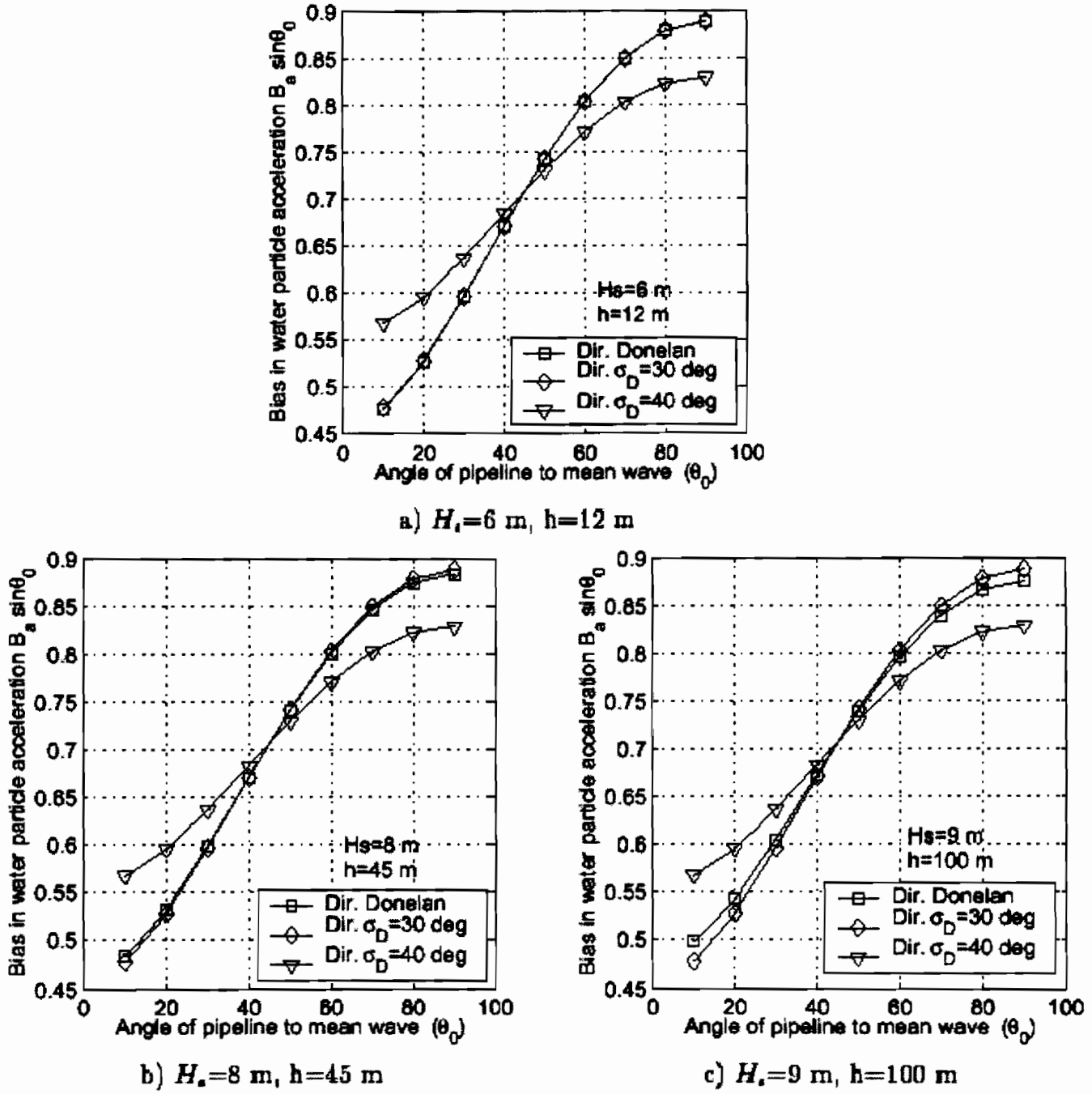

a) H_s=6 m, h=12 m

b) H_s=8 m, h=45 m

c) H_s=9 m, h=100 m

Fig. 4.9 Bias in water particle acceleration due to wave spreading

Figure 4.10 shows the coherence function of the water particle velocity for a range of separation distances (Eqs. 4.33 and 4.38). In general, the coherence function has a spatial periodicity and decays with an increase in the separation distance between the points of interest. For a directional wave system, the coherence function is in general a function of the dimensionless separation distance, pipeline orientation and the frequency. When the spreading function is assumed to be frequency-independent, the coherence becomes a function of only the dimensionless separation distance and orientation. This feature in the coherence model for the wave loads separates it from the generally used coherence models for wind and seismic load effects.

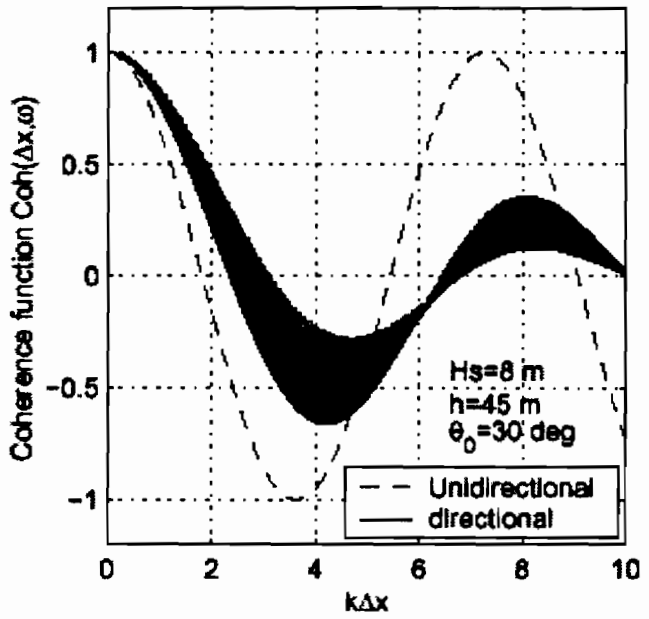

a) H_s=8 m, h=45 m, θ_0=30 deg, frequency dependent spreading function

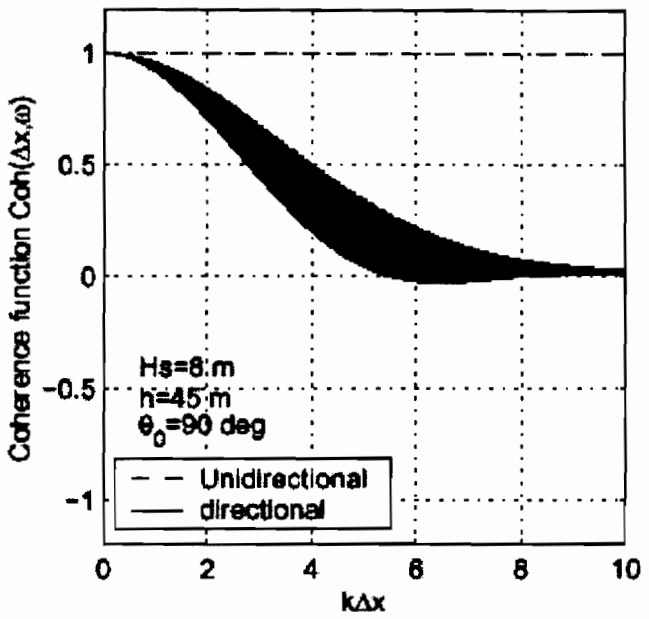

b) H_s=8 m, h=45 m, θ_0=90 deg, frequency dependent spreading function

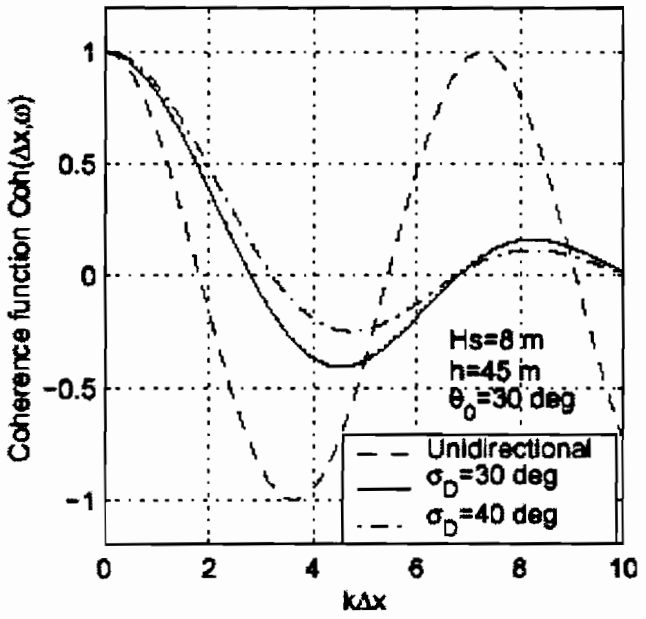

c) H_s=8 m, h=45 m, θ_0=30 deg, frequency independent spreading function

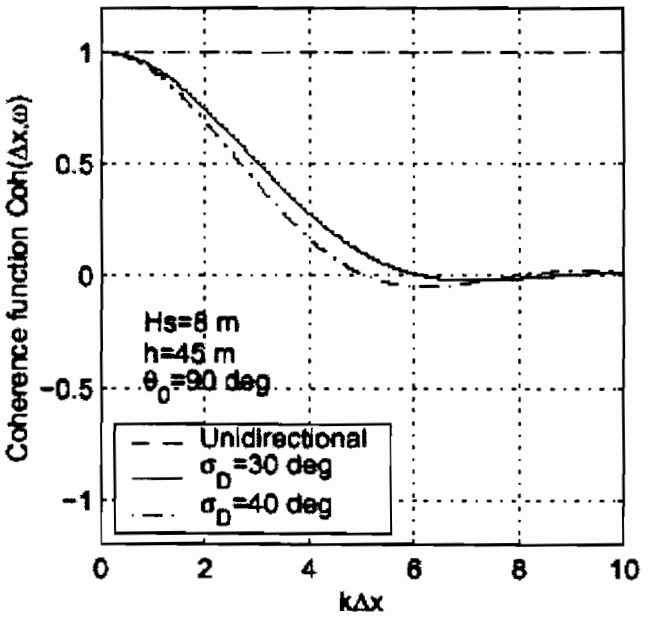

d) H_s=8 m, h=45 m, θ_0=90 deg, frequency independent spreading function

Fig. 4.10 Coherence functions of unidirectional and directional water particle velocities

Figures 4.11 and 4.12 show the joint acceptance functions for pipeline segments as a function of the dimensionless lengths and segment lengths, respectively (Eq. 4.60).

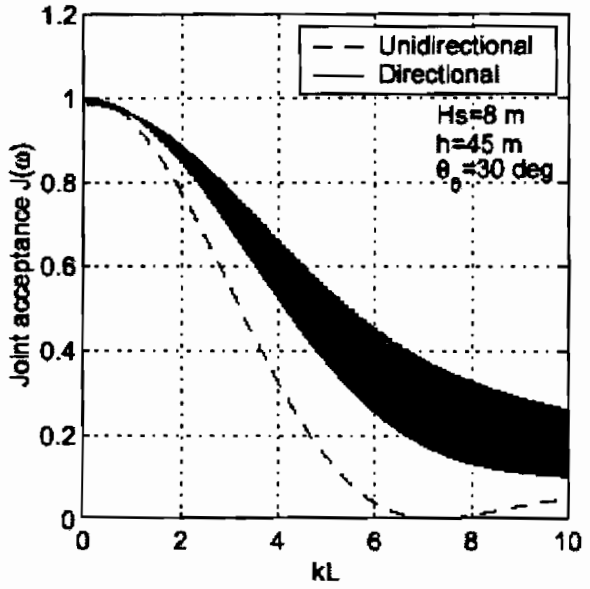

a) H_s=8 m, h=45 m, θ_0=30 deg, frequency dependent spreading function

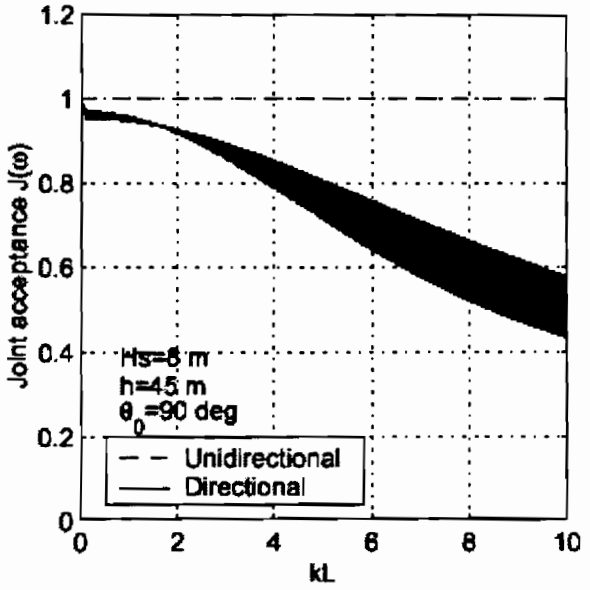

b) H_s=8 m, h=45 m, θ_0=90 deg, frequency dependent spreading function

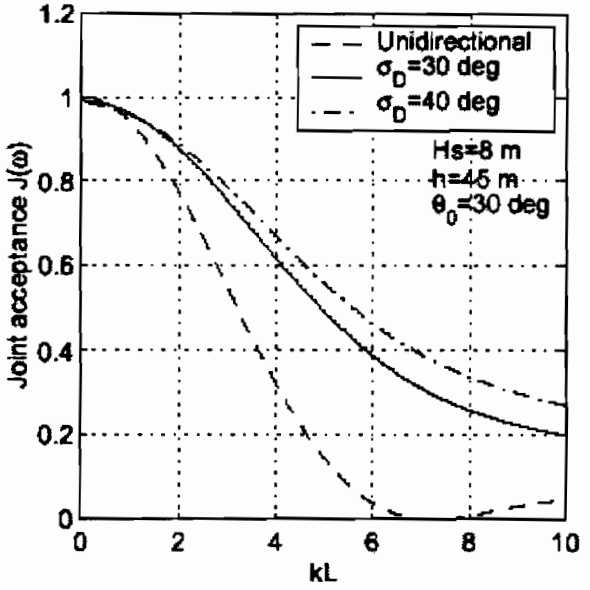

c) H_s=8 m, h=45 m, θ_0=30 deg, frequency independent spreading function

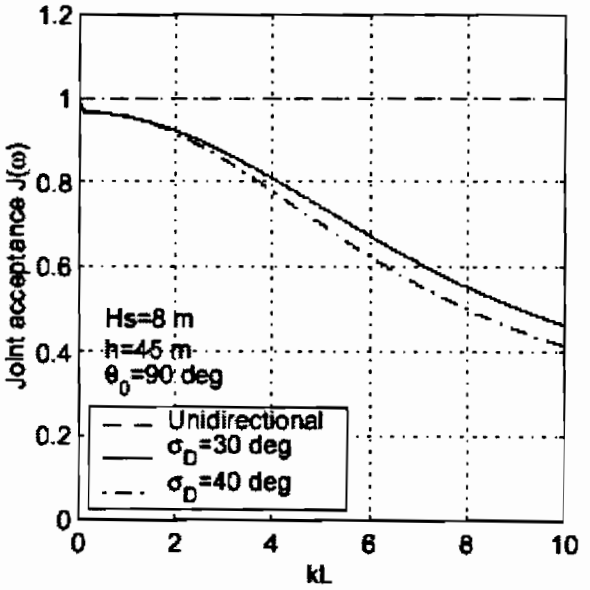

d) H_s=8 m, h=45 m, θ_0=90 deg, frequency independent spreading function

Fig. 4.11 Joint acceptance functions of unidirectional and directional water particle velocities

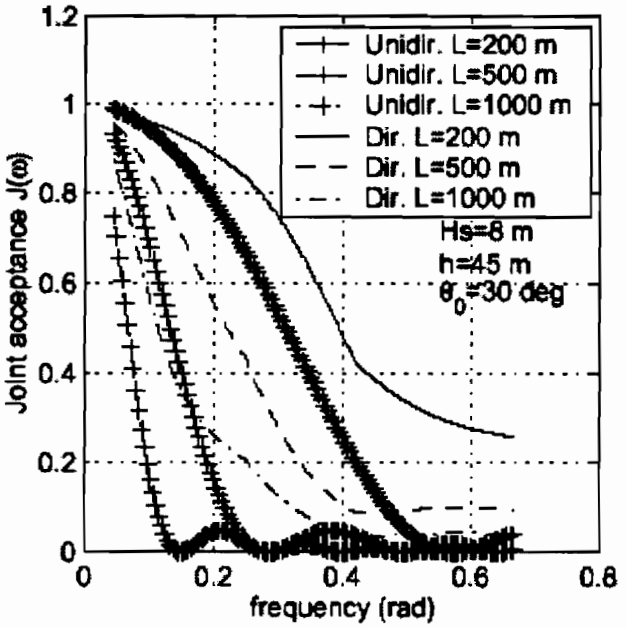

a) H_s=8 m, h=45 m, θ_0=30 deg, frequency dependent spreading function

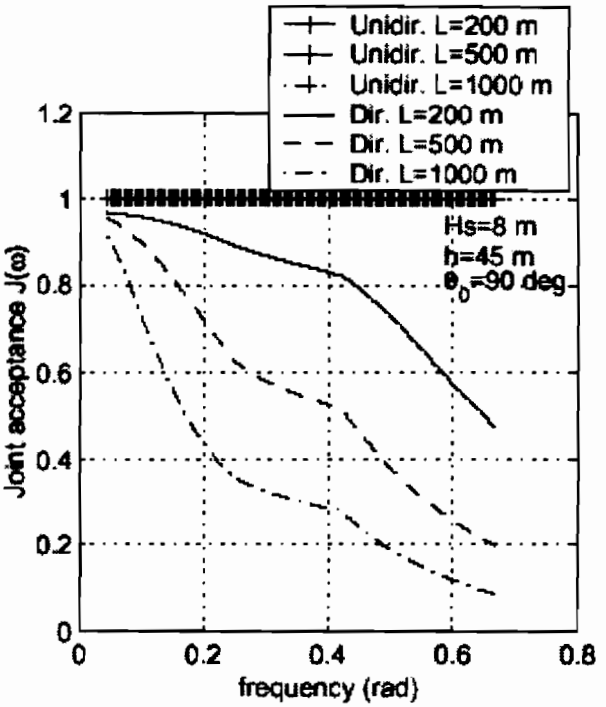

b) H_s=8 m, h=45 m, θ_0=90 deg, frequency dependent spreading function

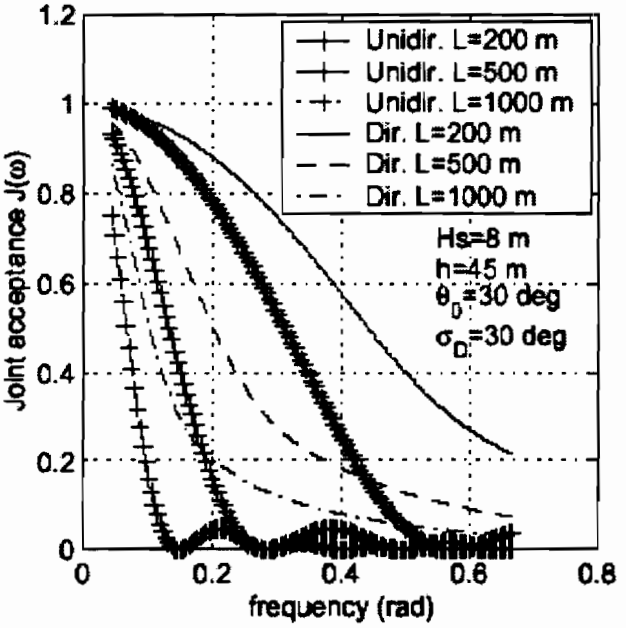

c) H_s=8 m, h=45 m, θ_0=30 deg, frequency independent spreading function, σ_D=30 deg

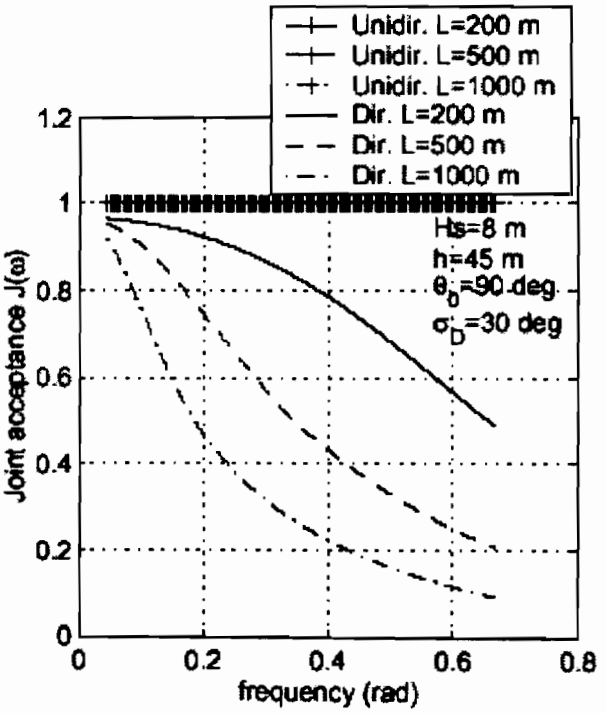

d) H_s=8 m, h=45 m, θ_0=90 deg, frequency independent spreading function, σ_D=30 deg

Fig. 4.12 Joint acceptance functions for pipeline segments with different lengths

Figures 4.13 and 4.14 indicate the bias, $B_{vc,}$ in water particle velocity due to spatio-temporal correlation for unidirectional and directional wave systems, respectively (Eq. 4.61). This bias also represents the bias in the hydrodynamic drag component without the current action, and the bias in the inertial force, due to the spatio-temporal correlation. It is noted that the effect of spatio-temporal correlation is highly influenced by the orientation and the wave environment (water depth and wave height, etc.).

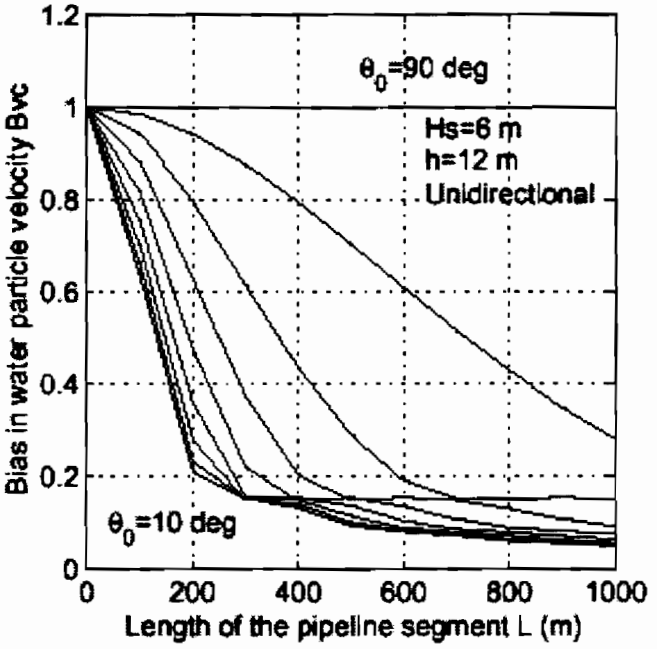

a) H_s=6 m, h=12 m, θ_0=10 - 90 deg

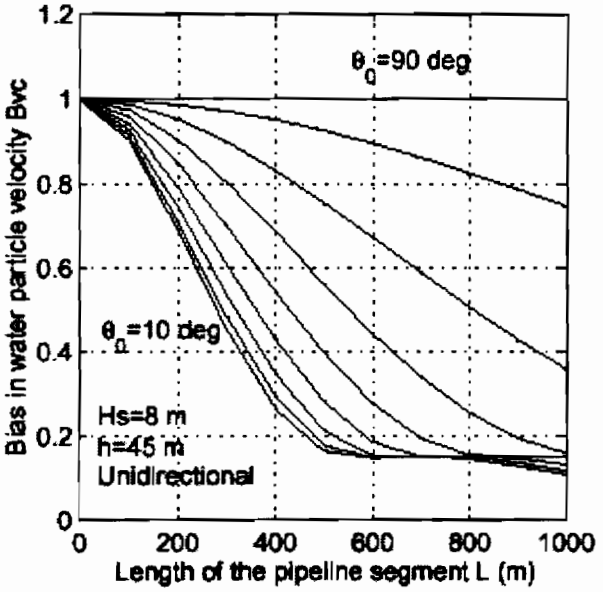

b) H_s=8 m, h=45 m, θ_0=10 - 90 deg

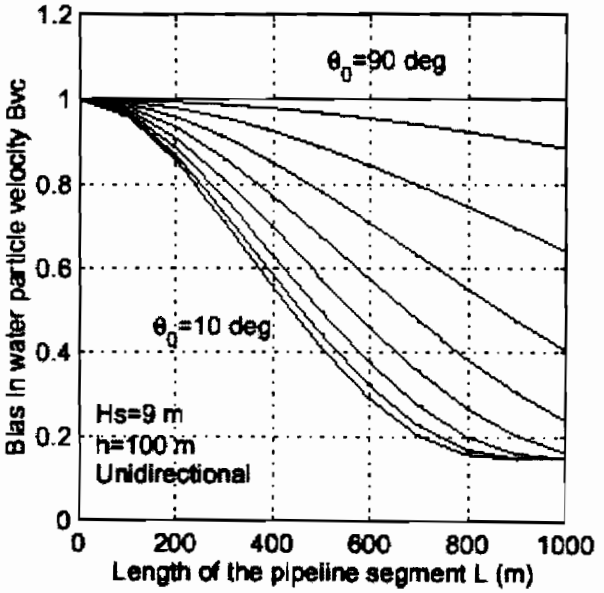

c) H_s=9 m, h=100 m, θ_0=10 - 90 deg

Fig. 4.13 Bias in water particle velocity due to spatio-temporal correlation for unidirectional wave system

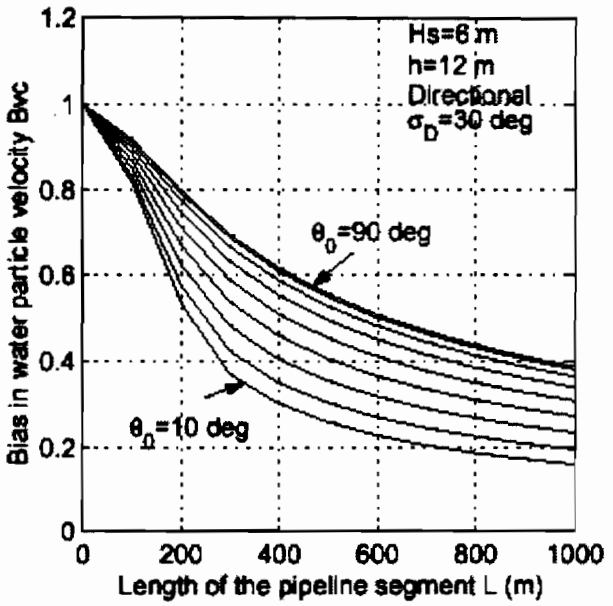

a) H_s=6 m, h=12 m, θ_0=10 - 90 deg

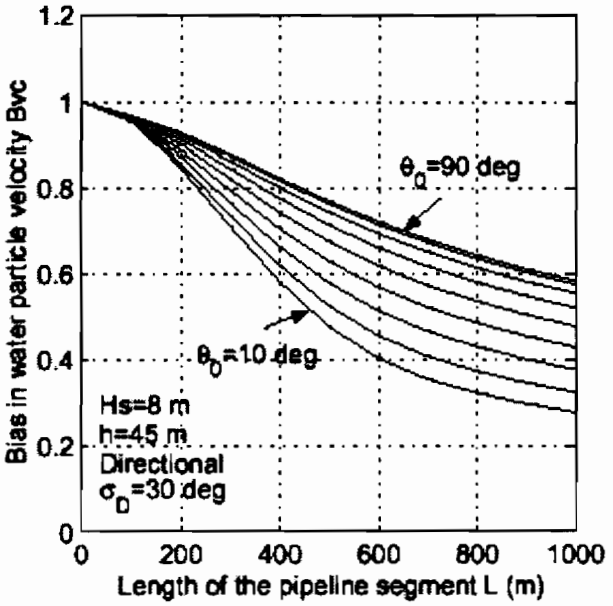

b) H_s=8 m, h=45 m, θ_0=10 - 90 deg

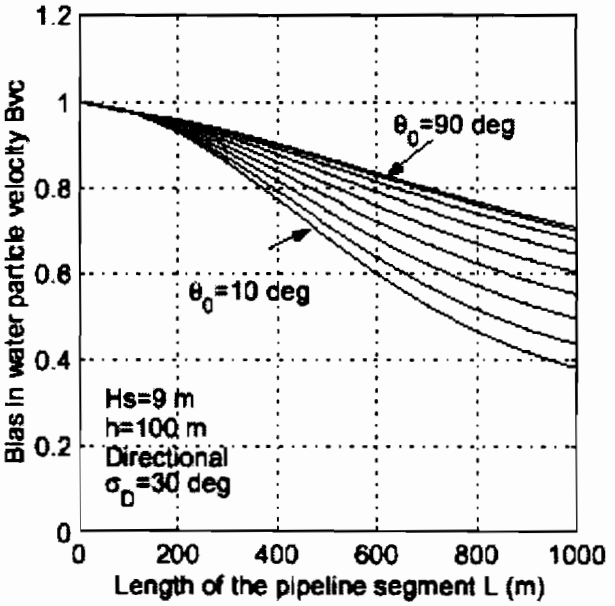

c) H_s=9 m, h=100 m, θ_0=10 - 90 deg

Fig. 4.14 Bias in water particle velocity due to spatial-temporal correlation for directional wave system (frequency independent spreading function, σ_D=30 deg)

Figure 4.15 shows their comparison with different spreading function models. Almost identical results have been obtained for different spreading models assumed in this study. Figures 4.16 and 4.17 demonstrate that the bias in the water particle acceleration is almost the same as in the velocity component. The bias in the hydrodynamic forces under the combined action of currents and waves exhibits dependence on the ratio of the steady current to the fluctuating water particle velocity. In this study, for the sake of illustration, the effects of the ratio between currents and water particle velocities on the force coefficients have been neglected, since the emphasis is only placed on the directional wave spreading effects. In Fig. 4.18, the ratios between the current velocities and the RMS water particle velocities normal to the axis of the pipeline segment for unidirectional (Eq.

4.50) and directional spreading waves (Eq. 4.49) are presented. Figure 4.19 shows the statistical linearization coefficients α_0 and α_1 associated with the mean and fluctuating components of the drag force as functions of the ratio between the current velocity and the RMS water particle velocity.

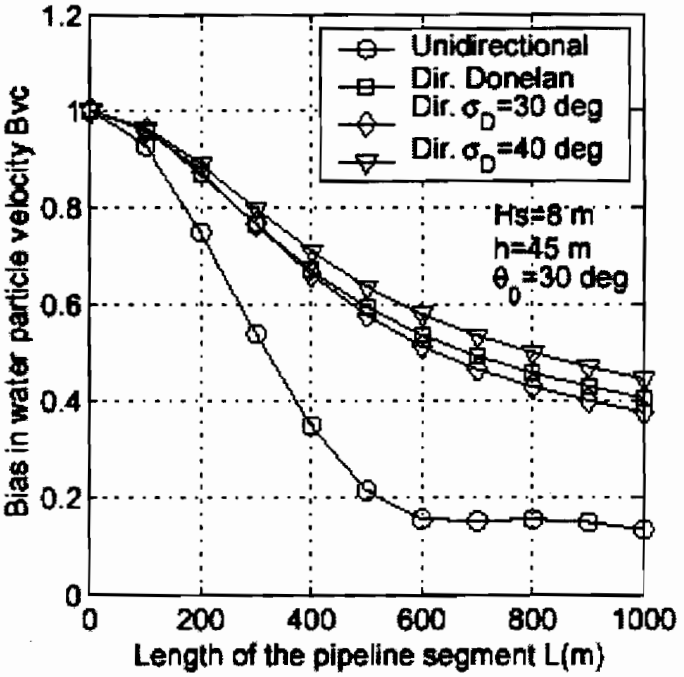

a) H_s=8 m, h=45 m, θ_0=30 deg

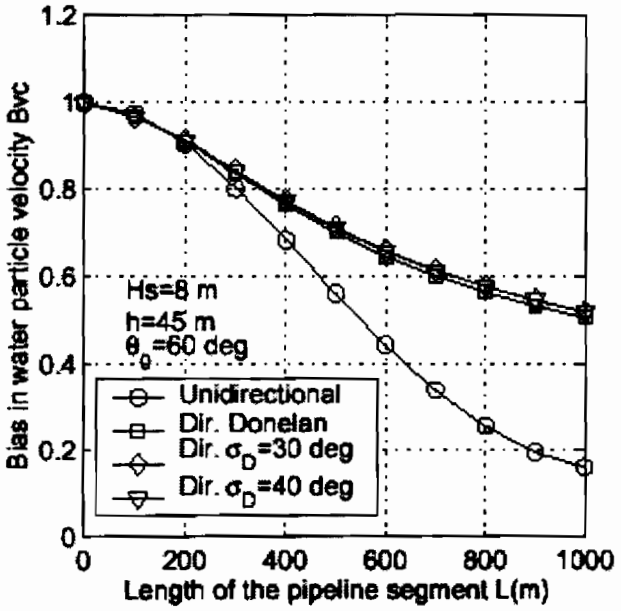

b) H_s=8 m, h=45 m, θ_0=60 deg

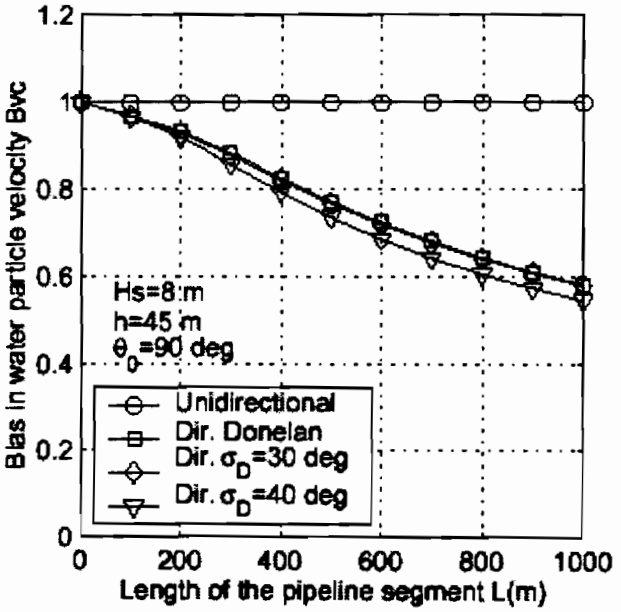

c) H_s=8 m, h=45 m, θ_0=90 deg

Fig. 4.15 Comparison of bias in water particle velocity due to spatio-temporal correlation for unidirectional and directional waves with different spreading functions

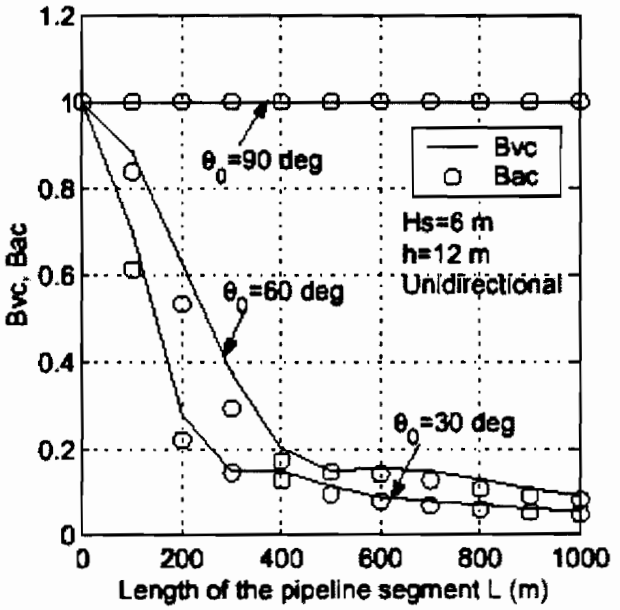

a) H_s=6 m, h=12 m

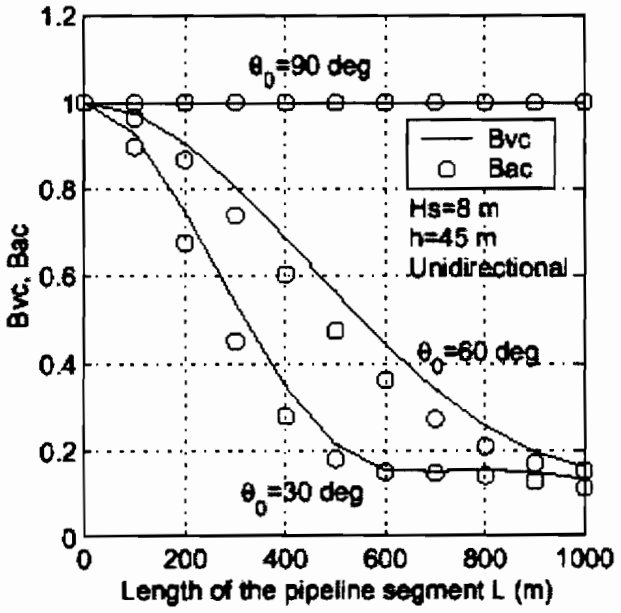

b) H_s=8 m, h=45 m

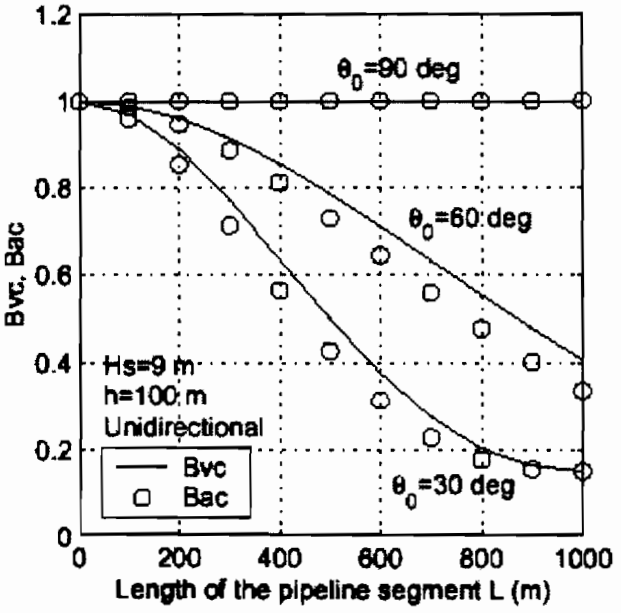

c) H_s=9 m, h=100 m

Fig. 4.16 Comparison of bias in water particle velocity and acceleration due to spatio-temporal correlation (Unidirectional wave system)

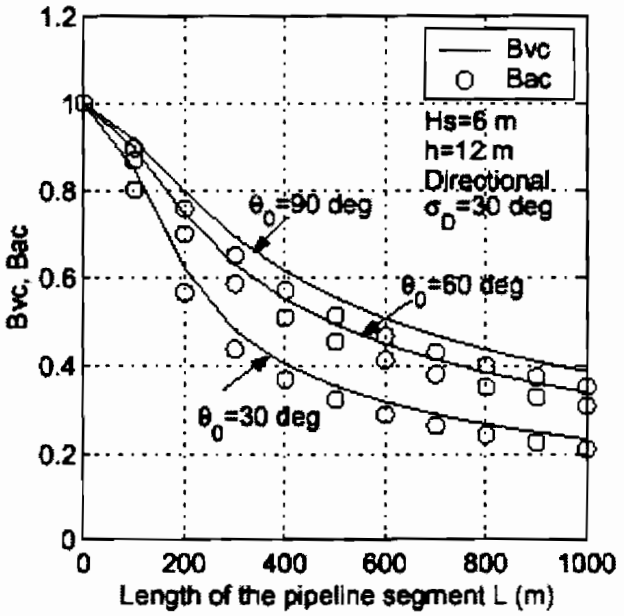

a) H_s=6 m, h=12 m

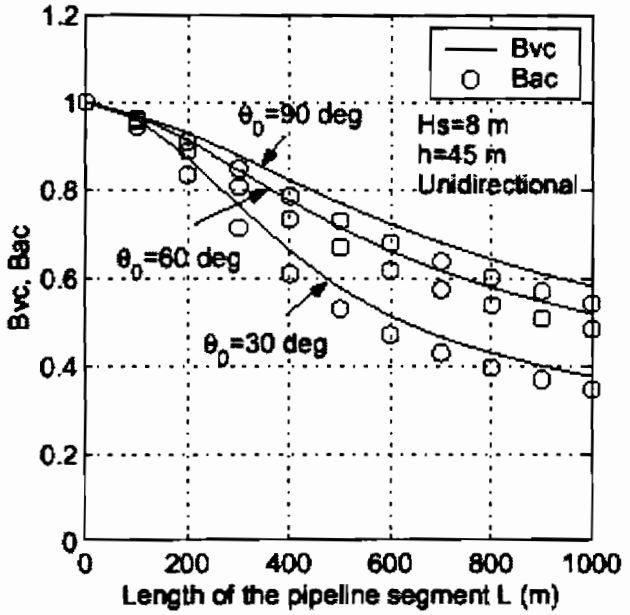

b) H_s=8 m, h=45 m

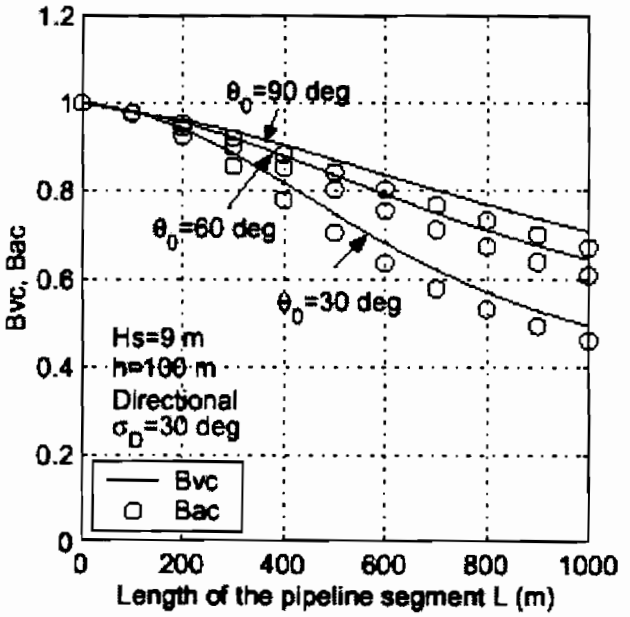

c) H_s=9 m, h=100 m

Fig. 4.17 Comparison of bias in water particle velocity and acceleration due to spatial-temporal correlation (Directional wave system, σ_D=30 deg)

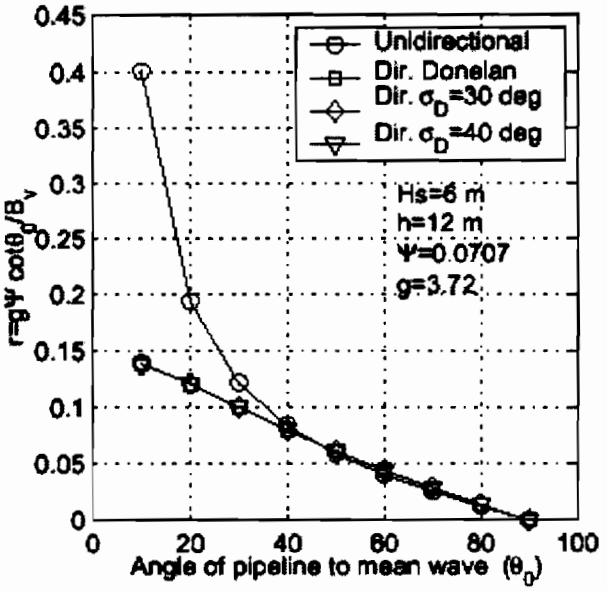

a) H_s=6 m, h=12 m, Ψ=0.0707

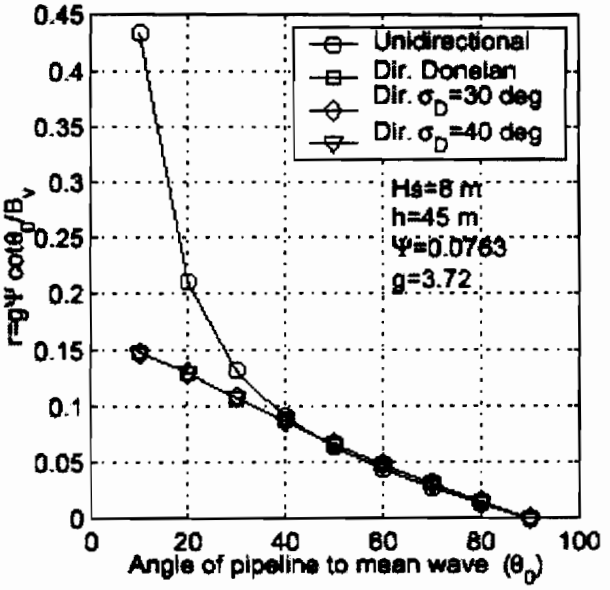

b) H_s=8 m, h=45 m, Ψ=0.0763

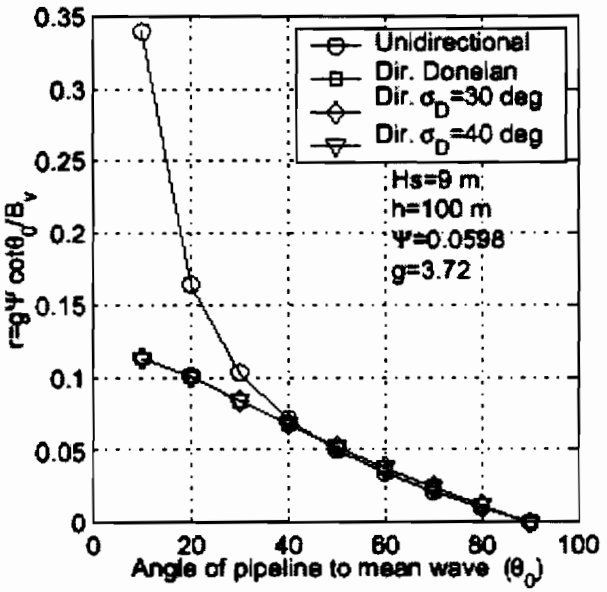

c) H_s=9 m, h=100 m, Ψ=0.0598

Fig. 4.18 Ratios between the current and RMS water particle velocities

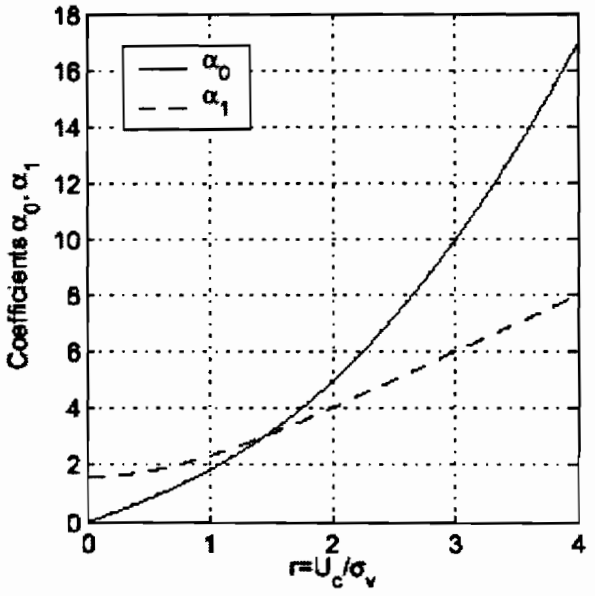

Fig. 4.19 Linearization coefficients α_0 and α_1 of nonlinear drag force component

Figures 4.20 and 4.21 show the bias, $B_{FD}{}^{u}$ and $B_{FD}{}^{0}$, in the drag forces (Eqs. 4.66 and 4.76) computed by using the components of the water particle kinematics and current velocity normal to the pipeline axis, or by employing simply their amplitudes regardless of direction, respectively. In Fig. 4.22, the results similar to Fig. 4.21 without currents are presented. In Fig. 4.23, the bias in the inertial force component is shown. Since the inertial forces do not dependent on the current velocity, therefore, the bias without currents is the same as with the currents. It is noted that the biases in the hydrodynamic drag and inertia forces are strongly dependent on the wave environment, orientation and the length

of the pipeline segments. Figure 4.24 presents the influence of the ratio between the design current and the water particle velocity on the bias in the drag forces. The ratio between the components of the current velocity and water particle velocity normal to the pipeline axis is affected by the pipeline orientation. This is reflected in the bias in the wave forces through the changes in the mean and fluctuating components of the hydrodynamic forces.

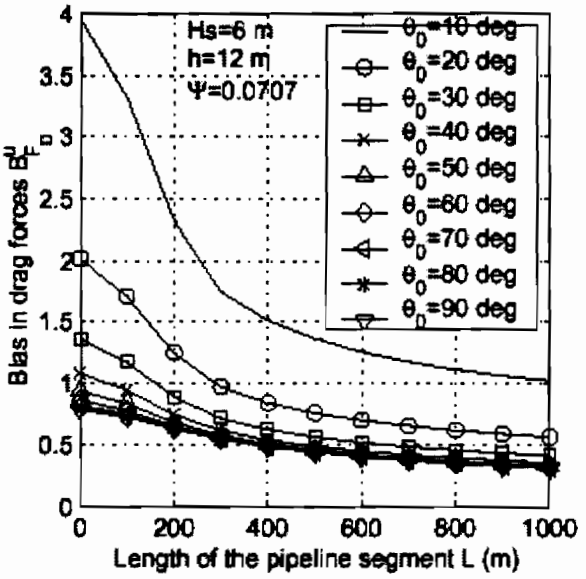

a) H_s=6 m, h=12 m, Ψ=0.0707

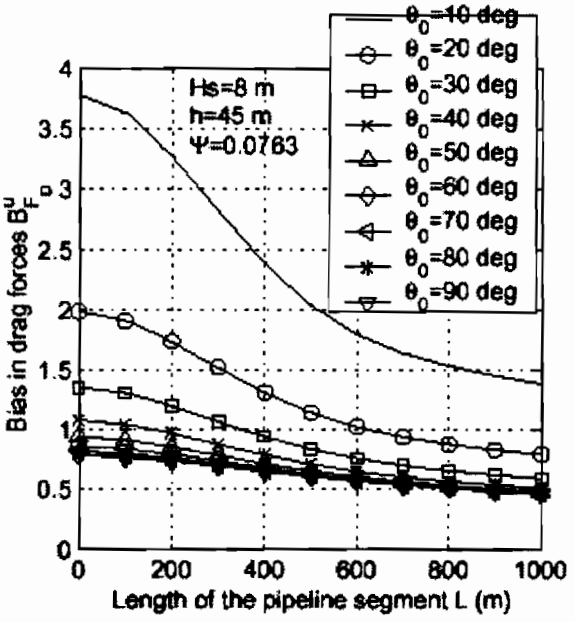

b) H_s=8 m, h=45 m, Ψ=0.0763

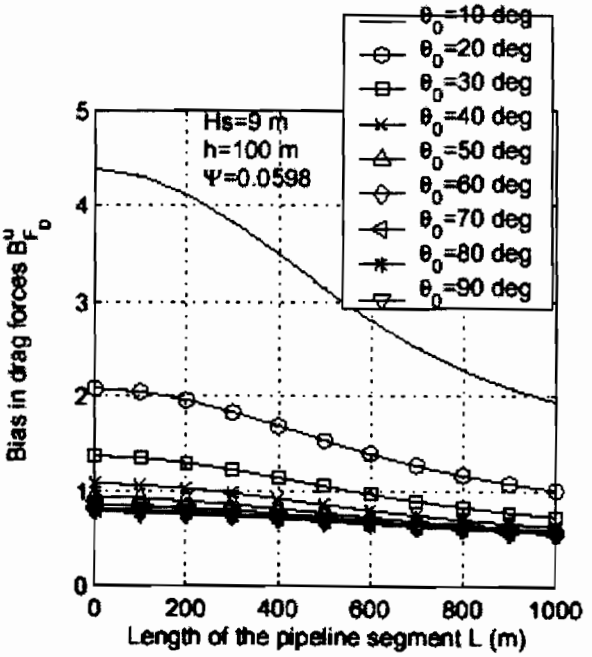

c) H_s=9 m, h=100 m, Ψ=0.0598

Fig. 4.20 Bias in drag force under combined wave and current action (w/ consideration of the pipeline orientation in the design force, σ_D=30 deg)

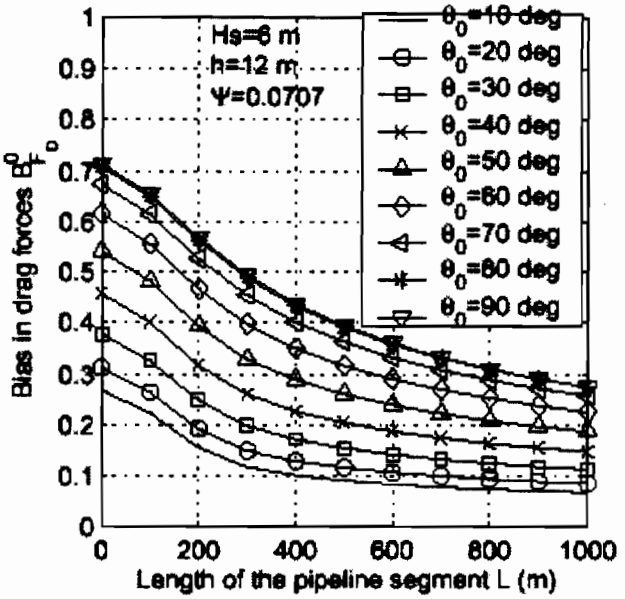

a) H_s=6 m, h=12 m, Ψ=0.0707

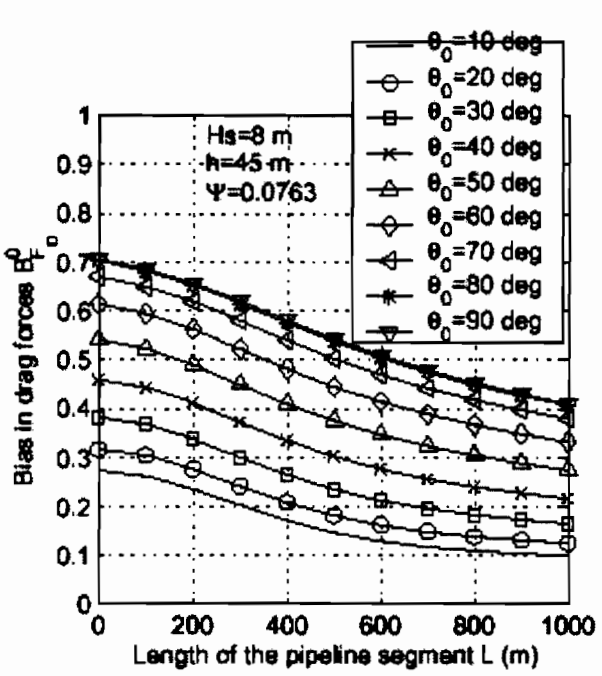

b) H_s=8 m, h=45 m, Ψ=0.0763

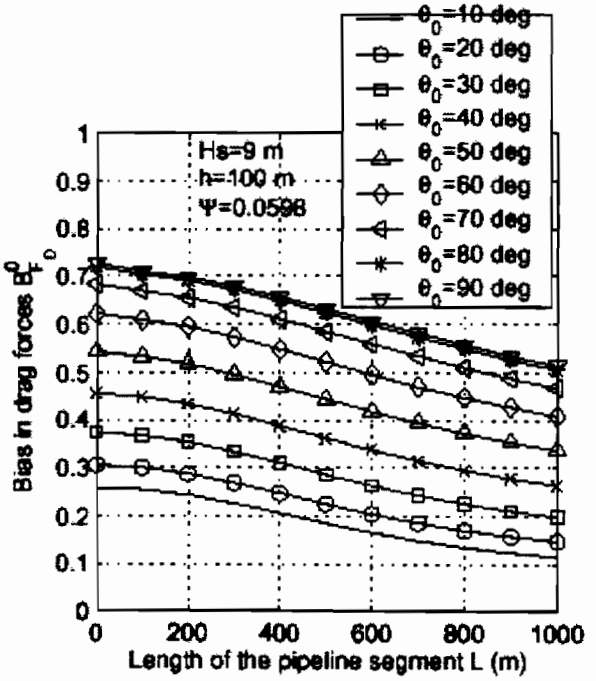

c) H_s=9 m, h=100 m, Ψ=0.0598

Fig. 4.21 Bias in drag force under combined wave and current action (w/o consideration of the pipeline orientation in the design wave force, σ_D=30 deg)

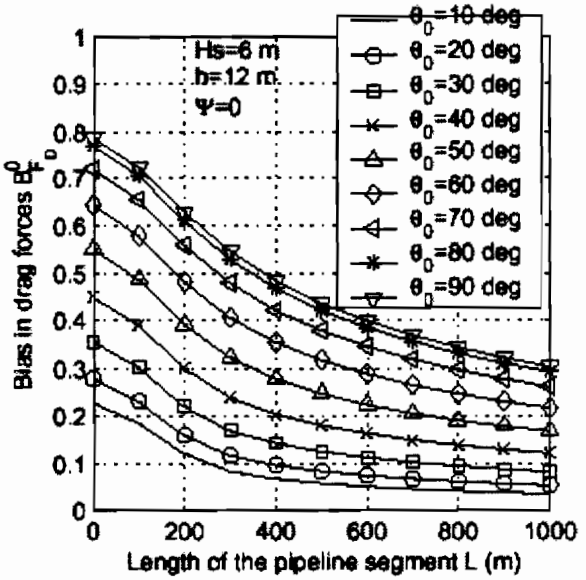

a) H_s=6 m, h=12 m, Ψ=0

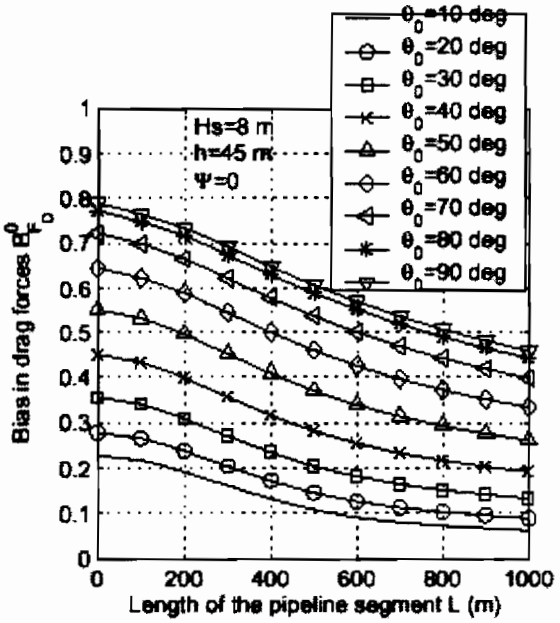

b) H_s=8 m, h=45 m, Ψ=0

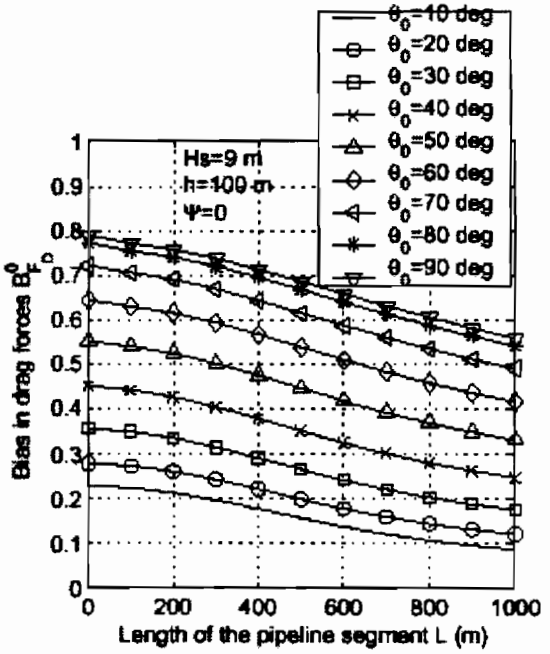

c) H_s=9 m, h=100 m, Ψ=0

Fig. 4.22 Bias in drag force under wave action (w/o consideration of the pipeline orientation in the design wave force, σ_D=30 deg)

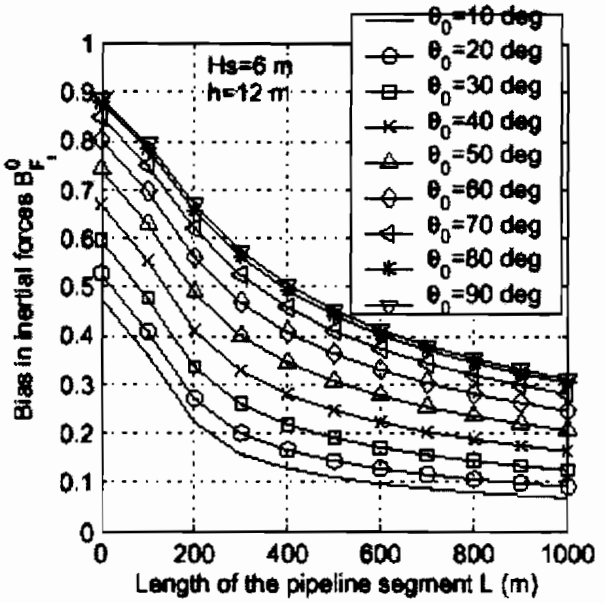

a) H_s=6 m, h=12 m, Ψ=0.0707

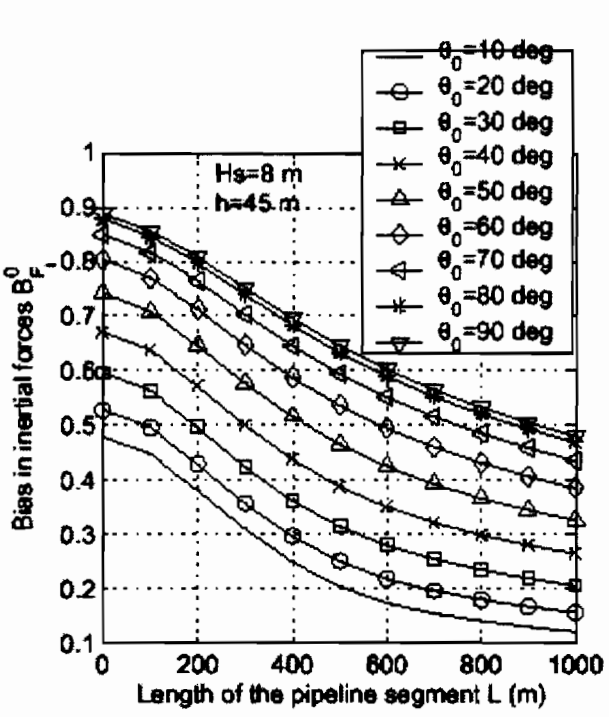

b) H_s=8 m, h=45 m, Ψ=0.0763

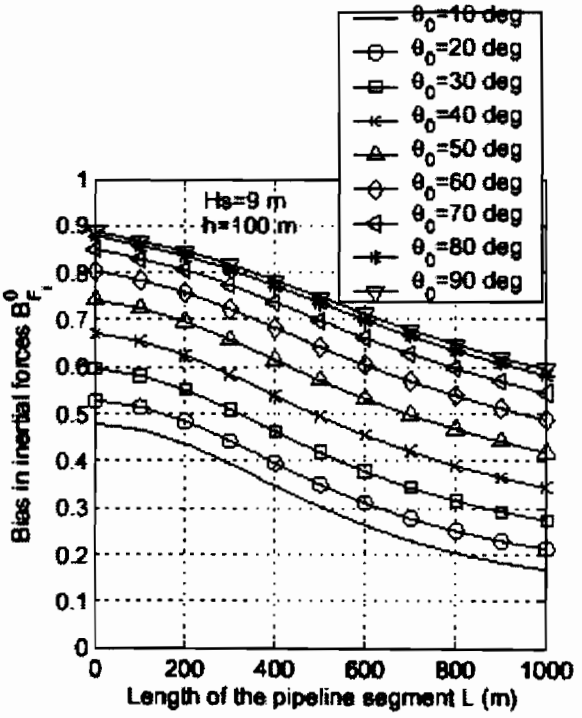

c) H_s=9 m, h=100 m, Ψ=0.0598

Fig. 4.23 Bias in inertial force under combined wave and current action (w/o consideration of the pipeline orientation in the design force, σ_D=30 deg)

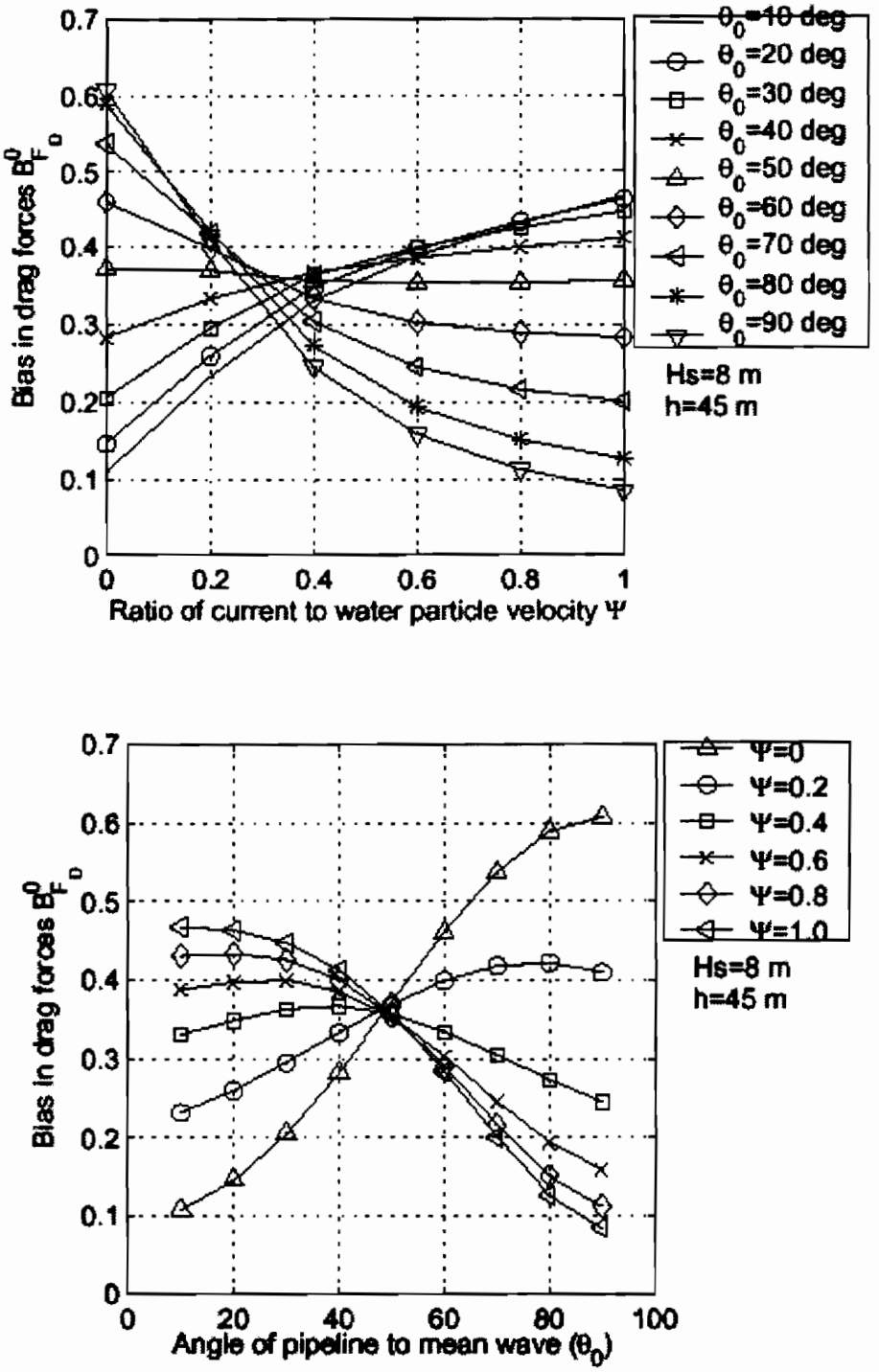

Fig. 4.24 Bias in drag forces for different ratios of currents to water particle velocities Ψ (H_s=8 m, h=45 m, L=500 m, σ_D=30 deg)

4.7 **Concluding Remarks**

This study provides an overall analysis framework to estimate the hydrodynamic loads on marine pipeline supported on sea bed under directionally spreading seas. This condition is very prevalent in hurricane prone areas of the Gulf of Mexico and Bay of Campeche, and impacts the development of oil field in the U.S. and Mexico. The analysis procedure developed here is used to conduct a detailed parameter study to delineate the influences of the directionally spreading seas and the pipeline orientation with respect to the mean direction of wave propagation. The results are expressed in terms of biases for convenient design application.

The key findings from this study are summarized as follows:

- The near sea bottom water particle kinematics are strongly influenced by the directional wave spreading and the orientation of the pipeline with respect to the direction of wave propagation. Both water particle velocity and acceleration exhibit similar biases due to wave spreading.
- The directional wave effects are described in terms of a coherence function commonly used in the representation of turbulence and ground motion. For frequency domain loading analysis, the coherence is described in terms of a joint acceptance function (a transfer function), which is a function of the spreading features. Since the spreading function may be a function of the frequency, accordingly this dependence on the frequency is reflected in the coherence/joint acceptance function. The frequency dependency of the coherence function in directionally spreading waves separates it from the coherence models of turbulence and ground motion characteristics, which can be conveniently expressed in a dimensionless frequency.
- The bias in water particle kinematics due to spatio-temporal correlation is strongly influenced by directional spreading, spectral description of wave elevation, and the pipeline orientation. Both water particle velocity and acceleration exhibit similar biases.
- The frequency dependence of the spreading function has insignificant influence on the biases in water particle velocity, thus the use of frequency independent function is suggested for computational efficiency.
- The analysis of hydrodynamic forces acting on a fixed pipeline segment under the combined action of waves and currents suggests that the bias in forces depend on the bias in particle velocity due to wave spreading and also on the current velocity. The influence of currents in directionally spreading seas is also affected by the orientation of the pipeline segment.
- The formulation presented in this study provides a definite improvement over current design approaches. It helps to quantity the biases present in various design quantities. Future work would focus on developing close-form expressions for biases. This would facilitate introduction of these improved estimations of wave load effects in codes and standards.
- In the current work, the hydrodynamic loads are estimated utilizing the Morison equation. A follow-up work is needed to develop improved hydrodynamic loading models for stationary and mobile pipeline segments and to capture the influence of water-soil surrounding medium on the pipeline stability.

4.8 Future Work

The completion of the initial phase of this study has enabled an accurate estimate of the various biases introduced under different wave surface environments for fixed pipeline. In the following, immediate extensions are suggested which would aid in developing a complete design approach for the pipeline to ensure its integrity under hurricane conditions. This would not only contribute to the hydrodynamic loading, but would also provide guidance on the indirect loading introduced by the translation of the embedment medium around the pipeline under wave action. This aspect of pipeline load effects needs a broader understanding as not only the hydrodynamic forces on pipelines are substantially altered when the seabed becomes mobile under the wave action, but also the pipeline resistance in soil. Some of the specific items for future work are listed below:

2) In order to validate the wave force model in directional seas presented in this study, laboratory and full-scale experiments are essential. The experiments may be performed in two phases. The first part may concern quantifying the coherence models for the wave surface fluctuations in directional seas, and the second may focus on assessing the forces on a pipeline in unidirectional and directional seas. These experiments would also shed light on our understanding of the mechanisms involved in the complex phenomenon of wave-sea bottom-pipeline interaction.
3) Develop close-form expressions for various biases reflected here under the assumption that the coherence can be expressed in terms of a frequency independent spreading function.
4) Refine hydrodynamic loading models based on experimental observations and theoretical considerations. The loading models would include both drag and lift components for a stationary pipeline segment.
5) Develop simple equivalent models that capture the essence of hydrodynamic loading on pipeline due in part to the dynamic water-soil medium surrounding the pipeline.
6) Develop uncertainties associated with the problem parameters, propagate uncertainties, and access their impact on the pipeline safety and integrity. This information will be invaluable towards the development of a probability based design of pipeline.

4.9 References

Bea, R., et al., (1998a), "Risk Assessment and Management Based Criteria for Design and Requalification of Pipelines and Risers in the Bay of Campeche," OTC 8695, Proceedings of the Offshore Technology Conference, Houston, TX.

Bea, R., et al., (1998b), "Risk Assessment and Management Based Hurricane Wave Criteria for Design and Requalification of Platforms in the Bay of Campeche," OTC 8692, Proceedings of the Offshore Technology Conference, Houston, TX.

Banner, M. L., (1990), "Equilibrium spectra of wind waves," *J. Phys Ocean*, Vol. 20, pp. 966-984.

Borgman, L. and Hudspeth, R., (1992), "Sea Floor Wave-Induced Kinematics for Design of Pipeline," Proceedings of Civil Engineering in the Oceans V, ASCE (Editor: R.T. Hudspeth).

Borgman, L.E., (1990), "Irregular Ocean Waves: Kinematics and Forces," The Sea, Vol. 9, Ocean Engineering Science, John Wiley.

Cardone, V.J., and Ramos, R., (1998), "Wave, Wind and Current Characteristics of Bay of Campeche," OTC 8697, Proceedings of the Offshore Technology Conference, Houston, TX.

Collins, J.I., (1995), "Damage to Unburied Flowlines in the Gulf of Mexico During Hurricane Andrew," OTC 7859, Proceedings of the Offshore Technology Conference, Society of Petroleum Engineers, Richardson, TX.

Donelan M.A., Hamilton, J. and Hui, W.H., (1985), "Directional spectra of wind-generated waves," Phil. Trans. Royal Soc. Lond., Vol. A315, pp. 509-562.

Grace, R.A. and Zee, G.T.Y., (1981), "Wave Forces on Rigid Pipes Using Ocean Test Data," Journal of the Waterway, Port, Coastal and Ocean Division, American Society of Civil Engineers, Vol. 107, No. WW2, pp. 71-92, NY.

Hale, J.R., Lammer, W.F. and Jacobsen, V., (1989), "Improved Basis for Static Stability Analysis and Design of Marine Pipelines," OTC 6059, Proceedings of the Offshore Technology Conference, Society of Petroleum Engineers, Richardson, TX.

Jacobsen, V., Bryndum, M.B. and Bonde, C., (1989), "Fluid Loads on Pipelines: Sheltered or Sliding," OTC 6056, Proceedings of the Offshore Technology Conference, Society of Petroleum Engineers, Richardson, TX.

Kareem, A. and Song, X., (1998), "Probabilistic Response Analysis of a Coupled Platform-Tether System Under Multi-Directional Seas," Proceedings of the 1998 OMAE Converence, ASCE, Lisbon.

Kareem, A., Zhao, J., and Tognarelli, M. A., (1995), ``Surge response statics of tension leg platforms under wind and wave loads: a statistical quadratization approach," Prob. Engrg. Mech., 10(4), pp. 225-240

Kareem, A., Deodatis, G. and Shinozuka, M., (1997), "Modelling of Coherence for Stochastic Representation of Wind, Wave, and Seismic Load Effects," Proceedings of 7th ICOSSAR, Kyoto, Japan.

Lambrakos, K.F., Chao, J.C., Beckman, H. and Brannon, H.R., (1987), "Wade Model of Hydrodynamic Forces on Pipelines," Ocean Engineering, Vol. 14, No. 2, pp. 117-136, Elsevier Publishers, NY.

Lambrakos, K.F., (1982), "Marine Pipeline Dynamic Response to Waves from Directional Wave Spectra," Ocean Engineering, Vol. 9, No. 4.

Lammaert, W., Hale, J.R. and Jacobsen, V., (1989), "Dynamic Response of Submarine Pipelines Exposed to Combined Wave and Current Action," OTC 6058, Proceedings of the Offshore Technology Conference, Society of Petroleum Engineers, Richardson, TX.

Mitwally, H. and Novak, M., (1989), "Wave Force of Fixed Offshore Structures in Short-Crested Seas," J. Engrg. Mechanics, ASCE, Vol. 115, No. 3, pp. 636-655

Morris, D.V., Webb, R.W. and Dunlap, W.A., (1988), "Self-Burial of Laterally Loaded Offshore Pipelines in Weak Sediments," OTC 5855, Proceedings of the Offshore Technology Conference, Society of Petroleum Engineers, Richardson, TX.

Pierson, W. J. and Moskowitz, L., (1964), "A proposed spectral form for fully developed wind seas based on the similarity theory of S. A. Kitaigorodskii," J. of Geophys. Res., Vol.69, No.24, pp. 5180-5190.

Pipeline Research Committee, (1993), ``Submarine Pipeline On Bottom Stability,'' Brown &Root, Report to American Gas Association (AGA), Houston, TX

Soedigdo, I. R., Lambrakos, K. F. and Edge B. L., (1999), ``Prediction of Hydrodynamic Forces on Submarine Pipelines Using an Improved Wake II Model," Ocean Engineering, 26, pp. 431-462

Valdez, V.M., Bayazitoglu, Y.O., Weiss, R.T., Valle, O.L., and Hernandez, T., (1997), "Inspection and Evolution of Offshore Pipelines in the Bay of Campeche," OTC 8499, Proceedings of the Offshore Technology Conference, Houston, TX.

Zimmerman, M., Hudspeth, R., Leonard, J., Tedesco, J., and Borgman, L., (1986), "Dynamic Behavior of Deep Ocean Pipeline," J. of Waterways, Port, Coastal and Ocean Engineering, Vol.112, No.2.

4.10 Symbols

Superscripts

u - Unidirectional wave
0 - Unidirectional wave without the orientation of pipeline

Subscripts

u - Unidirectional wave
ξ - Sea surface elevation
D - Drag force
I - Inertia force
rms - Root-mean-square value
max - Maximum value

General

A - Spectral amplitude
B_v - Bias in the water particle velocity due to wave spreading
$B_{\dot{v}}$ - Bais in the water particle acceleration due to wave spreading
B_{vc} - Bias in water particle velocity due to spatio-temporal correlation for spreading wave
B_{FD} - Bias in darg force
B_{FI} - Bias in inertial force
C_M - Inertial force coefficient
C_D - Drag force coefficient
coh - Coherence function of water particle velocity
D - Directional spreading function
f_D - Hydrodynamic drag on the pipeline per unit length
F_D - Hydrodynamic drag on the pipeline segment
g - Peak factor
h - Water depth
H_s - Significant wave height
H_{max} - Maximum wave height
$H_{v\xi}$ - Transfer function between sea surface elevation and water particle velocity

J	- Joint acceptance function
k	- Wave number
L	- Length of the pipeline segment
r	- Ratio between the normal components of the current velocity and RMS water particle velocity to the pipeline axis
R	- Ratio between the power spectra for unidirectional and directional seas
S	- Power spectral density
t	- Time
U_{cd}	- Design maximum current velocity
U_{wd}	- Design water particle velocity
U_c	- Current velocity normal to the pipeline axis
U_w	- Water particle velocty normal to the pipeline axis
v	- Water particle velocity
x, y, z	- Cartesian coordinate
Φ	- Water particle velocity potential
Ψ	- Ratio between the design maximum current velocity and water particle velocity
θ	- Direction of wave propagation of an elementary wave relative to the x-axis
θ_0	- Mean direction of wave propagation relative to the x-axis
σ_D	- Variance of spreading
σ_ξ	- Variance of the wave elevation
ω	- Wave velocity
ω_p	- Peak frequency of spectrum
ξ	- Sea surface elevation

5.0 Pipeline System Considerations

5.1 Systems and Elements

In development of RAM PIPE REQUAL, it was important to discriminate between pipeline ''elements', 'segments' and 'systems' (Fig. 5.1). A pipeline system can be decomposed into sub-systems of series and parallel elements (Melchers, 1987; Orisamolu and Bea, 1993; 1999). A series sub-system is one in which the failure of one of the elements leads to the failure of the system. Examples of a series sub-system would be a pipeline that is comprised of joints of pipe (segments). The cross section of these segments could be idealized as a series of elements.

A parallel system is one in which the failure of the system only occurs when all of the elements have failed. An example of a parallel system would be several pipelines that serve the same distribution point, given that the pipelines can all carry the required production.

5.2 Series Systems

A series (weak-link) system fails when any single element fails. In probabilistic terms, the probability of failure of a series system can be expressed in terms of the unions of the probabilities of failure of its N elements as (Madsen, Krenk, Lind, 1986; Melchers, 1987; Orisamolu, Bea, 1993):

$$Pf_{system} = (Pf_1) \cup (Pf_2) \cup ... (Pf_N)$$

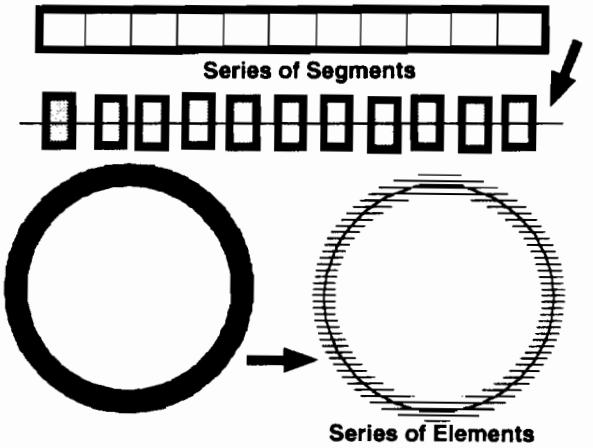

Fig. 5.1. Pipeline system comprised of segments and elements

For a series system comprised of N elements, if the elements have the same strengths and the failures of the elements are independent ($\rho = 0$), then the probability of failure of the system can be expressed as:

$$Pf_{system} = 1 - (1 - Pf_i)^N$$

If Pfi is small, as is usual, then approximately:

$$Pf_{system} \approx N\, Pf_i$$

If the elements are independent and have different failure probabilities:

$$Pf_{system} \approx \sum_{i=1}^{N} Pf_i \leq 1$$

Note that the last two equations are only applicable when the probabilities of failure of the elements are very small.

If the elements are perfectly correlated then:

$$Pf_{system} = \text{maximum } (Pf_i)$$

5.3 Correlations

There can be a variety of ways in which correlations can be developed in elements and between the segments that comprise a pipeline system. Important sources of correlations include:

- capacity and demand correlations,
- element to element characteristics correlations, and
- failure mode correlations.

The correlation coefficient, ρ, expresses how strongly two variables, X and Y, are related to each other. ρmeasures the strength of association between the magnitude of two variables. The correlation coefficient ranges between positive and negative unity ($-1 \leq \rho \leq +1$). If $\rho = 1$, they are perfectly correlated, so that knowing X allows one to make perfect predictions of Y. If $\rho = 0$, they have no correlation, or are 'independent,' so that the occurrence of X has no affect on the occurrence of Y and the magnitude of X is not related to the magnitude of Y. Independent random variables are uncorrelated, but uncorrelated random variables (magnitudes not related) are not in general independent (their occurrences can be related).

The correlation coefficient can be computed from data in which the results of n samples of X and Y are developed ($\underline{X}$ and $\underline{Y}$ are the mean values of the variables X and Y):

$$\rho = \frac{\sum X\,Y - n\,\underline{X}\,\underline{Y}}{\sqrt{\left(\sum X^2 - n\,\underline{X}^2\right)\left(\sum Y^2 - n\,\underline{Y}^2\right)}}$$

The term in the numerator of this expression is the covariance (CoV) between the two marginal distributions, X and Y. The terms in the denominator are the standard deviations of the two distributions, X and Y.

Frequently, the correlation coefficient can be quickly and accurately estimated by plotting the variables on a scattergram that shows the results of measurements or analyses of the magnitudes of the two variables (Fig. 5.2, 5.3, 5.4). Two strongly positively correlated variables will plot with data points that closely lie along a line that indicates as one variable increases the other variable increases. Two strongly negatively correlated variables will plot with data points that closely lie along a line that indicates as one variable increases, the other variable decreases. If the plot does not indicate any systematic variation in the variables, the general conclusion is that the correlation is very low or close to zero.

In general, paired pipeline elements and segments are strongly positively correlated (Fig. 5.2, 5.3, 5.4). These test data were taken from samples of delivered pipeline joints and were not intentionally paired from the same plate or runs of steel. High degrees of correlation of pipe properties were also found by Jaio, et al (1997) for samples of the same pipe steel plate.

These results have extremely important implications regarding the relationship between the reliability of a pipeline system and the reliability of the pipeline system elements and segments. The probability of ***failure of the pipeline system will be characterized by the probability of failure of the most likely to fail element – segment that comprises the system.***

There can be a correlation between the strength of the elements and the loadings imposed on or induced on the elements. Frequently, this source of correlation is either ignored in the reliability characterization (through the assumption of independent – non-correlated demands and capacities), or introduced through an evaluation in which the performance characteristic/s of the element are evaluated conditionally on the occurrence of the demands. For Lognormally distributed correlated demands and capacities, The Safety Index is determined as follows:

$$\beta = \frac{\ln(R_{50} / S_{50})}{\sqrt{\sigma_{\ln R}^2 + \sigma_{\ln S}^2 - 2\rho_{RS}\sigma_{\ln R}\sigma_{\ln S}}}$$

Positive correlation of the demands (S) and capacities (R) results in an effective decrease in the total uncertainty and an increase in the Safety Index. Positive correlation implies that as the loadings increase, the capacities increase. This is a beneficial effect. However, for negative correlation between R and S, there is the opposite effect; the Safety Index decreases. In this case ignoring the demand - capacity correlation would result in 'unconservative' estimates of the Safety Index.

Correlations can also be developed between the failure modes of the elements – segments that comprise a system. Cornell (1987) has developed a useful expression to determine the approximate correlation coefficient between the probabilities of failure of a system's components (or correlation of failure modes) as:

$$\rho_{fm} \approx \frac{V^2_S}{V^2_R + V^2_S}$$

where V^2_S and V^2_R are the squared coefficients of variation of the load (S) and capacity (R), respectively. It is often the case for pipeline systems that the coefficients of variation of the loadings are equal to or larger than those of the capacity. Thus, the correlation of the probabilities of the failure of the system's components are generally very close to unity, and there is a high degree of correlation between the system's failure modes. Again, this indicates that the probability of failure of the system is well approximated with the probability of failure of the system's most likely to fail segment or element.

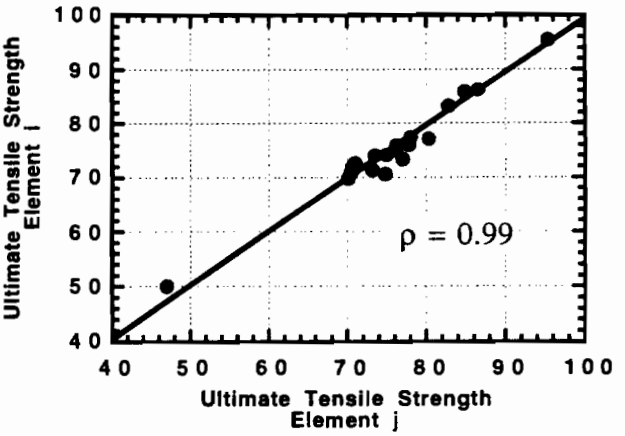

Fig. 5.2. Correlation of measured ultimate tensile strengths of paired pipeline steel samples

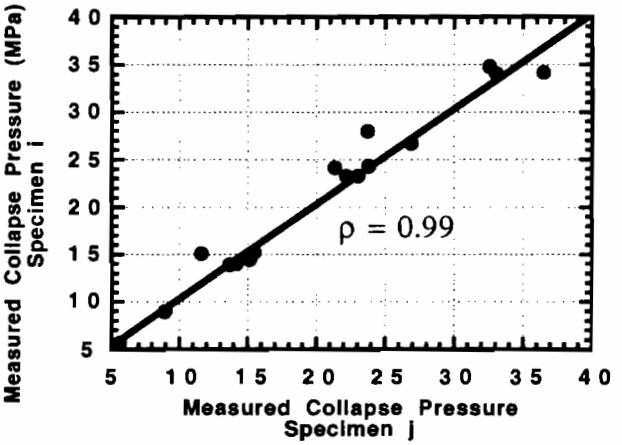

Fig. 5.3. Correlation of measured collapse strengths of paired steel pipeline samples

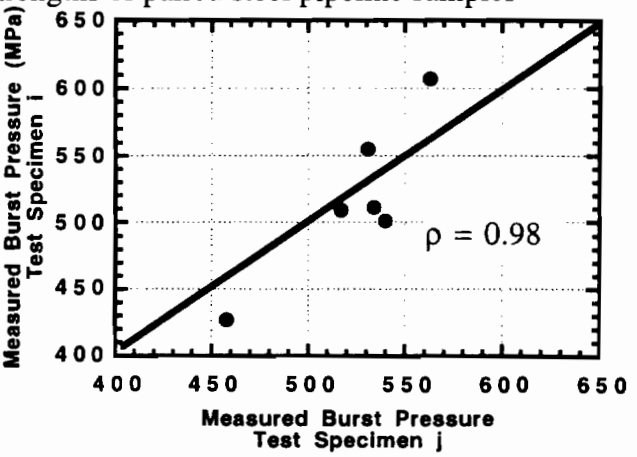

Fig. 5.4. Correlation of measured burst strengths of paired steel pipelines

5.4 Fully Probabilistic Approach

The fully probabilistic approach represents the most formal and rigorous framework for the propagation of uncertainties through engineering analytical or numerical models (Orisamolu, Bea, 1993; 1999). It provides a methodology via which the probabilistic attributes of the output variable can be accurately derived directly from those of the input variables.

Consider a function $z = z(x)$ that depends on several random variables $\left(\underset{\sim}{x}\, x_1, x_2, x_3, \ldots, x_n\right)$. Then z is also itself a random variable. In the most general case, the independent random variables, x_i, would have different probabilistic attributes, namely: probability distribution function, statistical parameters, and possibly a correlation between the random variables. In the full probabilistic approach, there are two broad categories of methods that are employed to derive the probabilistic attributes of z from those of its dependent variables.

These methods include the simulation methods and the probability integration methods. Simulation methods generally rely on the generation of sample values of the random variables that are then substituted into the functional expression for z(x), and later processed to establish the probabilistic attributes for z(x). The probability integration methods, on the other hand, utilize an integration approach to compute a series of point probability values of the function z(x) by evaluating the integrate:

$$P = P\left(z \le z_i\right) = \int \cdots \int_{\tilde{z}(x) \le 0} f_x(x)dx$$

where $f_x(x)$ is the joint probability density function (pdf) of the random vector and the integrand is defined over the region $\tilde{z}(x) = z(x) - z_i \le 0$.

Several probability reliability algorithms are available for carrying out the operation defined in the foregoing Equation. These are well documented in classical monographs such as the book by Madsen et al.(1986). Fig. 5.5 illustrates most of the different techniques that have been developed and applied in the reliability engineering community.

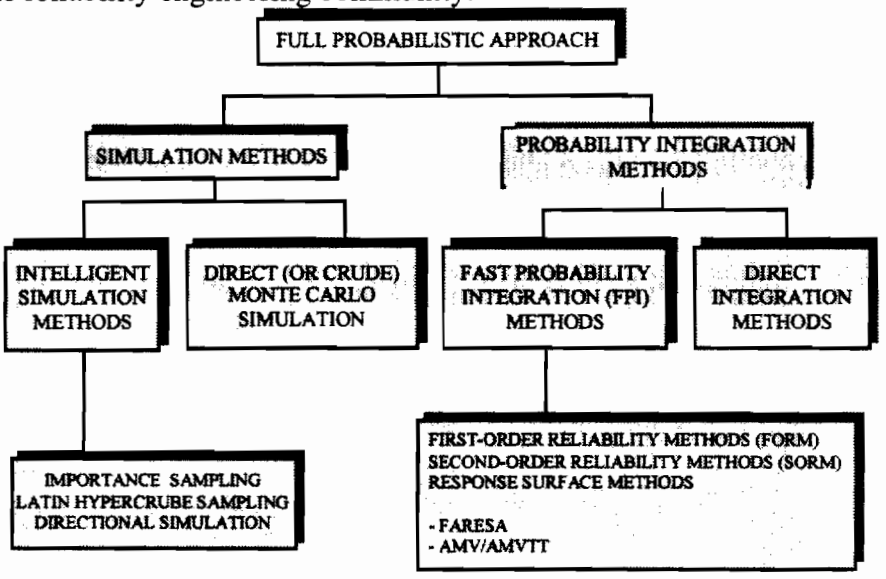

Fig. 5.5. Different techniques of the full probabilistic approach

5.5 Probabilistic Relationship Between Experimental and Numerical Databases

In development of probability based guidelines for requalification and design of pipelines, it has become popular to utilize numerical databases in which Finite Element Analysis (FEA) results are used in lieu of physical experimental results. This approach has much appeal because it is much less expensive to generate FEA results to cover a wide range of many important parameters than to perform the same number of physical tests. This approach requires development of a probabilistic relationship between a limited experimental database and a more extensive numerical database.

The probabilistic modeling uncertainty factor, B_M, is typically defined as follows:

$$B_M = \frac{B_{EXP}}{B_{ANA}}$$

where B_{EXP} represents the 'experimental' value (e.g. burst pressure) of interest and B_{ANA} is the value predicted using the analytical models. In this case, the set of experimental values are generated using FEA.

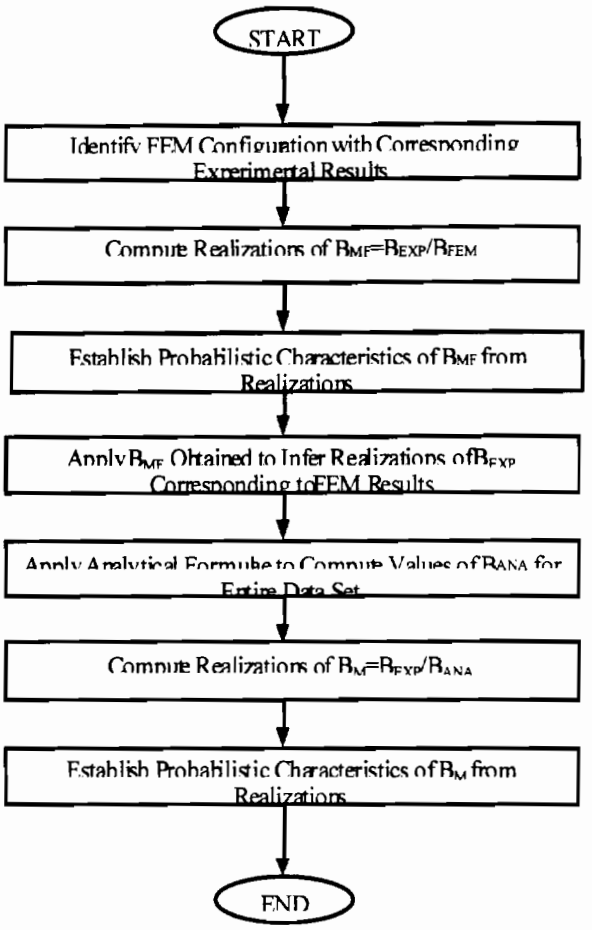

Fig. 5.6. Development of probabilistic basis for use of simulated test data in development of criteria

Now, we have a set of numerical results generated via the use of advanced FEA methods. Although these values are generally believed to be more accurate than the explicit analytical models, there are still some differences between the results and the true (experimental) results. We introduce a new modelling uncertainty random variable, B_{MF}, which is defined as:

$$B_{MF} = \frac{B_{EXP'}}{B_{FEM'}}$$

where $B_{FEM'}$ represents the subset of finite element values and $B_{EXP'}$ represents the corresponding experimental values. The random variable B_{MF}, is used to 'correct' the entire FEA data set B_{FEM} and the result can be written as:

$$B_{EXP} = B_{MF}\ B_{FEM}$$

This approach hinges on using representative experimental results to establish the probabilistic characteristics of the random variable, B_{MF}. Once B_{MF} has been established, the population of B_{EXP} that is available for the characterization of B_M can be expanded to the same number as the number of FEA results. This process is schematically illustrated in Fig. 5.6.

In the case that will be illustrated here, one-to-one comparisons of FEA results with experimental results were not available. However, one-to-one comparisons could be developed between the analytical model that was proposed for the pipeline collapse pressure criteria (identified as

Timoshenko elastic formulation) and the experimental data. Similarly, one-to-one comparisons could be developed between the analytical model and the FEA results. In this case the FEA results are 'corrected' with a random variable that represents the error between the experimental results and the analytical model:

$$B_{MF} = \frac{B_{EA}}{B_{FA}}$$

where:

$$B_{EA} = \frac{B_E}{B_A}, \text{ and}$$

$$B_{FA} = \frac{B_F}{B_A}.$$

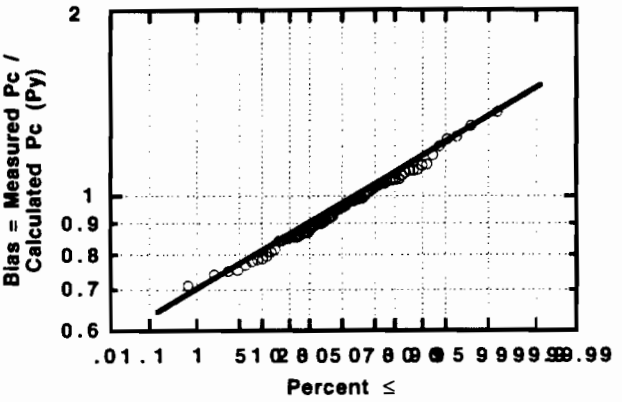

Fig. 5.7. Bias in Timoshenko Elastic formulation based on results from seamless pipe tests (Logarithmic Normal distribution scales)

A database of 74 collapse pressure tests on seamless pipeline test specimens was assembled (Bea, et al, 1998). The collapse pressure analyses were performed using the Timoshenko Elastic formulation. The results are summarized in Fig. 5.7. The median bias is B_{EA50} = 1.0 and the Coefficient of Variation of the Bias is V_{BEA} = 12.4 %.

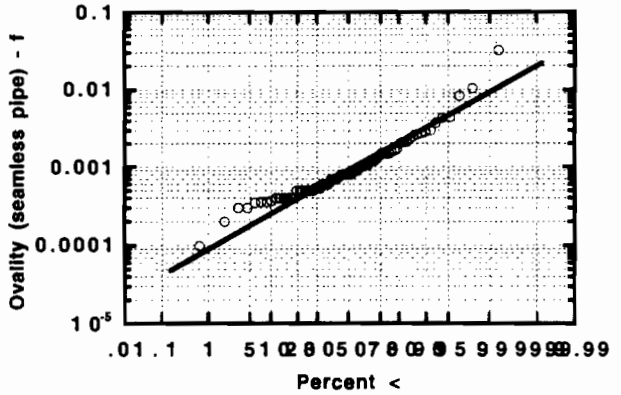

Fig. 5.8. Measured ovalities of seamless pipeline test specimens (Logarithmic Normal distribution scales)

Because of its importance in determining the collapse pressures, the ovality of the seamless pipeline test specimens were evaluated. The results are summarized in Fig. 5.8. The median ovality is f_{50} = 0.1% and the ovality of the test specimens has a Coefficient of Variation of V_f = 90 %.

A database of 44 simulated 'tests' on collapse pressures of X-52 and X-77 pipe were provided by Igland (1997). This database included only those simulations that did not include residual stresses. The simulations that included residual stresses produced results that were 'unusual' when compared with physical test data.

Figure 5.9 summarizes results from the statistical analysis of the simulated test data Bias. The Timoshenko Elastic model was used to calculate the collapse pressures. Four ovalities were used in the calculations: f = measured, f = 0.001 (e.g. high quality seamless pipe), f = 0.01 (low quality fabricated pipe), and f = 0.005.

The formulation based on f = 0.005 produced a median Bias B_{FA50} = 1.0 and a coefficient of variation of the bias of V_{BFA} = 4.0 %. The formulation based on the measured ovalities and SMYS times 1.1 produced a median Bias of B_{FA50} = 0.96 and Coefficient of Variation of the Bias of V_{BFA} = 4.1 %. The formulation based on the measured ovalities and the simulation model yield strengths produced a median Bias of B_{FA50} = 0.90 and Coefficient of Variation of the Bias of V_{BFA} = 8.7 %.

If one used the seamless pipeline test data, a median bias of B_{EA50} = 1.0 and Coefficient of Variation of the Bias of 12.4 %. The simulation data analyzed in the same way as the test data developed a median bias of B_{FA0} = 0.90 and Coefficient of Variation of the Bias of 8.7 %. Given that the requalification analysis would be based on f = 0.005, B_{FA50} = 1.0 and a coefficient of variation of the bias of V_{BFA} = 4.0 %.

To develop the required model bias, the simulation based test data median bias would have to be multiplied by a median Bias correction factor of B_{MF} = 1.11; thus, B_{M50} = 1.11. The model bias Coefficient of Variation would be:

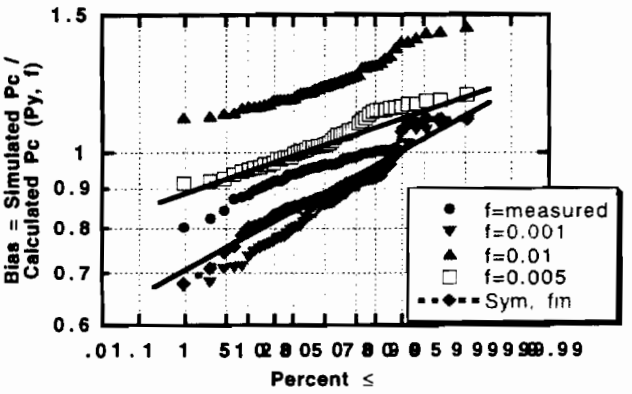

Fig. 5.9. Bias from Simulated Test Data for Various Ovalities (Logarithmic Normal distribution scales)

$$V_{BM} = [0.12^2 + 0.04^2]^{0.5} = 12.6\%$$

It would not be correct to use the results directly from the FEA model. If this were done, it would result in an under-estimate of the model bias and the model bias uncertainty.

5.6 Example of Full Probabilistic Approach

The full probabilistic approach can be generally applied to establishing the probabilistic response (i.e. the full cumulative distribution function) or for reliability assessment with reference to a design (or performance) limit state condition. Here, we employ the burst design equation to illustrate the application of the approach.

The burst design equation for a pipe segment of diameter D, wall thickness t and ultimate tensile strength can be expressed as:

$$P_B = \frac{2t\sigma_U}{D}$$

where P_B is the burst pressure predicted by the analytical expression, and σ_U is the ultimate tensile strength (UTS). The particular value of UTS to be employed is usually stipulated as the specified minimum tensile strength (SMTS). Failure with reference to this formulation occurs when the applied (operating) pressure, P_A, exceeds the burst pressure, that is, the limit state condition is given by:

$$g(x) = P_B - P_A$$

or

$$g(x) = \left\{ \frac{B_M \bullet 2t\sigma_U}{D} - P_A \right\}$$

where B_M is the modelling uncertainty factor associated with the fact that the burst pressure formulation does not give perfect predictions. The parameter B_M is a random variable whose realisations are given by the various values of the ratio of the actual (experimental) burst pressures to the predicted burst pressures.

The probability of failure is given by:

$$P_f = \mathrm{Prob}\{g(x) \leq 0\}$$

and is computed herein using advanced reliability analysis algorithms: FORM (First Order Reliability Method) and SORM (Second Order Reliability Method) (Madsen, et al, 1986; Melchers, 1987). First, however the rigorous probabilistic characterisation of B_M and σ_U are performed using a software system called PRADAC: Probabilistic Data Characterisation Program.

Based on the pipe burst test data base, it was established that B_M is best-fit modeled with a Lognormal probability distribution. A summary of the probabilistic attributes for the burst data is given in Table 5.1. It can be seen that the mean value is B_M = 1.1, the variance is 0.168E-02 (or the Coefficient of Variation is 3.73%). Applying this information to the calculation of P_F for various values of the operating pressure (for a given wall thickness) is shown in Fig. 5.10. Similar plots for different values of thickness for a given operating pressure are also illustrated in Fig. 5.11. It is important to note that the FORM and SORM results are very close to those from the RAM PIPE REQUAL approach summarized earlier in this report.

Table 5.1. Summary of statistical analysis of pipeline burst pressure data
(Number of Records: 14, Number of Selected Distributions: 3)

Selected Distributions and Their Bounds

Type	Lower Bound
Normal	
Lognormal	0.000E+00
Weibull	0.000E+00

Estimated Distribution Parameters (MOM –Method of Moment)

Type	Mean	Variance	Par1	Par2	Par3	Par4
Normal	0.111E+01	0.168E-02	0.111E+01	0.409E-01	0.000E+00	0.000E+00
Lognormal	0.111E+01	0.168E-02	0.000E+00	0.368E-01	0.105E+00	0.000E+00
Weibull	0.111E+01	0.168E-02	0.000E+00	0.113E+01	0.341E+02	0.000E+00

Confidence Intervals of Mean

Conf. Level	Alpha value	Lower limit	Upper limit
0.8000	0.2000	0.10970E+01	0.11265E+01
0.8500	0.1500	0.10950E+01	0.11285E+01
0.9000	0.1000	0.10923E+01	0.11311E+01
0.9500	0.0500	0.10881E+01	0.11354E+01
0.9900	0.0100	0.10788E+01	0.11447E+01

Confidence Intervals of Variance

Conf. Level	Alpha value	Lower limit	Upper limit
0.8000	0.2000	0.11159E-02	0.33715E-02
0.8500	0.1500	0.10717E-02	0.38514E-02
0.9000	0.1000	0.10192E-02	0.47255E-02
0.9500	0.0500	0.94799E-03	0.72512E-02
0.9900	0.0100	0.83408E-03	

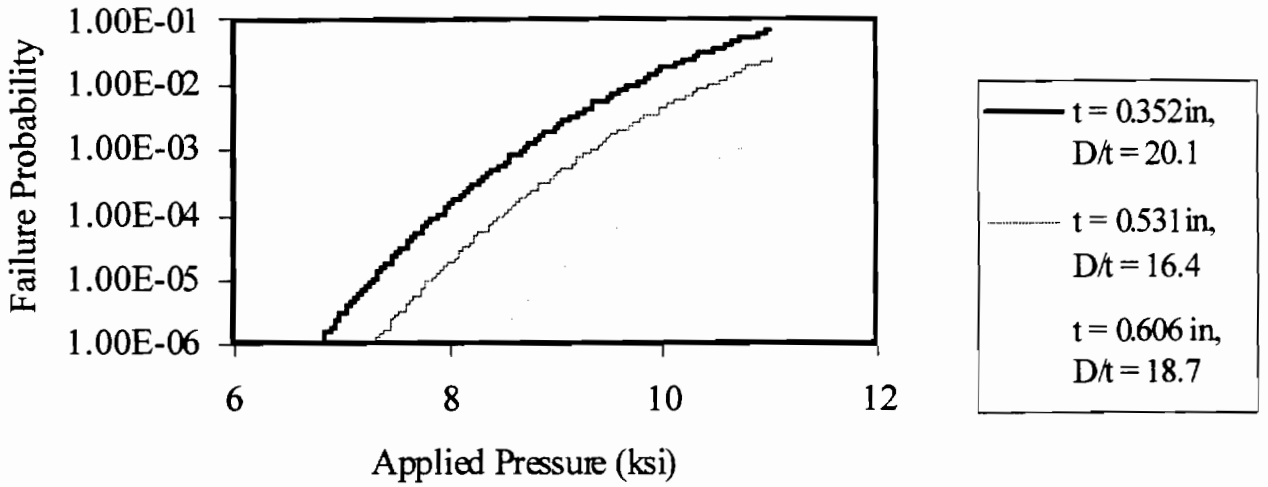

Fig. 5.10. Failure probability as function of applied pressure (Logarithmic scale) for various pipeline diameters and thicknesses

Fig. 5.11. Failure probability as function of pipeline wall thickness for various pressures

5.7 Pipeline System Reliability Modeling Using a Fully Probabilistic Approach

The application of system reliability modeling capabilities is warranted when there are multiple defects and/or multiple failure modes to consider for a given pipeline segment or series of segments. If one thinks about a pipeline structure that is in service, most practical analyses to determine the probability of failure would fall into this category. Typically, a pipeline has several defects (e.g., corrosion) along its length which may cause structural integrity concerns from several failure mode considerations (e.g., burst, compressive local buckling, collapse, etc). For such structures, several approaches have been employed. Some approaches erroneously ignore the correlations arising from these multiple defects and/or failure modes: correlations that are naturally induced by virtue of the commonality of material properties, loading and operational conditions, and the models employed for failure prediction.

This section summarizes the features of system reliability modeling within the framework of a fully probabilistic approach. The next section demonstrates its application to assessment of the reliability characteristics of the burst pressures of corroded pipelines.

Failure Probability

The system reliability problem consists of one that is aimed at the computation of probabilities of multiple events. In general, system models are classified as either series or parallel systems. Complicated systems usually consist of a combination of both series and parallel systems. A series system is defined as a system which fails if any of its components fails. It failure event is hence the union of the individual component failure events. A parallel system however, fails only if all its components fail, and its failure event is the intersection of component failure events. Detailed expositions of these models and the algorithms that are used for probability calculations were briefly summarized in Orisamolu and Bea (1993; 1998).

For pipeline structural reliability modeling under multiple defects and/or multiple failure modes, a series system reliability model is the suitable probabilistic model. The series system model can be envisioned to consist of several pipeline segments, each with one or more defects, and the integrity being evaluated with reference to limit state criteria such as burst, collapse, compressive local buckling, etc. In reliability language, the evaluation of a particular defect on a given segment with

reference to a particular limit state condition is a component. As such the model for the evaluation of given section of a pipeline with several defects along many of the segments that make up the pipeline is given by a series system of components as shown in Fig. 5.12.

Fig. 5.12. Pipeline series system configuration

The system probability of failure for a series system of n components, Pfs, is given by:

□ EMBED Equation.3 □□□

For any two components whose limit state functions are defined by gi and gj with failure defined as events Ei and Ej, respectively, the system failure probability is given by:

□ EMBED Equation.3 □□□

in which the last term in the equation accounts for the equation correlations between the two events.

The expression EMBED Equation.3 is explicitly given by:

$\Pr ob(E_i \bigcap E_j) = \iint_{E_i \cap E_j} f_{g_i g_j}(g_i g_j) dg_i dg = \Phi(-\beta_i, -\beta_j, \rho_{ij})$ where f_{gigj} is the joint probability density function of the resultant random variables g_i and g_j, Φ is the two-dimensional standard normal CDF, β_i and β_j are the reliability indices for the components variables gi and gj, and ρij is the correlation coefficient between the two components.

Several techniques are available for the computation of P_{f_s} just as there are several methods for the estimation of component failure probabilities. Using first-order reliability methods (FORM) for example, it can be shown that the system failure probability for a parallel system of n components is given by:

$$P_{f_s} = \Phi_n\left(-\overline{\beta}, [\rho_{ij}]\right)$$

where Φ_n is the n-dimensional standard normal CDF, $\overline{\beta}$ is the n-dimensional vector containing all reliability indices of components, and $[\rho_{ij}]$ is the correlation coefficient matrix of the various components. The series system problem which is of relevance to the pipeline configuration illustrated in Figure A.5 is usually treated as the complement of the parallel system problem, and the corresponding P_{f_s} is given by

$$P_{f_s} = 1 - \Phi_n(-\overline{\beta}, [\rho_{ij}])$$

With the exception of some few special cases, the evaluation of the foregoing equations is difficult, especially when a large number of components (n) is involved. Approximate techniques are available to handle this complicated problem. These techniques were summarised by Orisamolu and Bea (1993) in a previous effort, and include probability bounding techniques, and improved bimodal bounds (Ahamed, Koo, 1990), as well as the probabilistic network evaluation technique (PNET). More advanced system-based FORM and SORM methods are also available (Orisamolu, Bea, 1993).

System Reliability Example for Corroded Pipeline

In this development, we employ improved bimodal bounds that take into effect the intersection of joint failure probabilities to demonstrate the application as well as the importance of using system

reliability models in pipeline reliability assessment. The examples involve the reliability assessment of a pipeline segment with several corrosion defects with reference to burst and pressure collapse.

In this development, the burst pressure of corroded pipe is given by (Bea, et al, 1998):

$$\frac{2.2t\sigma_u}{D.SCF}$$

The pressure collapse equation for corroded pipe is given by:

$$Pcd = 0.5\{Pud+Ped*Kd-[(Pud+Ped*kd)^2-4.*Pud*Ped]^{0.5}\}$$

where

$$Pud = \frac{5.1t_{d\_u}}{D}$$

$$Ped = 2E(t_d/D)^3 \frac{}{1-v^2}$$

$$Kd = 1.3f\,(D/t_d),\ t_d = t - d$$

A section of the pipe with 11 corrosion defects that are randomly distributed along the pipe segment was selected for analysis. Component reliability analysis was carried out on the basis of the burst capacity equation and the pressure collapse equation. System reliability analysis was also executed using the equations developed in the previous Section. Table 2 gives the value, probability distribution and coefficient of variation of the random variables that are used in the analysis. These values are representative of a section of a real corroded pipeline.

The following nomenclature is used in Fig. 5.13 to Fig. 5.18:

- Increasing corrosion depth means that all the 11 pits are of different depth with the smallest or nominal pit of 0.0531 in. The remaining pits are increased in steps of 10%.
- Decreasing corrosion depth means the depth of the pits decreases in steps of 10% from the nominal pit value.
- Fixed corrosion depth means that all the pits have the same nominal depth of 0.0531in.
- The number of pits as indicated on the x-axis of the bar charts means the number of corrosion pits that are used for system reliability analysis starting with the pit with nominal depth.

Table 5.2. Values of Random Variables Used for Reliability Analysis

Random Variable	**Distribution Type**	**Mean Value**	**COV (%)**
Applied Pressure (P)	Lognormal	5.000Ksi	10
Wall thickness(t)	Fixed	0.531in	
Modeling Uncertainty (B_m) for Compressive Buckling Model	Lognormal	1.000	45
Modeling Uncertainty (B_m) For Burst Capacity Model	Lognormal	1.000	24
Pipe Diameter (D)	Fixed	9.929in	

Ultimate Tensile Strength σ_u	Lognormal	126.0	15
Corrosion Depth	Gumbel	0.0531in	10
Young's Modulus (E)	Fixed	3000Ksi	
Poisson Ratio	Fixed	0.300	
Ovality Constant (f)	Fixed	0.001	
Specific Minimum Tensile Strength	Fixed	100.0	

Figure 5.13 shows the results of system reliability evaluated for a pipeline segment with a different number of corrosion defects based on burst criteria only. It can be seen that the system failure probability increases as the number of defects increase. It is important to note, however, the following:

- It is incorrect to select the corrosion defect with the worst failure probability as a representation of the reliability of the pipeline segment. This practice is, indeed, dangerously non-conservative as the additional contributions to the pipeline failure probability that are introduced by virtue of the presence of the other defects are not accounted for; and
- It is equally incorrect to sum up the various failure probabilities for the individual defects. Physically, this neglects the correlations between the components (representing the safety margins of the individual defects with reference to the failure criteria). Such a practice is also mathematically erroneous because it could lead to failure probabilities greater than unity - a violation of one of the fundamental axioms of probability!

For a practical pipeline reliability assessment, therefore, the results shown in Fig. 5.13 to Fig. 5.18 clearly demonstrate that the full probabilistic approach is capable of handling the correlations between elements (or segments) of the pipeline as well as between different failure modes on the same or different segments. Indeed, a rigorous framework is available for the direct (and accurate) estimation of the values of these correlations. Using FORM procedures, for example, the correlation coefficient, ρ_{ij}, between two components with limit state functions (or safety margins) g_i and g_j are given by:

$$\rho_{ij} = \alpha_i \alpha_j^T$$

where α_i and α_j are the unit direction vectors at the design point (or most probable point) in the standard normal (U) space.

For the specific examples considered in this work so far, we have computed some typical values of ρ_j and found them to be generally 0.99 and 1.0. This clearly shows that the assumption of statistical independence as practiced by many reliability analysts is not correct! It also confirms what should be expected from physical considerations because these high correlations are naturally induced by virtue of the commonality of material properties, demands (loadings, pressures), structural dimensions and modelling uncertainties in many situations.

The following results can be inferred from Fig. 5.13 to Fig. 5.18 for the specific example considered:

- The failure probability of the system increases with increase in the depth of corrosion pit.
- Pits that are below a certain nominal threshold values do not change the value of the system reliability i.e. they do not make any significant contribution to failure probability.
- For increased accuracy, system reliability analysis must take into consideration all possible mechanical failure modes (See Figures A.7 and A.8). We see from the graphs that the predicted system failure probability based on a combination of burst capacity model and pressure collapse

model is significantly different and higher than the system failure probability predicted by the individual failure modes.

Results presented in Table 5.3 to Table 5.5 are based on the burst capacity model described earlier. Table 5.3 summarizes the effect of uncertainty in the modeling uncertainty factor on the failure probability of a component. The variability in the predicted probability shows the need to accurately account for variability in the modeling uncertainty factor. Similar results were obtained for the pressure collapse formulation (Bea, et al, 1998).

Table 5.4 shows the system reliability for the 11 corrosion pits with the same depth. It is seen from the table that system failure probability increases with the number of pits. Furthermore, it is also seen that the system failure probability (0.6838E-03) is not a simple summation of the component failure probabilities. This illustrates the need to execute system reliability analysis when the number of components is greater than one. Similar results were obtained for collapse pressure.

These results clearly show that additional attention must be paid to the system reliability and correlation issues in development of design and requalification criteria for pipelines. In these cases, the results show that the probability of failure for the pipeline system is well evaluated as the probability of failure of the most likely to fail element.

Table 5.3. Effect of uncertainty of the COV of modeling uncertainty factor of burst capacity formulation

COV (%)	Probability of Failure
10	0.2132E-02
15	0.4075E-02
20	0.7633E-02
25	0.1309E-01

Table 5.4. System reliability analysis for corrosion pits with the same depth of corrosion.

No of pits with same corrosion depth	Probability of Failure
1	0.6590E-03
2	0.6838E-03
3	0.7085E-03
4	0.7332E-03
5	0.7579E-03
6	0.7826E-03
7	0.8073E-03
8	0.8320E-03
9	0.8567E-03
10	0.8814E-03
11	0.9061E-03

Table 5.5. Effect of uncertainty of the COV of modeling uncertainty factor of pressure collapse formulation

Coefficient of Variation (%)	Probability of Failure
20	0.3275E-13
25	0.1618E-09
30	0.3795E-07
35	0.7953E-06
40	0.1095E-04
45	0.7162E-04
50	0.2906E-03

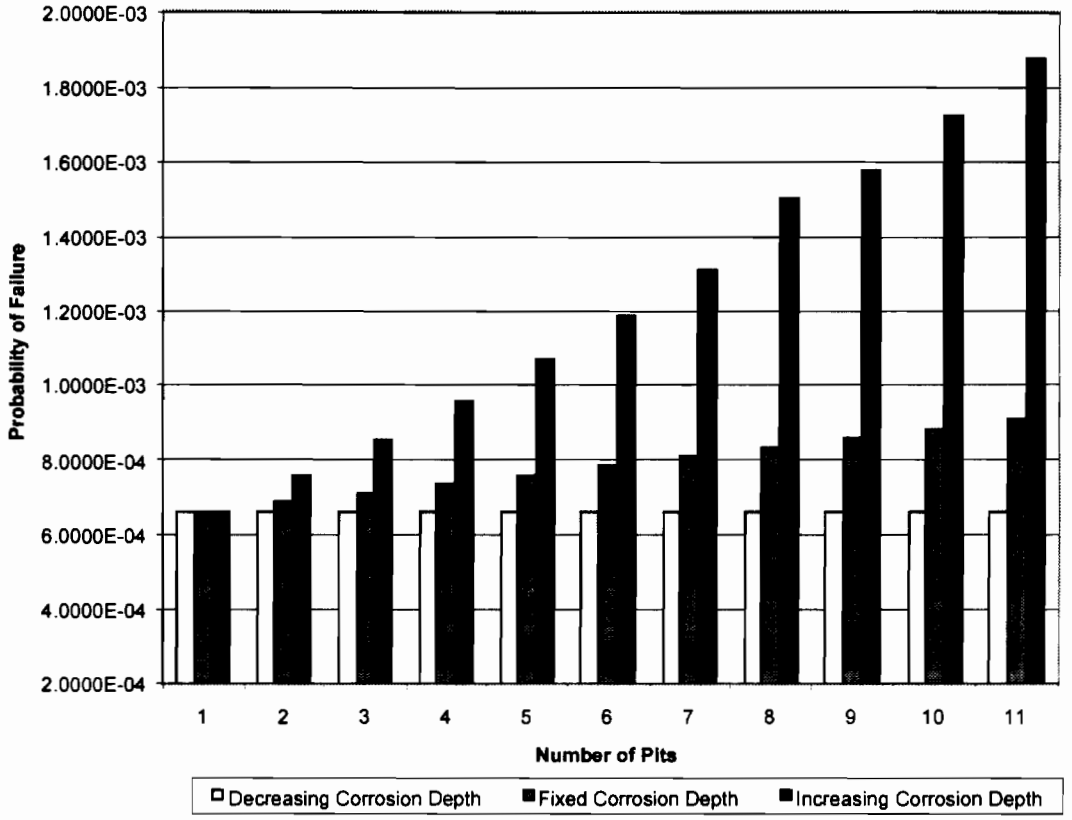

Fig. 5.13. Probability of system failure based on burst capacity failure mode

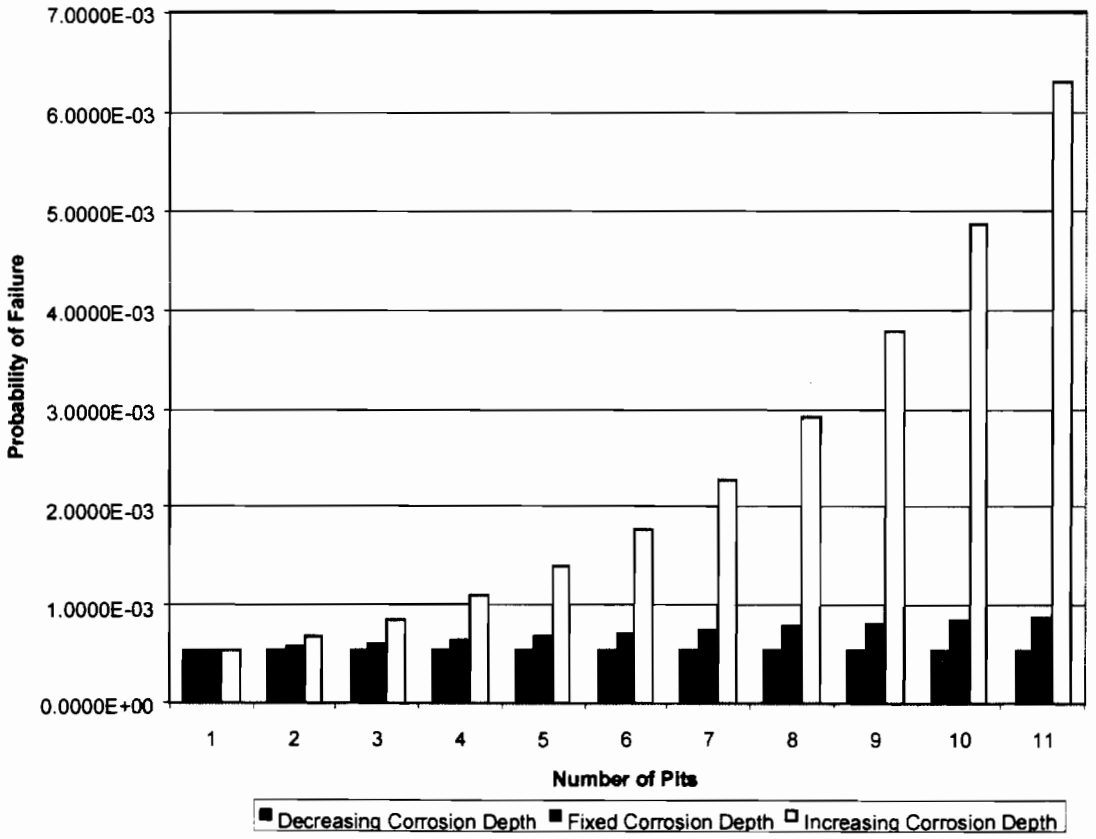

Fig. 5.14. Probability of system failure based on collapse pressure failure mode

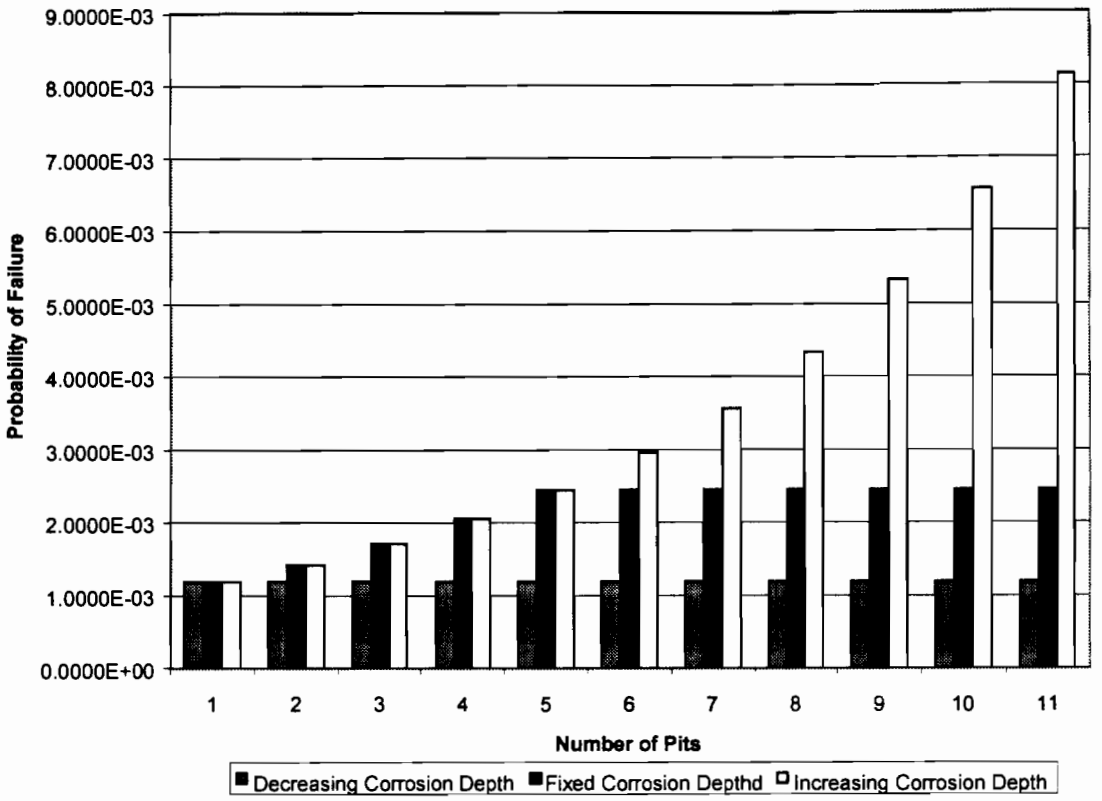

Fig. 5.15. Probability of system failure based on burst capacity and collapse pressure failure modes

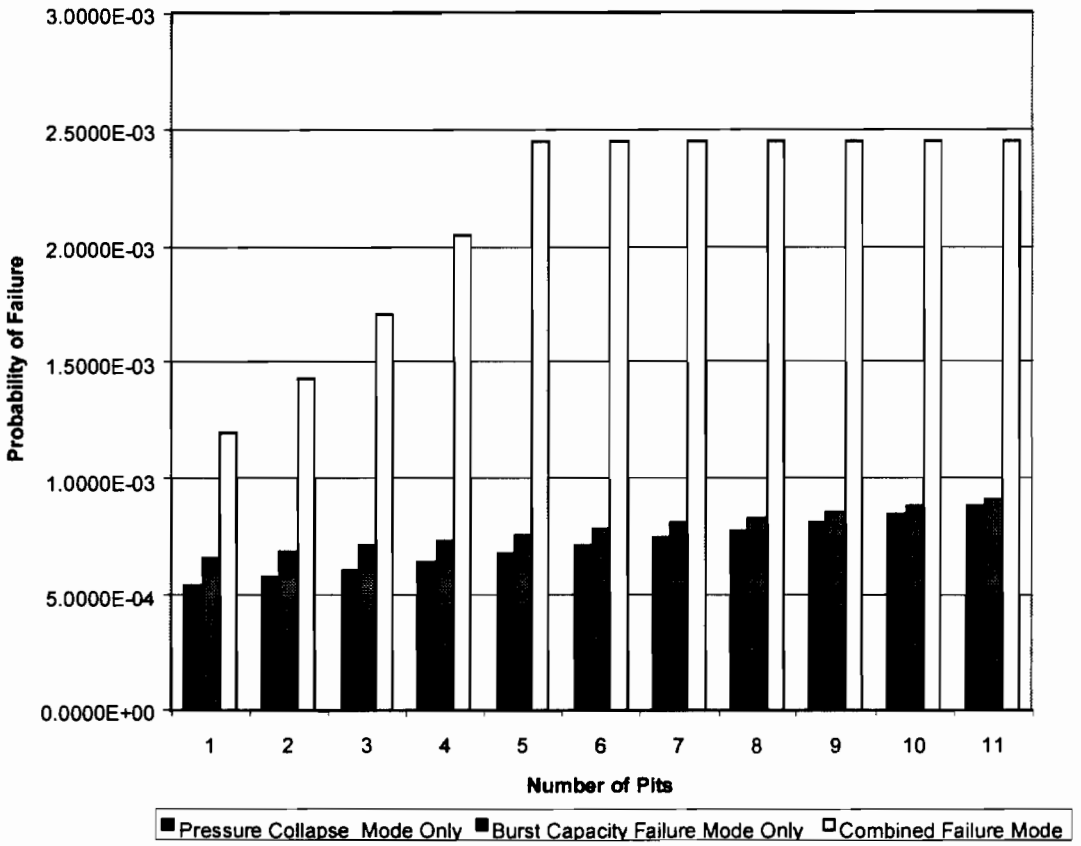

Fig. 5.16. Probability of system failure for corrosion pits of the same depth

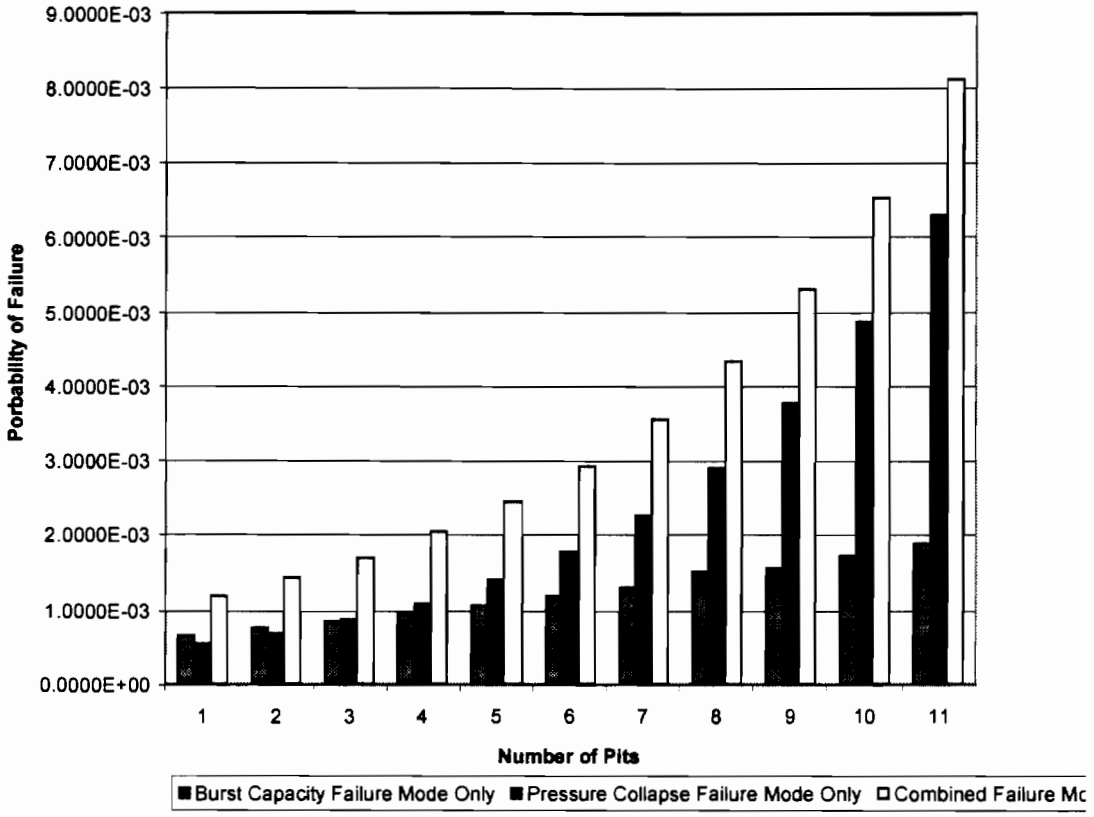

Fig. 5.17. Probability of system failure b for corrosion pits of increasing depth

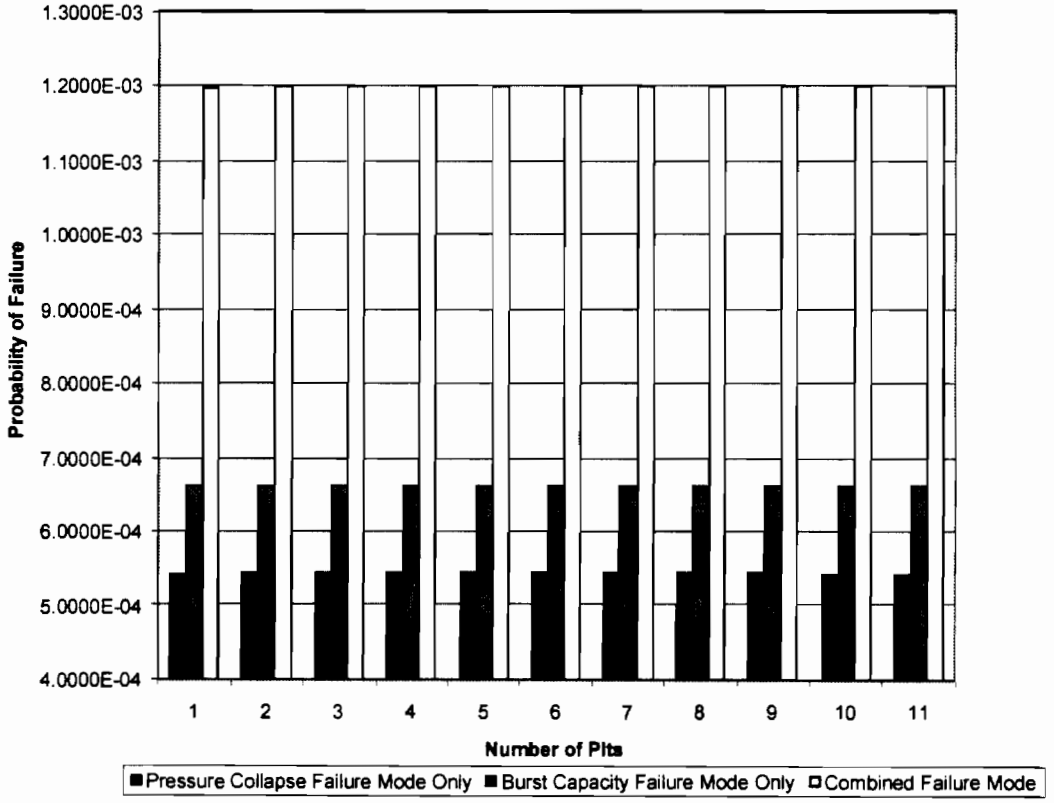

Fig. 5.18. Probability of system failure based on burst capacity for corrosion pits of the decreasing depth

6.0 More on Pipeline Corrosion

6.1 Introduction

Experience with Gulf of Mexico and North Sea pipelines and risers (oil, gas, mixed) clearly shows that the primary operating hazard to the integrity of pipelines and risers is corrosion (Bea, et al, 1999). For pipelines, the primary hazard is internal corrosion. For risers, the primary hazard is external corrosion, especially in the vicinity of the waterline and in the atmospheric zone immediately above the waterline and splash zone protection.

There are three fundamental approaches to evaluate corrosion effects in the reassessment of existing pipelines:

- use of instrumentation and inspections to detect and quantify corrosion defects,
- use of corrosion coupons to quantify corrosion rates, and
- use of analytical models and indirect indicators of corrosivity and corrosion rates.

6.2 Corrosion

Corrosion is a very complex electro-chemical-mechaniccal process that is a function of what is transported in the pipeline or riser, what surrounds the exterior of the pipeline or riser, and how the corrosion is managed. Both pipeline wall thickness and strength can be diminished. Primary corrosion rate determining parameters include temperature, water composition (pH, salinity), and concentration (collection & stagnation sectors); product composition (chemical composition, pH); operational parameters including flow rates, regime, pressures, and oil-water wetting; steel – weld properties including macro and micro structure, alloying elements, and consumables; sulphate reducing bacterial (SRB) count and types; deposits - coatings on the steel surfaces; steel cracking (stress corrosion fatigue); erosion due to the transport of solids and 'stray' currents associated with electrical operating equipment and, and other metals that can come into or are placed in contact with the pipeline.

Anything that can accelerate the transport of electrons from a cathode to an anode will accelerate corrosion, and vice versa. In general, all of the parameters cited can be expected to change during the life of a pipeline because the sources of oil, water, and gas transported through a pipeline are changing and because the external environmental and operational conditions are continuously changing. Similar statements can be made regarding the effects of changes in space along the length and around the perimeter of the pipeline.

Corrosion management is paramount if corrosion is to be controlled in pipelines and risers. Management processes include cathodic protection, dehydration, inhibition, coatings, use of bactericides, pH neutralizers, inspections, instrumentation, and use of coupons to indicate corrosion rates. Once the steel has been lost and its properties degraded, they can not be restored other than by replacement (liners, sleeves). For long-life pipelines, corrosion management, or lack thereof, can pay dividends.

Petroleos Mexicanos (PEMEX) have developed an extensive database on measured (ultrasonic measurements) corrosion in pipelines and risers in the Bay of Campeche (Lara, et al, 1998). Fig. 6.1 identifies the locations in which corrosion was measured. The reported corrosion is based on the maximum loss of metal thickness reported at each location along the pipeline. Two locations are of particular interest: Zone E and Zone F. Zone E is at the lower section of the riser. Zone F is in the expansion loop portion of the pipeline. The reported corrosion in these zones is internal.

The pipelines range in diameter from 406 mm to 914 mm. The pipelines generally transport low sulfur oil, gas, and oil and gas that ranges in temperature from 30° C (average water temperature) to

110° C with an average of about 80° C. Bacterial counts are low due to the generally very high temperature products. These pipelines are cathodically protected with sacrificial anodes supplemented with pipeline coatings.

Fig. 6.2 summarizes corrosion rate data from all of the pipelines in Zones E and F. The median corrosion rate is 0.015 inches per year for both Zones. The corrosion rate has a Coefficient of Variation of 68 %. Fig. 6.3 and Fig. 6.4 summarize data for the oil, and gas service pipelines as a function of their age. The term 'average' refers to the average of the maximum wall thickness loss over a given period of time.

There is a definite decrease in the corrosion rates with time for all services. The initial rates of corrosion for gas lines are generally about half those associated with the oil lines. The rate of corrosion is much higher early in the life of the pipeline.

Fig. 6.5 and Fig. 6.6 summarize pipeline corrosion rates for pipelines that are 17 to 19 years old. The median rate of corrosion for oil pipelines is 0.015 in / yr (15 mills per yr, mpy). The oil pipelines corrosion rate has a Coefficient of Variation (COV) of 40%. The median rate of corrosion for gas pipelines is 0.010 in/yr (10 mpy). The gas pipelines corrosion rate has a COV of 40%.

This is extremely useful data for the prediction of corrosion rates for this particular population of pipelines. Due to the unique characteristics of the products and environment, the data can not be easily applied to other populations of pipelines.

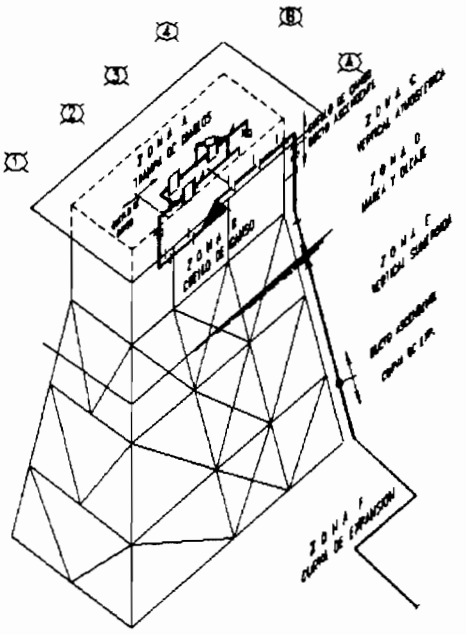

Fig. 6.1. Zones for corrosion gauging inspections

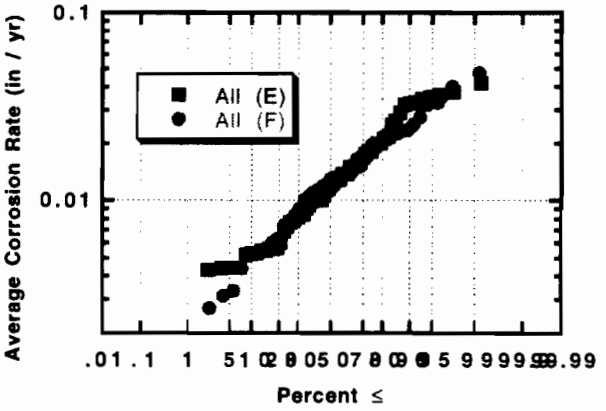

Fig. 6.2. Corrosion rate data for all pipelines (Lognormal probability scales)

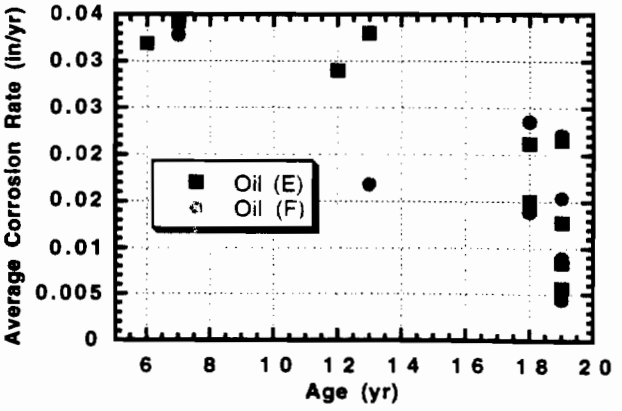

Fig. 6.3. Oil service corrosion rates as function of pipeline age

6.3 Corrosion Effects on Burst Capacity

The formulations developed during this study (RAM PIPE REQUAL) (Bea, et al, 1998) to assess the burst capacities of pipelines subjected to general corrosion are:

$$Pbd = 2.0\ t\ SMTS / (D - t)\ SCF$$

$$Pbd = 2.4\ t\ SMTS / (D - t)\ SCF$$

$$SCF = 1 + 2\ (d / R)^{0.5}$$

where Pbd is the burst pressure capacity of the corroded pipeline, t is the nominal wall thickness (including the corrosion allowance), D is the pipeline outside diameter, SMTS is the specified minimum tensile strength (-3σ), and SCF is a stress concentration factor that is due to the corrosion

features. The SCF is a function of the depth of corrosion, d (d≤t), and the pipeline radius, R. This formulation was chosen because study of the failure mechanisms associated with burst of naturally corroded mild steel pipelines (corroded over more than 10% of the circumference) indicated that it was the corrosion feature induced local stress increase that was controlling the rupture of the pipeline wall (ductile tearing mode of failure). The SCF (maximum hoop stress / nominal hoop stress) that is due to a notch of depth d in the pipeline cross section that has a radius R (Miller, 1987). Note that Eq. 1 and Eq. 2 do not explicitly incorporate the area (length, width) of the pipeline that is corroded. The area is included implicitly in the radius of the corrosion feature (the pipe radius) and the definition of the SCF (plain strain condition). The hoop stress coefficient of 2.0 in Eq. 1 is multiplied by 1.2 in Eq. 2 to develop an unbiased estimate of the median transverse ultimate tensile strength of the pipeline steel.

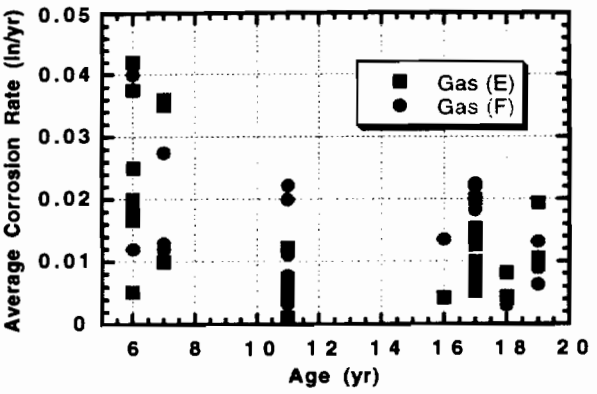

Fig. 6.4. Gas service corrosion rates as function of pipeline age

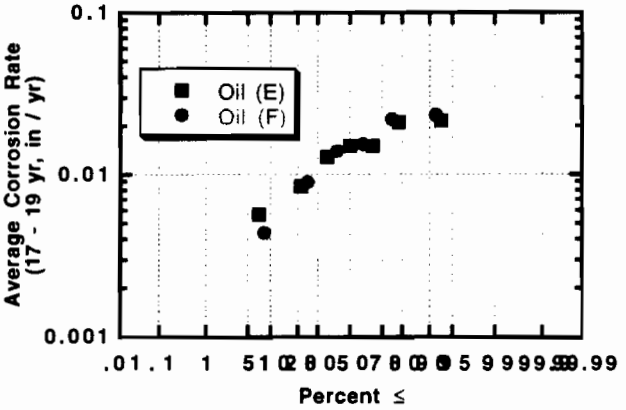

Fig. 6.5. Oil pipeline corrosion rates for ages 17 – 19 years (Lognormal probability scales)

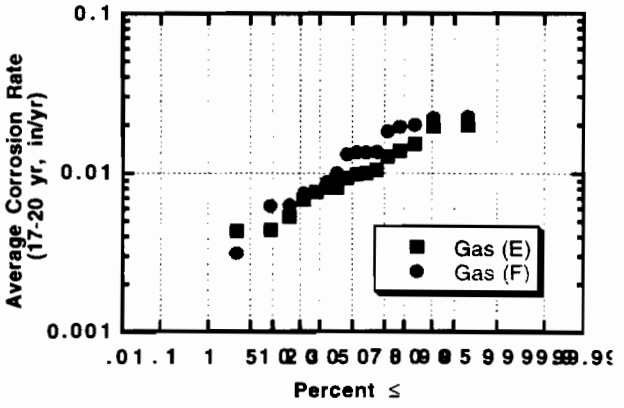

Fig. 6.6. Gas pipeline corrosion rates for 17 – 19 years (Lognormal probability scales)

A test database consisting of 151 burst pressure tests on corroded pipelines was assembled from tests performed by the American Gas Association, NOVA, British Gas, and the University of Waterloo (Bea, et al, 1998). The Pipeline Research Committee of the American Gas Association published a report on the research to reduce the excessive conservatism of the B31G criterion (Kiefner and Vieth 1989). 86 test data were included in the AGA test data. The first 47 were used to develop the B31G criterion, and were full scale tests conducted at Battelle Memorial Institute. The rest of the 86 tests were also full scale and were tests on pipe sections removed from service and containing real corrosion.

Two series of burst tests of large diameter pipelines were conducted by NOVA during 1986 and 1988 to investigate the applicability of the B31G criterion to long longitudinal corrosion defects and long spiral corrosion defects. These pipes were made of grade 414 (X60) steel with an outside diameter of 4064 mm and a wall thickness of 50.8 mm. Longitudinal and spiral corrosion defects were simulated with machined grooves on the outside of the pipe. The first series of tests, a total of 13 pipes, were burst. The simulated corrosion defects were 203 mm wide and 20.3 mm deep producing a width to thickness ratio (W/t) of 4 and a depth to thickness ratio (d/t) of 0.4. Various lengths and orientations of the grooves were studied. Angles of 20, 30, 45 and 90 degrees from the circumferential direction, referred to as the spiral angle, were used. In some tests, two adjacent grooves were used to indicate interaction effects. The second series of tests, a total of seven pipes, were burst. The defect

geometries tested were longitudinal defects, circumferential defects, and corrosion patches of varying W/t and d/t. A corrosion patch refers to a region where the corrosion covers a relatively large area of pipe and the longitudinal and circumferential dimensions were comparable. In some of the pipes, two defects of different sizes were introduced and kept far enough apart to eliminate any interaction.

Hopkins and Jones (1992) conducted five vessel burst tests and four pipe ring tests. The pipe diameter were 508 mm. The wall thickness was 102 mm. The pipe was made of X52. The defect depth was 40% of the wall thickness. Jones et al (1992) also conducted nine pressurized ring tests. Seven of the nine were machined internally over 20% of the circumference, the reduced wall thickness simulating smooth corrosion. All specimens were cut from a single pipe of Grade API 5L X60 with the diameter of 914 mm and wall thickness of 22 mm.

As part of a research project performed at the University of Waterloo, 13 burst tests of pipes containing internal corrosion pits were reported by Chouchaoui, et al (1992). In addition, Chouchaoui et al reported the 8 burst tests of pipes containing circumferentially aligned pits and the 8 burst tests of pipes containing longitudinally aligned pits.

The database was analyzed to determine the statistics of the Bias where the Bias is the ratio of the test burst pressure (rupture of the pipe wall) divided by the predicted (analytical) burst pressure. Analysis of the test data based on Eq. 1 (Fig. 6.7) indicated a median Bias of 1.2 and a Coefficient of Variation (COV) of the Bias of 22 %. Analysis of the test data based on Eq. 2 indicated a median Bias of 1.0 and a COV of the Bias of 22 %. The 1.2 factor was found to be the ratio of the expected ultimate tensile strength to the nominal tensile strength.

Fig. 6.8 summarizes the test database in the form of the measured burst pressure for the corroded condition divided by the burst pressure for no corrosion (Pbm / Pbo) versus the corrosion depth divided by the nominal wall thickness of the pipeline specimens (d/t). There is a large scatter in the Pbm / Pbo for larger values of d/t. Note that even at values of d/t ≥ 0.7, the pipeline can sustain as much as 80% of the uncorroded burst pressure (and as low as 40%).

The DNV (1999, 1993) and the B31G (effective area) (1993) formulations to determine the burst pressures of corroded pipelines include parameters to define the area (length, width, plan geometry) characteristics of the corrosion features. The formulation developed during this study does not include explicit parameters to define the area characteristics of the corrosion features. The 151 physical test database was analyzed to determine if there were

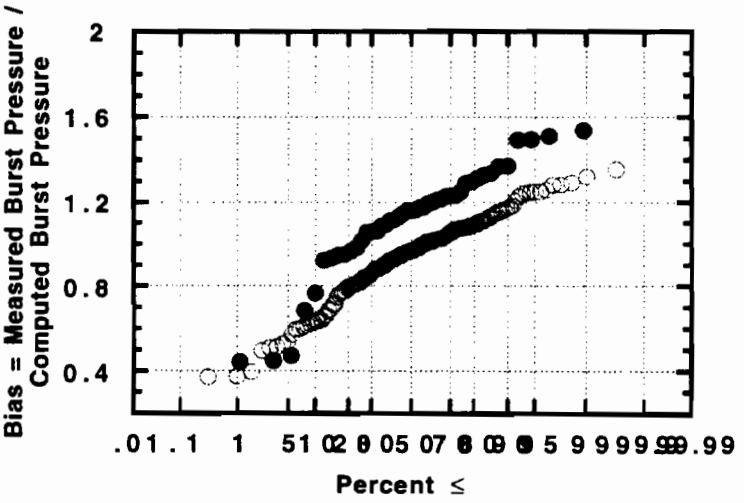

Fig. 6.7. Bias in design formulations based on SMTS

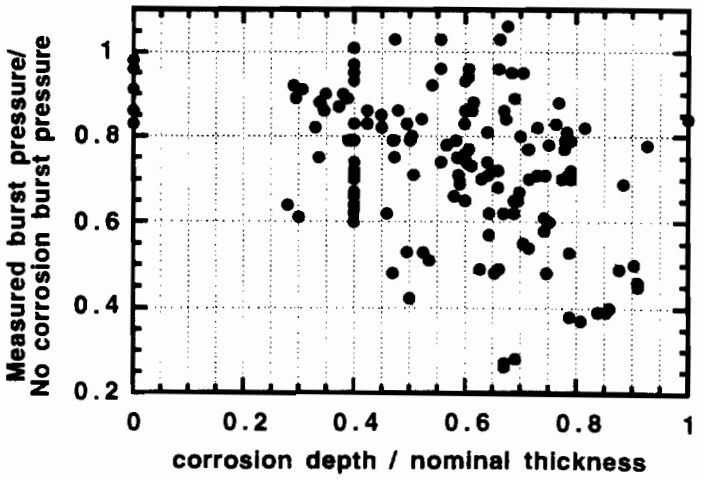

Fig. 6.8. Variation in burst pressure ratio with d/t

definitive trends in the burst pressures that depended on the corrosion area characteristics. The test burst pressures are normalized by the hoop stress at the specified minimum tensile strength (SMTS). The results are summarized in Fig. 6.9, Fig. 6.10, and Fig. 6.11 for the corrosion area defined in terms of its length, its area (length times width), and the term included in the DNV and B31G formulations (square root of the square of the length of the corrosion feature divided by the pipe diameter times the wall thickness), respectively. No definitive trends in the test burst pressures with the corrosion area characteristics were found.

To investigate this finding farther, the DNV (1999), B31G (1993), and the RAM PIPE REQUAL formulations were used to determine the burst pressure bias (measured burst pressure divided by predicted burst pressure). The results for the 151 physical tests are summarized in Fig. 6.12 and Fig. 6.13. These tests included specimens that had corrosion depth to thickness ratios in the range of 0 to 1 (Fig. 13). The statistical results from the data summarized in Fig. 12 are summarized in Table 6.1. The formulation developed during this study has the median bias closest to unity and the lowest COV of the bias. The DNV 99 formulation has a lower bias than B31G, but the COV of the Bias is about the same as for B31 G. The B31G mean Bias and COV in Table 1 compares with values of 1.74 and 54 %, respectively, found by Bai, et al (1997). The burst pressure test data were reanalyzed to include only those tests for d/t = 0.3 to 0.8. The bias statistics were relatively insensitive to this partitioning of the data.

A last step in the analysis of the physical test database was to analyze the Bias statistics based on only naturally corroded specimens (40 of 151 tests). The results are summarized in Fig. 6.14 and Table 6.2. The Bias statistics for the DNV 99 and B31G formulations were affected substantially. The results

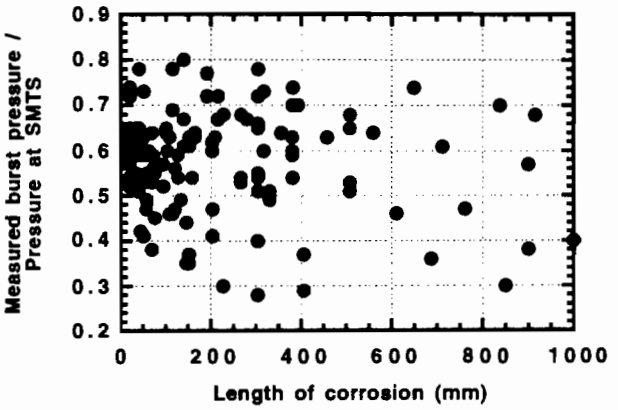

Fig. 6.9. Pipeline test burst pressures as function of length of corrosion

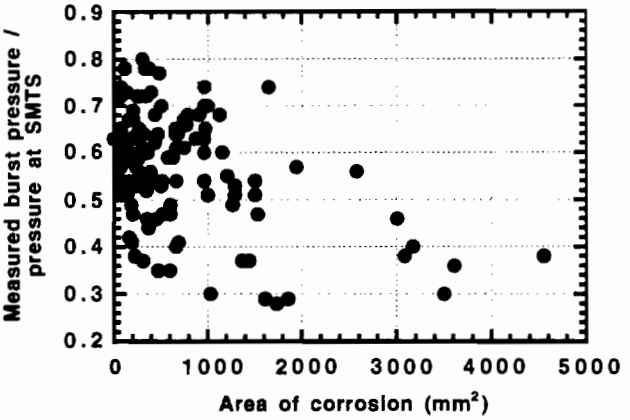

Fig. 6.10. Pipeline test burst pressures as function of area of corrosion

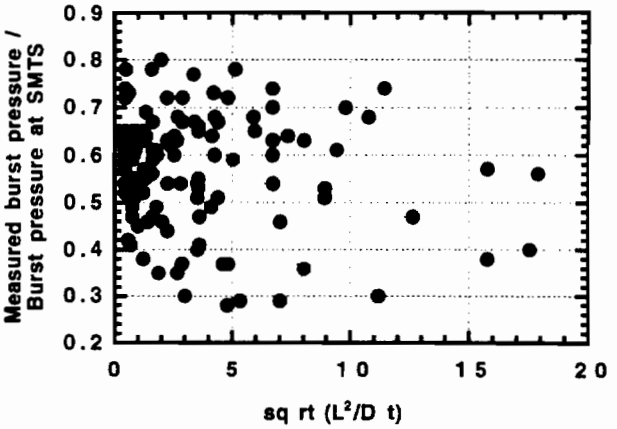

Fig. 6.11. Pipeline test burst pressures as function of corrosion area parameter

Table 6.1. Summary of Bias statistics for three burst pressure formulations (d/t = 0 to 1)

Formulation	B mean	B_{50}	V_B %
DNV 99	1.46	1.22	56
B 31 G	1.71	1.48	54
RAM PIPE	1.01	1.03	22

Table 6.2. Summary of Bias statistics for three burst pressure formulations – naturally corroded tests

Formulation	B mean	B_{50}	V_B %
DNV 99	2.10	1..83	46
B 31 G	2.51	2.01	52
RAM PIPE	1.00	1.1	26

indicate that the machined specimens develop lower burst pressures than their naturally corroded counterparts.

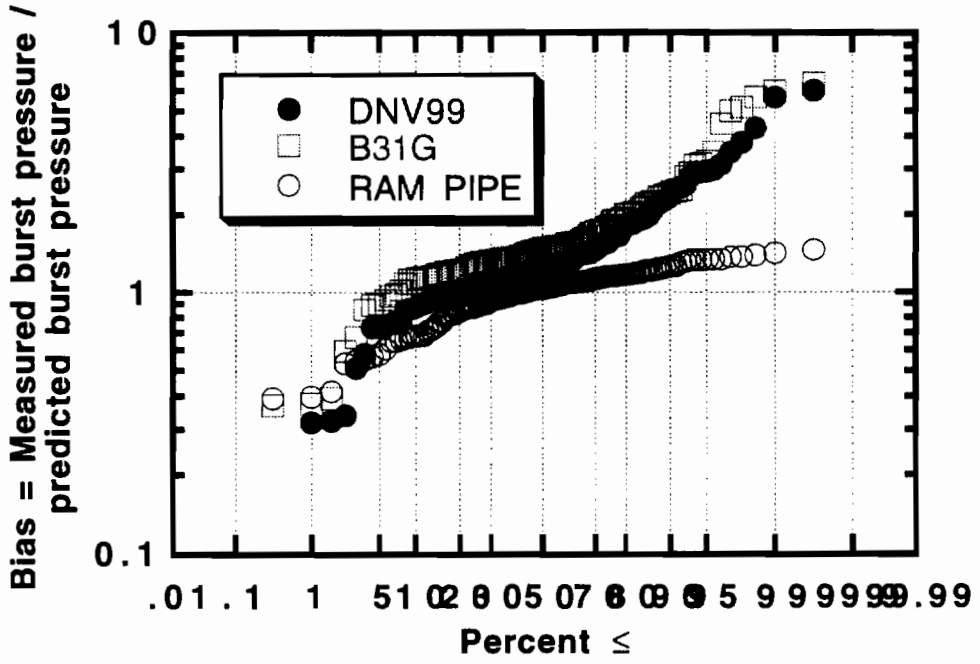

Fig. 6.12. Bias in burst pressure formulations (Lognormal probability scales)

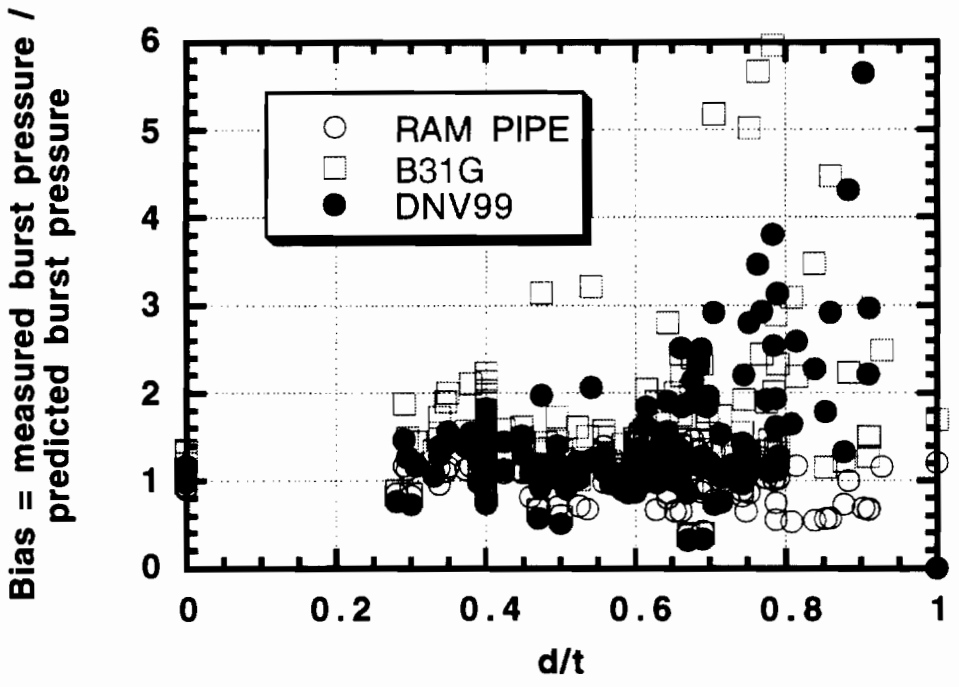

Fig. 6.13. Bias in burst pressure formulations as function of corrosion depth to wall thickness ratio (d/t)

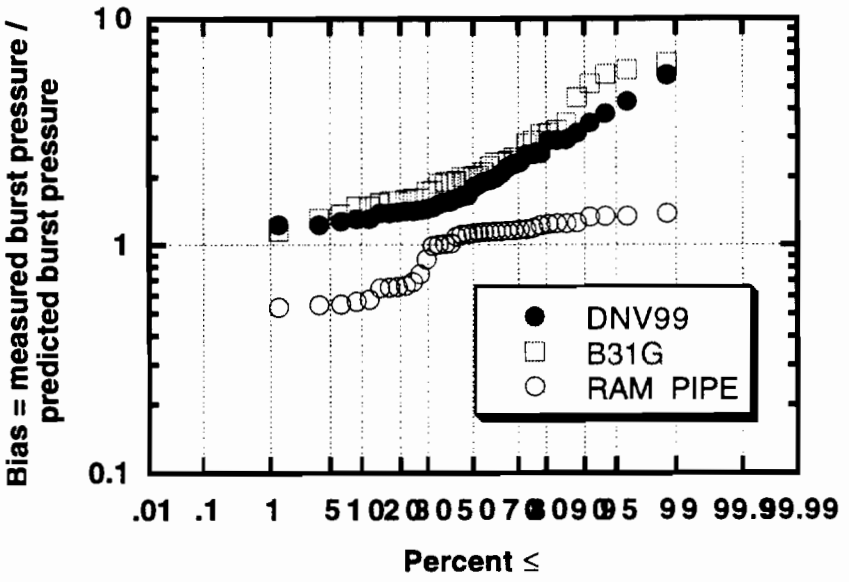

Fig. 6.14. Bias in burst pressure formulations for naturally corroded test specimens (Lognormal probability scales)

6.4 Corrosion – Time Dependent Reliability

Pipeline reliability is a time dependent function that is dependent on the corroded thickness of the pipeline ($t_{ci/e}$). The corroded thickness is dependent on the rate of corrosion and the time that the pipeline or riser is exposed to corrosion. This time dependency can be clarified with the following expression for a time dependent Safety Index:

$$\beta = \ln (Kp\ t - Kp\ t_{ci/e}) / \sigma_{lnp/R}$$

where:

$Kp = (2.4\ SMTS / D\ SCF\ Po)$

Po is the median maximum operating pressure. $t_{ci/e}$ is the wall thickness loss due to internal and external corrosion. $\sigma_{lnp/R}$ is the total uncertainty (standard deviation of the logarithms) in the burst pressure capacity and the maximum operating pressure. The foregoing formulation is based on Lognormally distributed burst pressure capacities and peak internal pressures.

If one defines:

$$Kp\ t = FS_{50}$$

where FS_{50} is the median factor of safety in the burst capacity of the pipeline or riser. Then:

$$\beta = \ln (FS_{50} - FS_{50}\ (t_{ci/e} / t)) / \sigma_{lnp/R}$$

As the pipeline corrodes, the reduction in the pipeline or riser wall thickness leads to a reduction in the median factor of safety that in turn leads to a reduction in the Safety Index (or an increase in the probability of failure). In addition, as the pipeline corrodes, there is an increase in the total uncertainty due to the additional uncertainties associated with the corrosion rates and their effects on the burst capacity of a pipeline or riser.

An analytical model for the increase in total uncertainty as a function of the corrosion can be expressed as:

$$\sigma_{lnp/R}|t = \sigma_{lnp/R}|to\ (1 - t_{ci/e} / t)^{-1}$$

where $\sigma_{lnp/R}|t$ is the uncertainty at any given time, t, $\sigma_{lnp/R}|to$ is the uncertainty at time t = 0, $t_{ci/e}$ is the corroded thickness and t is the initial thickness. When $t_{ci/e}$ / t = 0.5 the initial uncertainty would be increased by a factor of 2. Results for $\sigma_{lnp/R}|to$ = 0.2 and = 0.30 and FS_{50} = 2.0 (same as median bias used previously) are summarized in Fig. 6.15.

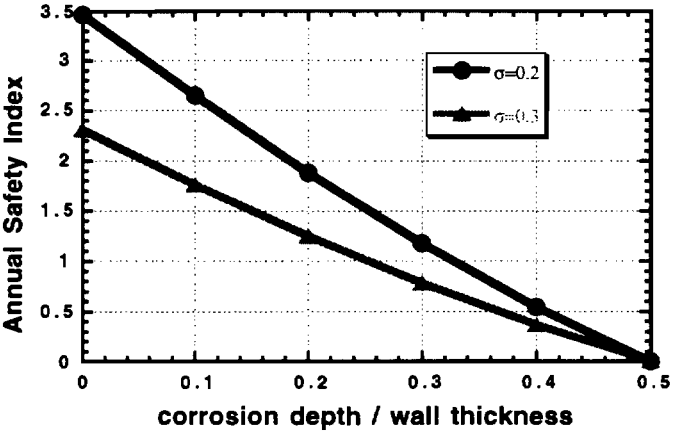

Fig. 6.15. Influence of corrosion depth and uncertainty on annual Safety Index

Additional insight into the change in the uncertainty associated with the pipeline capacity associated with the loss of wall thickness due to corrosion, can be developed by the following:

$$\bar{t}' = \bar{t} - \bar{d}$$

t' is the wall thickness after the corrosion, t is the wall thickness before corrosion, and d is the maximum depth of the corrosion loss. Bars over the variables indicate mean values.

Based on First Order – Second Moment methods, the standard deviation of the wall thickness after corrosion can be expressed as:

$$\sigma_{t'} = \sqrt{\sigma_t^2 + \sigma_d^2}$$

The Coefficient of Variation (COV = V) can be expressed as:

$$V_{t'} = \frac{\sigma_{t'}}{\bar{t}'} = \frac{\sqrt{(V_t \bar{t})^2 + (V_d \bar{d})^2}}{\bar{t} - \bar{d}}$$

A representative value for the COV of t would be 2%. A representative value for the COV of d would be Vd = 40%. Fig. 6.16 summarizes the foregoing developments for a 16-in. ((406 mm) diameter pipeline with an initial wall thickness of t = 0.5 in. (17 mm) that has an average rate of corrosion of 10 mpy (0.010 in. / yr, 0.25 mm / yr). The dashed line shows the results for the uncertainties associated with the wall thickness. The solid line shows the results for the uncertainties that include those of the wall thickness, the prediction of the corrosion burst pressure, and the variabilities in the maximum operating pressure.

At the time of installation, the pipeline wall thickness COV is equal to 2%. But, as time develops, the uncertainties associated with the wall thickness increase due to the large uncertainties associated with the corrosion rate – maximum depth of corrosion. The solid line that reflects all of the uncertainties converges with the dashed line that represents the uncertainties in the

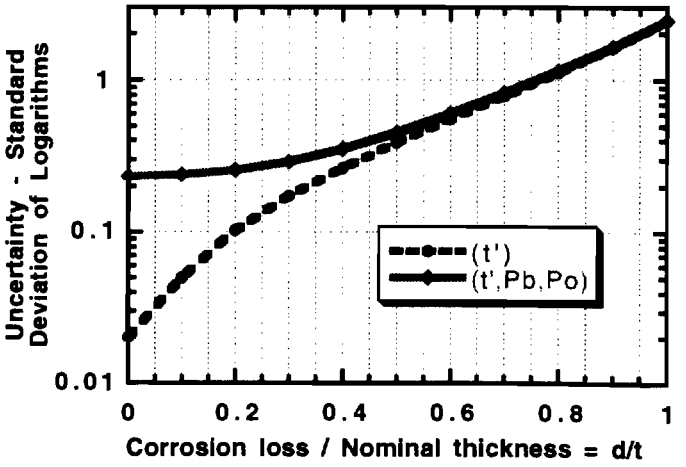

Fig. 6.16. Uncertainty in pipeline wall thickness and burst pressure capacity as a function of the normalized loss in pipeline wall thickness.

remaining wall thickness, until at a time of about 20 years, the total uncertainty is about the same as that of the remaining wall thickness (Vt-d ≈ 25 %). As more time develops, there is a dramatic increase in the COV associated with the remaining wall thickness. These uncertainties are dominated by the uncertainties attributed to the corrosion processes.

These observations have important ramifications on the probabilities of failure – loss of containment of the pipeline. After the 'life' of the pipeline is exceeded (e.g. 20 to 25 years), one can expect there to be a rapid and dramatic increase in the uncertainties associated with the corrosion processes. In addition, there will be the continued losses in wall thickness. Combined, these two factors will result in a dramatic increase in the probability of failure of a pipeline.

Fig. 6.17 summarizes example results for a 16-in. (406 mm) diameter, 0.5 in (13 mm) wall thickness pipeline that has a maximum operating pressure (MOP) of 5,000 psi (34.5 Mpa). The COV associated with the MOP is 10 %. The pipeline is operated at the maximum pressure, and at 60 % of the maximum operating pressure for a life of 0 to 50 years. The average corrosion rate was taken as 10 mpy. For the 60 % pressured line, during the first 20 years, the annual probability of failure rises from 1E-7 to 5 E-3. After 20 years, the annual probability of failure rises very quickly to values in the range of 0.1 to 1. Perhaps, this is why the observed pipeline failure rates associated with corrosion in the Gulf of Mexico are in the range of 1 E-3 per year (Bea, et al, 1999).

Fig. 6.18 shows the time dependent operating pressures for a 762 mm diameter, 25 mm wall thickness, X60 pipeline that transports crude oil over a distance of 50 km (Collberg, Cramer, Bjornoy, 1996). The operating pressures decrease from a maximum of 3,000 psi (20.7 Mpa, inlet) at the time of commissioning to a maximum of 2,300 psi (15.9 Mpa) at 20 years.

The corrosion in the pipeline is modeled as a time dependent process that is organized into three stages (Fig. 6.19). The first stage (5 years) is when there is no significant water-cut in the oil stream. The pipeline is effectively

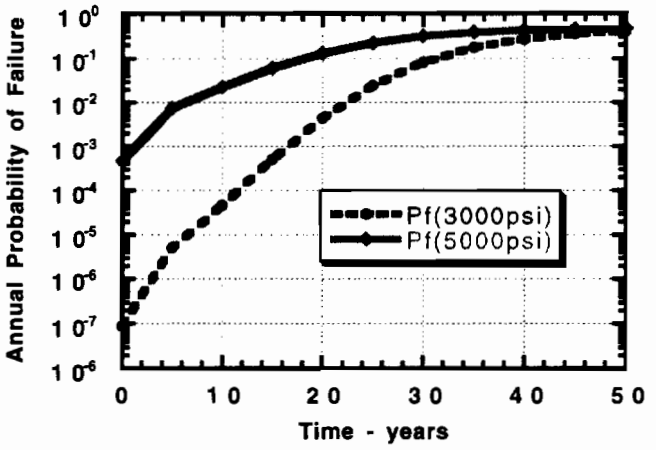

Fig. 6.17. Example pipeline failure rates as function of exposure to corrosion

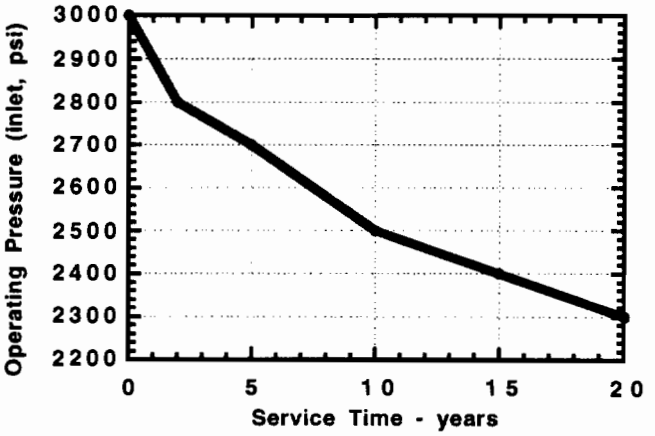

Fig. 6.18. Example pipeline service time maximum operating pressures

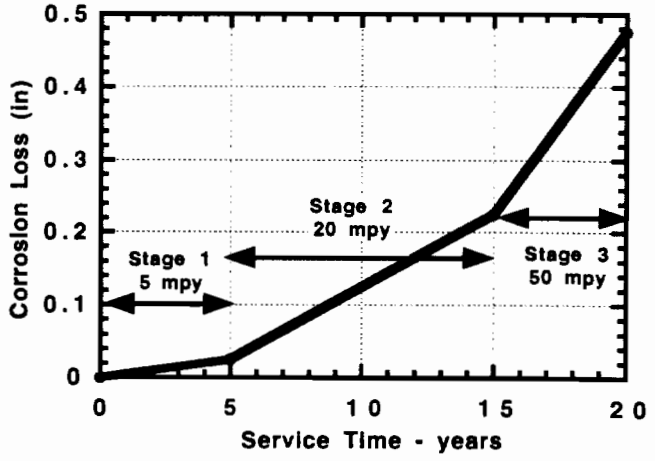

Fig. 6.19. Example pipeline loss of wall thickness due to corrosion

protected by the oil wetting of the steel. The best estimate average corrosion rate during Stage 1 is estimated to be 5 mpy. The second stage (10 years) is when there is a significant (above 40 %) water cut in the oil stream. Salt water is in contact with significant portions of the horizontal sections of the pipeline. The best estimate average corrosion rate during this stage is estimated to be 20 mpy. The third stage (5 years) is when there is significant SRB count (above 1E4) due to water flooding of the reservoir with untreated sea water. The best estimate average corrosion rate during this period is estimated to be 50 mpy.

Fig. 20 summarizes the result of the evaluation of the annual probabilities of loss of containment as a function of the service time. This example recognizes the time changes of the operating pressures (COV = 10 %), corrosion rates, and uncertainties associated with the corrosion losses (COVd = 40 %).

In Stage 1, there is a relatively rapid rise in the probabilities of failure early in the life of the pipeline due to the increased uncertainties associated with the corrosion damage and the prediction of the burst pressure capacities of the corroded pipeline. In Stage 2, there is a leveling off of the probabilities of failure due to the compensating effects of the lowered operating pressures and the increased corrosion rate and uncertainties associated with the corrosion damage. In Stage 3, there is again a rapid increase in the probabilities of failure due to the large increase in corrosion damage associated with the sulphate reduction bacteria (SRB) effects.

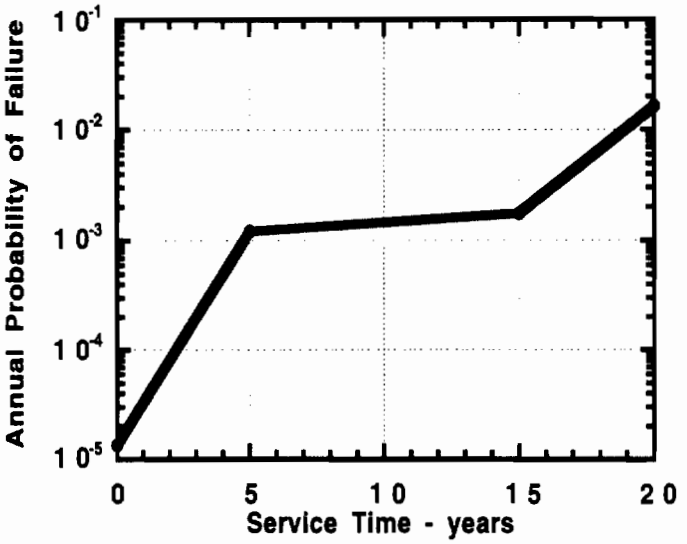

Fig. 6.20. Probabilities of failure as function of service period

7.0 Acknowledgements

The names on the cover of this report do not include the management, engineering, and operating personnel of PEMEX and IMP that provided extensive information, data, analysis results, and financial support to perform this project. Special appreciation is expressed to Oscar Valle, Leonel Lara, Juan Matias, Ernesto Heredia, Juan Horrillo, Rafael Ramos, Roberto Ortega, and Victor Valdes.

Appreciation is expressed to Dr. Charles Smith, Mr. Bob Smith, and Mr. Alex Alvarado of the U. S. Minerals Management Service. Dr. Smith, Mr. Smith and Mr. Alvarado provided technical guidance, data on pipeline failures in the Gulf of Mexico, information on pipeline capacities, and financial support to perform this project.

This project was conducted in conjunction with a project for PEMEX and IMP to develop criteria and guidelines for design of marine pipelines and risers. This project received significant technical input and direction from Dr. Al Mousselli (ApTech, Houston, Texas), Dr. Yong Bai (J. P. Kenny, Stavanger, Norway), and Dr. I. R. (Wally) Orisamolu (Martec, Halifax, Canada). This input and direction had direct influences on the developments in this project.

Important insights were also developed from discussions with Johannes Rosenmoller (In-line instrumentation, Rosen Engineering, Lingen, Germany), Sam Mishael (Chevron Corporation, San Francisco, California), and Khlefa Esaklul (corrosion, BP, Houston, Texas).

8.0 References

Advanced Mechanics and Engineering Ltd. (AME) (1991) "Pipeline and Riser Loss of Containment Study - 1990" Report to Health and Safety Executive, OTH 91, 337, HSE Books, London

Advanced Mechanics and Engineering Ltd. (AME) (1995) "PARLOC 942 The Update of Loss of Containment Data for Offshore Pipelines" Report to Health and Safety Executive, OTH 93, 424, HSE Books, London

Advanced Mechanics and Engineering Ltd. (AME) (1993) "The Update of Loss of Containment Data for Offshore Pipelines" Health and Safety Executive Books, Scheffield, J.K., T95468, London

Ahmed, S., and Koo, B., (1990) "Improved Reliability Bounds of Structural Systems", ASCE Journal of Structural Engineering, Vol. 116, Pp. 3138-3147

Allen, D.W., Lammert, W.F., HAle, J.R., and Jacobsen, V., (1989) "Submarine Pipeline On-Bottom Stability: Recent AGA Research", Proceedings of Offshore Technology Conference, OTC 6055, Society of Petroleum Engineers, Richardson, TX.

American Petroleum Institute API RP 1111 (1997) "Design, Construction, Operation, and Maintenance of Offshore Hydrocarbon Pipelines (Limit State Design)"

American Petroleum Institute (API) (1980) "Bulletin 5C2 on Performance Properties of Casing, Tubing and Drill Pipe", Production Department, Dallas, USA

American Petroleum Institute, (1993) "Recommended Practice for Planning, Designing and Constructing Fixed Offshore Platforms - Load and Resistance Factor Design (RP 2A-LRFD), Washington, D.C.

Andersen, T.L., (1990) "Elastic-Plastic Fracture Mechanics-A Critical Review", Ship Structure Committee Report, Washington, D.C.

Ang, A. H-S, and Tang, W.H., (1984) "Probability Concept in Engineering Planning and Design" Vol. I & II, John Wiley & Sons, Inc., New York

ASME B31G (1993) "Manual for Determining the Remaining Strength of Corroded Pipelines", American Society of Mechanical Engineers

Bai, Y., et al (1993) "Tube Collapse under Combined Pressure, Tension and Bending", International Journal of Offshore and Polar Engineering, Vol. 3, pp. 99-115

Bai, Y., et al (1994) "Ultimate Limit States for Pipes under Combined Tension and Bending", International Journal of Offshore and Polar Engineering, Vol. 4 pp312-319

Bai, Y., et al (1997a) "Reliability Based Design & Requalification Criteria for Longitudinally Corroded Pipelines", Proceedings of 8th International Conference on Offshore and Polar Engineering

Bai, Y., et al (1997b) "Tube Collapse under Combined External Pressure, Tension and Bending", Journal of Marine Structure

Bai, Y., et al (1997c) "Limit State Based Design of Offshore Pipelines", Proceedings of the 18th Offshore Mechanics and Arctic Engineering,

Bai et al (1998a) "Analytical Collapse Capacity of Corroded Pipes", The 19th International Offshore Mechanics and Arctic Engineering Conference

Bai et al (1998b) "Design Through Analysis Applying Limit State Concepts and Reliability Methods", Proceedings of the 8th International Offshore and Polar Engineering Conference, Montreal Canada

Bal, C., and Rosenmoeller, J., (1997) "Can Pipeline Risk Assessment Studies Rely on Rosen Intelligent Pig Surveys", Proceedings of the International Conference on Pipeline Rehabilitation & Maintenance, Abu Dhabi, UAE.

Batte, A.D., Fu, F., Kirkwood, M. G., and Vu, D., (1997) "New Methods for Determining the Remaining Strength of Corroded Pipelines", The Proceedings of the 18th Offshore Mechanics and Arctic Engineering Conference, Yokohama, Japan

Bea, R.G. (1992) "Marine Structural Integrity Program (MSIP)", Ship Structure Committee Report SSC 365, Washington, DC

Bea, R. G., (1998) "Reliability Assessment & Management (RAM) Criteria for Design & Reassessment of Pipelines and Risers in the Bay of Campeche", Report to Petroleos Mexicanos and Instituto Mexicano del Petroleo

Bea, R. G., (1997) "Risk Based Criteria for Design & Requalification of Pipelines and Risers in the Bay of Campeche", Report to Petroleos Mexicano, Instituto Mexico del Petroleo, and Brown and Root International Inc., Marine Technology and Management Group, University of California at Berkeley.

Bea, R.G., (1998) "Marine Structural Integrity Programs: Inspection, Maintenance, Repairs", Proceedings of International Symposium on Offshore Hydrocarbons Exploitation Technologies", Petroleos Mexicanos and Instituto Mexicano de Petroleo, Cuidad del Carmen, Campeche, Mexico

Bea, R.G., (1998) "Risk Assessment & Management of Marine Pipelines : RAM PIPE", Proceedings of Risk Assessment & Management of Marine Pipeline Systems Workshop, Houston, TX

Bea, R.G., Xu, T., (1997) "In-Service Inspection Program for Marine Structures", Proceedings of the Offshore Mechanics and Arctic Engineering Conference, Yakohama, Japan, American Society of Mechanical Engineers, New York, New York

Bjorney, O.H., Cramer, E.H., and Sigurdson, G., (1997) "Probabilistic Calibrated Design Equation for Burst Strength Assessment of Corroded Pipes", Proceedings of the 7th International Offshore and Polar Engineering Conference, Honolulu, The International Society of Offshore and Polar Engineers, Golden, CO

British Standard Institute 8010 (1993) "Code of Practice for Subsea Pipeline" Part 3, London

Bruschi, R., Dumitrescu, A., Sintini, L., Tura, F., (1994) "Laying Large Diameter Pipelines in Deep Waters", Proceedings of the 13th International Conference on Offshore Mechanics and Arctic Engineering, ASME, Houston, Texas

Brushi, R., Malacari, L.E., Torselletti, E., and Vitali, L., (1995) "Concrete Coated Submarine Pipelines: Further Advances in Strain Concentration at Field Joints and Relevant Implications on Strain Based Design", OTC paper 7858, Proceedings of the Offshore Technology Conference, Houston, Texas

Bruschi, Roberto, Monti Paolo, Bolzoni, Gianluca, and Tagliaferri, Roberto (1995) "Finite Element Method as Numerical Laboratory for Analyzing Pipeline Response under Internal Pressure, Axial Load, and Bending Moment, Proceedings of the 14th Offshore Mechanics and Arctic Engineering, Copenhagen, Denmark

Brushi, R. Torselletti, E., and Lund, K.M., (1995) "SUPERB Phase 2M Project: Submarine Pipeline Installation Design Criteria", SINTEF, Trondheim, Norway

Bryndum, M.B., et al (1982) "Dynamic Lay Stresses for Pipelines ", OTC Paper 4267, Proceedings of the Offshore Technology Conference, Houston, Texas

Cannon, A.G., and Lewis, R.C.E., (1987) "Performance of Pipework in the British Sector of the North Sea, Safety and Reliability Directorate, United Kingdon Atomic Energy Authority, National Center of System Reliability, Report No. NCSR/GR/71

Chater, E., and Hutchinson, J. W., (1984) "On the Propagation of Bulges and Buckles", ASME Journal of Applied Mechanics, Vol. 106, pp269-277

Chouchaoui, B. A., et al (1992) "Burst Pressure Prediction of Line Pipe Containing Single Corrosion Pits using the Finite Element Methods", Proceedings of the 13th International Offshore Mechanics and Arctic Engineering

Corona, E., and Kyriakides, S., (1988) "On the Collapse of Inelastic Tubes under Combined Bending and Pressure", International Journal of Solids and Structures, Vol. 24, pp. 270-280

Crentsil, K., Hauptmann, E.G., and Hill, P. G., (1990) "Axial Rupture in Underwater Pipelines", Journal of Offshore Mechanics and Arctic Engineering, Vol. 112, pp151-156

Det Norske Veritas (1996) "Rules for Submarine Pipeline Systems", Hovik, Norway

Det Norske Veritas (1999) "Corroded Pipelines, Recommended Practice RP-F101", Hovik, Norway

Dyau J. Y. and Kyriakides S., (1991) "On the Response of Elastic Plastic Tubes under Combined Bending and Tension", Proceedings of Offshore Mechanics and Arctic Engineering Conference, Stavanger

E&P Forum (1984) "A Review of Submarine Pipeline Performance in the North Sea 1975-1982, Report No. 192, London, UK

Eder, M.F., Grove, R.B., Petwrs, S.W., and Miller, C.D., (1984) "Collapse Tests of Fabricated Cylinders under Combined Axial Compression and External Pressure", Report to American Petroleum Institute, CBI Industries, Inc., Dallas, TX

Edwards S. H., and Miller C. P. (1939) "Discussion on the Effect of Combined Longitudinal Loading and External Pressure on the Strength of Oil-Well Casing", Drilling and Production Practice, API, pp. 483-502

Ellians C. P., Supple W. J., and Walker A. C., (1984) "Buckling of Offshore Structures", Granada Publishing Ltd

Estefen S. F., Souza, A. P. F., and Alves, T. M., (1995) "Comparison between Limit State Equations for Deepwater Pipelines under External Pressure and Longitudinal Bending", Proceedings of the 16th Offshore Mechanics and Arctic Engineering, Copenhagen, Denmark

Fabian, O., (1981) "Elastic-Plastic Collapse of Long Tube under Combined Bending and Pressure Loads", Ocean Engineering, V.8, pp. 295-330

Felton L. P. and Dobbs M. W., (1967) "Optimum Design of Tubes for Bending and Torsion", Journal of Structural Division, ASCE 93, pp. 184-200

Fowler, J. R., (1990) "Pipe Collapse - Large Scale Tests", Stress Engineering Services, Inc. Report (PR-201-818), American Gas Association

Fujino, Y., Lind, N.c, (1977) "Proof-Load Factors and Reliability", Journal of Structural Division, Proceedings of the American Society of Civil Engineers, Vol. 103, No. ST4, New York

Gerard, G., Becker, H., (1957) "Handbook of Structural Stability, Part III Buckling of Curved Plates and Shells", New York Univeristy, National Advisory Committee for Aeronautics, Washington, DC

Glinedinst W.O. (1963) "Development of API Collapse Pressure Formulas", American Petroleum Institute, Dallas

Grace, R. A., and Zee, G.T.Y., (1981) "Wave Force on Rigid Pipes using Ocean Test Data", Journal of the Waterway, Port, Coast and Ocean Division, American Society of Civil Engineers, Vol. 107, No. WW2, pp. 71-92, NY

Greene T. W., (1924) "Strength of Steel Tubing under Combined Column and Transverse Loading Including Tests of Columns and Beams", Technologic Papers of the Bureau of Standards, Dept. of Commerce/USA, 258, pp243-276

Gresnight, A. M., et al (1996) "Effect of Local Buckling on Burst Pressure", Proceedings of the 6th International Offshore and Polar Engineering, Los Angeles, USA

Gresnight, A. M., et al (1998) "Plastic Deformation and Local Buckling of Pipelines Loaded by Bending and Torsion", Proceedings of the 8th International Offshore and Polar Engineering, Montreal, Canada

Grigoriu, M., and Hall, W.B., (1984) "Probabilistic Models for Proof Load Testing", Journal of the Structural Division, Proceedings of the American Society of Civil Engineers, Vol, 108, No. ST7, New York

Grigoriu, M., and Lind, N.C., (1982) "Probabilistic Models for Prototype Testing", Journal of Structural Engineering, Vol. 114, No. 3, American Society of Civil Engineers, New York

Hobbs, R. E. (1988) "In-Service Buckling of Heated Pipelines", Journal of Transportation Engineering, Vol. 110, pp. 175-189

Igland, R. T. (1997) Reliability Analysis of Pipelines During Laying Considering Ultimate Strength Under Combined Loads, Thesis, Department of Marine Structures, The Norwegian University of Science and Technology, Trondheim, Norway.

Instituto Mexicano del Petroleo (IMP) (1997), "Background on Pipelines in the Bay of Campeche, Information Compiled and Developed by the Pipeline Group for Pipeline Transitory Criteria", Deparatamento de Ingenieria Civil Acero, Mexico Cicty, Mexico

International Standard Organization (1996) "Pipeline Transportation System for the Petroleum and Natural Gas Industries", ISO DIS 13623

Jacobsen, V., Bryndum, M.B., and Bonde, C., (1989) "Fluid Loads on Pipelines: Sheltered or Sliding", Proceedings of Offshore Technology Conference, OTC 6056, Society of Petroleum Engineers, Richardson, TX

Jiao Guoyang, et al (1996) "The SUPERB Project: Wall Thickness Design Guidelines for Pressure Containment of Offshore Pipelines", Proceedings of 15th International Conference on Offshore Mechanics and Arctic Engineering, Florence, Italy

Jirsa J. O., Lee F. H., Wilhoit Jr. J. C., and Merwin J. E., (1972) "Ovaling of Pipelines under Pure Bending", OTC 1569, Offshore Technology Conference, Houston, TX

Johns T. G., and McConnell (1983) "Design of Pipelines to Resist Buckling at Depths of 1000 to 9000 Feet", 11th Pipeline Technology Conference, Houston, TX

Johnes, D.G., (1981) " The Significance of Mechanical Damage in Pipelines", British Gas Corporation, Research & Technology, Engineering Research Station, Newcastle Upon Tyne, UK

Khaliq, A.A., and Schilling, C.G., (1964) "Plastic Buckling Strength of Seamless Steel Tubes under Bending Loads", Report No. 57.019-800 (2) Applied Research Lab., U. S. Steel Corporation< Monroeville, PA

Kiefner, J. F., et al (1974) "Corroded Pipe: Strength and Repair Methods", 5th Symposium on Line Pipe Research, Pipeline Research Committee of American Gas Association

Kiefner, J. F., et al (1989) "A Modified Criterion for Evaluating the Remaining Strength of Corroded Pipe, RSTRENG" Project PR 3-805 Pipeline Research Committee, American Gas Association

Kim, H. O., (1992) "Plastic Buckling of Pipes under Bending and Internal Pressure", Proceedings of the Second International Offshore and Polar Engineering, San Francisco, USA

Kim J. Mork et al (1997) "The SUPERB Project & DNV 96: Buckling and Collapse Limit State", The 18th International Offshore Mechanics and Arctic Engineering Conference

Klever, F. J., (1992) "Burst Strength of Corroded Pipe: Flow Stress Revisited", OTC Paper 7029, Proceedings of Offshore Technology Conference.

Korol R. M., and Hudoba J., (1972) "Plastic Behavior of Hollow Structural Sections", Journal of Structural Division, ASCE, 98

Korol R. M., (1979) "Critical Buckling Strains of Round Tubes in Flexure", International Journal of Mechanical Science, 21, pp. 719-730

Kvernvold, O., Johnson, R., and Helgerson, T., (1992) "Assessment of Internal Pipeline Corrosion", Proceedings of International Conference on Offshore Mechanics and Arctic Engineering, Vol. 4, American Society of Mechanical Engineers, New York, NY

Kyogoku, T., Tokimasa, K., Nakanishi, H., and Okazawa, T., (1981) "Experimental Study on the Effect of Axial Tension Load on Collapse Strength of Oil Well Casing", Proceedings of the 13th Offshore Technology Conference, OTC Paper 4108, Houston, TX

Kyriakides, S., Corona, E., Mafhaven, R., and Babcock, C. D., (1983) "Pipe Collapse under Combined Pressure, Bending and Tension Loads", Proceedings of the Offshore Technology Conference, OTC Paper 6104, pp. 541-550

Kyriakides S. and Yeh M. K. (1985) "Factors Affecting Pipe Collapse", EMRL Report No. 85/1 (PR-106-404) Prepared for The American Gas Association

Kyriakides S., Corona E., Babcock C. D., and Madhavan R., (1987) "Factors Affecting Pipe Collapse- Phase II" EMRL Report No. 87/8 (PR-106-521), Prepared for the American Gas Association

Kyriakides, S., (1991) "Buckling Propagation", Advanced in Applied Mechanics

Lambrakos, K.F., Chao, J.C., Beckman, H., and Brannon, H.R., (1987) "Wake Model of Hydrodynamic Force on Pipelines", Ocean Engineering, Vol. 14, No. 2, pp. 117-136, Elsevier Publishers, NY

Lambrakos, K.F., Remselth, S., Sotberg, T., and Verley, R.L.P., (1987) "Generalized Response of Marine Pipelines", Proceedings of the Offshore Technology Conference, OTC 5507, Society of Petroleum Engineers, Richardson, TX

Lammaet, W., Hale, J.R., and Jacobsen, V., (1989) "Dynamic Response of Submarine Pipelines Exposed to Combined Wave and Current Action", Proceedings of the Offshore Technology Conference, OTC 6058, Society of Petroleum Engineers, Richardson, TX

Lara, L., Garcia, H., and Zavoni, H., (1998) "Categorization of Pipelines in the Bay of Campeche for Risk Based Design and Assessment", Subdireccion de ngenieria, Gerencia de Ingenieria de Detalle, Instituto Mexicano de Petroleos, Mexico, DF

Langner, C.G., (1974) "Buckling and Hydrostatic Collapse Failure Characteristics of High-D/T Line Pipe", Technical Progress Report No. 4-74, Project No. 84807, Battelle Memorial Institute

Li, Robin et al (1995) "DeepSea Pipeline Collapse under Combined Loads of External Pressure, Bending, and Tension", Proceedings of 5th International Offshore and Polar Engineering Conference

Loh, J. T., (1993) "Ultimate Strength of Dented Tubular Steel Members", Proceedings of 3rd International Offshore and Polar Engineering Conference

Lund, S., et al (1993) "Laying Criteria Versus Strain Concentration at Field Joints for Heavily Coated Pipelines", Proceeding of the 12th International Conference on Offshore Mechanics and Arctic Engineering, ASME, Glasgow, Scotland

Ma, K-T, Orisamolu, I.R., Bea, R.G., and Huang, R.T., (1997) "Towards Optimal Inspection Strategies for Fatigue and Corrosion Damage", Transactions, Society of Naval Architects and Marine Engineers, Jersey City, NJ

Madsen, H.O., Krent, S and Lind, N.C., (1986) "Methods of Structural Safety", Prentice Hall, Inc, Englewood Cliffs, New York

Mandke, J.S., Wu, Y.T., and Marlow, R.S., (1995) "Evaluation of Hurricane-Induced Damage to Offshore Pipelines", Final Report to Minerals Management Services, Southwest Research Institute, San Antonio, TX

Mao, Y., (1986) "The Interaction Between a Pipeline and an Erodible Bed", Doctoral Dissertation, Institute of Hydrodynamics and Hydraulic Engineering, Technical University of Denmark, Series Paper No. 39, Lyngby, Denmark

Marine Board (1994) "Improving the Safety of Marine Pipelines", National Research Council, National Academy of Engineering, National Academy Press, Washington, DC

Marlow, R.S., (1988) "Effects of External Hydrostatic Pressure on Tubular Beam Columns", Final Report to American Petroleum Institute, Southwest Research Institute, Dallas, TX

Mehdizadeh, P. (1976) "Casing Collapse Performance", Trans ASME Series B, 98, pp. 1112-1119

Mesloh, et al (1976) "The Propagation Buckle", Proceedings of the International Conference of Offshore Structures, Vol. 1

Mitwally, H.M., (1987) "Dynamic Analysis of Marine Structures", Doctoral Dissertation, Faculty of Graduate Studies, Engineering Science, The University of Western Ontario, London

Mohareb, M. E. et al (1994) "Deformational Behavior of Line Pipe", Structural Engineering Report No. 22, University of Alberta

Mork, K.J., et al (1997) "The SUPERB Project & DNV 96: Buckling and Collapse Limit State", The 18th International Offshore Mechanics and Arctic Engineering Conference

Murphey C. E., and Langner C. G., (1985) "Ultimate Pipe Strength under Bending, Collapse, and Fatigue", Proceedings of Offshore Mechanics and Arctic Engineering Conference, New Orleans

National Association of Corrosion Engineers (NACE) (1992) "Control of External Corrosion on Undergroud or Submerged Metallic Piping Systems", NACE RP 0169-92, New York, NY.

Neill, I. A. R. and Hinwood, J. B. (1998). "Wave and Wave-Current Loading on a Bottom-Mounted Circular Cylinder," International Journal of Offshore and Polar Engineering, The International Society of Offshore and Polar Engineers, Vol. 8, No. 2, Golden, CO.

Ness, O., and Verley, R., (1995) "Strain Concentrations in Pipelines with Concrete Coating: An Analytical Model", Proceedings of the 14th International Conference on Offshore Mechanics and Arctic Engineering, Copenhagen, Denmark

Ness, O., and Verley, R., (1996 "Strain Concentrations in Pipelines with Concrete Coating", International Journal of the Offshore Mechanics and Arctic Engineering, ASME, New York, USA

Nishioka K., Nara Y., Kyogoku T., Hirakawa K and Tokimasa K. (1976) "An Experimental Study on Critical Collapse Pressure of a Seamless Steel Tube for Well Casing under External Pressure", The Sumitomo Search, No. 15

Oceanweather (1996) "Update of Meteorological and Oceanographic Hindcast Data, Normals and Extremes, Bay of Campeche", Report to Brown & Root Energy Services, Houston, TX.

Orisamolu, I. R. and Bea, R. G. (1993). *Reliability of Offshore Structural Systems: Theory, Computation, and Guidelines for Applications*, Report to Engineering Branch of Canadian National Energy Board, Calgary, Alberta, Canada.

Orisamolu, I. R. and Bea, R. G. (1999). "Reliability Considerations in the Development of Guidelines for Requalification of Pipelines," Proceedings Offshore Mechanics and Arctic Engineering Workshop on Requalification of Marine Pipelines, St. Johns, Newfoundland, August.54

Ostapenko, A. and Grimm, D.F., (1979) "Local Buckling of Cylindrical Tubular Columns Made of A-36 Steel, Report to American Petroleum Institute, Dallas, TX

Palmer, A.C., and Martin, (1979) "Buckle Propagation in Submarine Pipelines", Nature V 254, No. 5495, pp. 46-48

Pipeline Research Committee (1993) "Submarine Pipeline On-Bottom Stability", Brown & Root, Report to American Gas Association (AGA), Houston, TX

Rammant, L.R., et al (1980)" Offshore Pipeline Installation Sensitivity Analysis for a Conventional Lay-Barge", Applied Ocean Research, Vol. 2

Ramberg W. and Osgood W.R. (1943) "Description of Stress-Strain Curve by the Three Parameters", NACA TN 902

Ricles, J. M., et al (1992) "Residual Strength of Damaged Offshore Tubular Bracing", Proceedings of Offshore Technology Conference, OTC 6938, Houston, TX

Schilling G. S. (1965) "Buckling Strength of Circular Tubes", Journal of Structural Division, ASCE 91, pp. 325-348

Serpas, R., (1998) "Transitory Criteria Applied for Assessment of Marine Pipelines, Application Examples, Assessment of Marine Pipelines 093 and 127", Taller de Applicacion de la la Edicion del Criterio Transitorio Para el Diseno y la Ealuacion de Lineas Submarinas en la Sonda de Campeche, Instituto Mexico del Petroleo, Mexico, DF

Sewart, G. et al (1994) "An Analytical Model to Predict the Burst Capacity of Pipelines", Proceedings of the 15th International Offshore Mechanics and Arctic Engineering

Shell International Exploration and Production B.V., (1996) "Specifications and Requirements for Intelligent Pig Inspection of Pipelines", Version 1, The Hague, The Netherlands

Sherman D. R., (1986) "Inelastic Flexural Buckling of Cylinders" In Steel Structures: Recent Research Advances and Their Applications to Design (Ed, M. N. Pavlovic), Elsevier Applied Science Publishers, pp. 339-357

Sherman D. R., (1984) "Supplemental Tests for Bending Capacity of Fabricated Pipes", Report, Dept. of Civil Engineering, University of Wisconsin-Milwaukee

Sherman, D.R., (1975) "Ultimate Capacity of Tubular Members", Report to Shell Oil Company, University of Wisconsin-Milwaukee

Sherman, D.R., (1983) "Bending Capacity of Fabricated Pipes", Dept. of Civil Engineering, Univeristy of Wisconsin-Milwaukee

Stephens M. J., Kulak G. L. and Montgomery C. J., (1982) "Local Buckling of Thin-Walled Tubular Steel Memebrs", Structural Engineering Report, 103, Dept. of Civil Engineering, Univeristy of Alberta

Simiu, E., and Scanlan, R.H., (1978) "Wind Effects on Structures: An Introduction to Wind Engineering", John Wiley & Sons, Brisbane, Australia

Simpson, S., (1983) "Accidents and Leakages: A Statistical Review", Pipelines and Offshore Environment, Barbican Center, London

SINTEF, (1989) "Reliability Data for Subsea Pipelines", Report No. STF75 A89037, Trondheim, Norway

Smith, C. S., Kirkwood, W., and Swan, J. W., (1979) "Buckling Strength and Post-Collapse Behavior of Tubular Bracing Members Including Damage Effects", The Second International Conference on Behavior of Offshore Structures, London, England

Sotberg, T., (1990) "Application of Reliability Methods for Safety Assessment of Submarine Pipelines", Doctotal Dissertation, Technical University of Norway, Trondheim, Norway

Sotberg, T., and Leira, B.J., (1994) "Reliability-based Pipeline Design and Code Calibration", Proceedings of 13th International Conference on Offshore Mechanics and Arctic Engineering, American Society of Mechanical Engineers, New York, NY

Sotberg, T., et al (1996) "A New Safety Philosophy for Submarine Pipeline Design", Proceedings of the 15th International Conference on Offshore Mechanics and Arctic Engineering, American Society of Mechanical Engineers, NY

Sotberg, T., Moan, T., Bruschi, R., Jiao, G., and Mork, K.J., (1997) "The SUPERB Project: Recommended Target Safety Levels for Limit State Based Design of Offshore Pipelines", Proceedings of the 16th International Conference on Offshore Mechanics and Arctic Engineering

Staneff, S.T., Ibbs, C.W., and Bea, R.G., (1996) "Risk-Management System for Infrastructure Condition Assessment", Journal of Infrastructure Systems, Vol. 1, No. 4, American Society of Civil Engineers, Herndon, VA

Sterinman, S.L., and Vojta, J.F., (1989) "Hydrostatic Beam Column Test (Phase II), Chicago Bridge & Iron, Prepared for the American Petroleum Institute, Washington, DC

Stephens, M.J., Kulak, G.L., and Montgomery, C.J., (1982) "Local Buckling of Thin-Walled Tubular Steel Members", Structural Engineering Report, 103, Dept. of Civil Engineering, University of Alberta

Stewart, G., Klever, F. J., and Ritchie, D., (1993) "An Analytical Model to Predict the Burst Capacity of Pipelines," Proceedings 13th International Conference on Offshore Mechanics and Arctic Engineering, American Society of Mechanical Engineers, New York, NY

Stewart, G., and Klever, F. J., (1996) "Accounting for Flaws in the Burst Strength of OCTG," Proceedings SPE Applied Technology Workshop on Risk Based Design of Well Casing and Tubing, Society of Petroleum Engineers, Richardson, TX

Taby, J., Moan, T., and Rashed S.M.H., (1991) "Theoretical and Experimental Study of the Behavior of Damaged Tubular Members in Offshore Structures", Norwegian Maritime Research, No. 211981

Tamano, T., Mimura, H., and Yanagimoto, S., (1982) "Examination of Commercial Casing Collapse Strength under Axial Loading", Proceedings of the 1st Offshore Mechanics and Arctic Engineering, ASME pp 113-118

Thomsen, A.K., and Leonhardsen, R.L., (1998) "Experience from Operation, Inspection, and Condition Monitoring of Offshore Pipeline Systems on the Norwegian Continental Shelf", Proceedings of the 8th International Offshore and Polar Engineering Conference, Montreal, Canada, Society of Offshore and Polar Engineers, Golden, CO

Timoshenko, S. P., and Gere, J. M., (1961) "Theory of Elastic Stability", McGraw-Hill International

Torselletti, E., and Maincon, P., (1994) "SUPERB Project Task B – Probabilistic Assessment and Calibration of Pipeline Installation, SINTEF Report, STF70 F94045, Trondheim, Norway

Tvergaard, V., (1976) "Buckling of Elastic-Plastic Oval Cylindrical Shells under Axial Compression", International Journal of Solids and Structures

Tvergaard V. (1979) "Plastic Buckling of Axially Compressed Circular Cylindrical Shells" Thin Walled Structures, 1, pp. 139-163

Valdez, V.M., Bayazitoglu, Y.O., Weiss, R.T., Valle, O.L., and Hernandez, T., (1997) "Inspection and Evaluation of Offshore Pipelines in the Bay of Campeche", Proceedings of the Offshore Technology Conference, OTC 8499, Society of Petroleum Engineers, Richardson, TX

Verley, R., and Ness, O.B., (1995) "Strain Concentrations in Pipelines with Concrete Coating Full Scale Bending Tests and Analytical Calculations", Proceedings of the 14th International Conference on Offshore Mechanics and Arctic Engineering, ASME, Copenhagen, Denmark

Walker, G.E., and Ayers, R.R., (1971) "Bending of Line Pipe Under External Pressure", Technical Information Record No. 3-71, Battelle Memorial Institute

Wilhoit Jr J. C., and Merwin J. E., (1973) "Critical Plastic Buckling Parameters for Tubing in Bending under Axial Tension", OTC Paper 1874, Offshore Technology Conference, Houston

Winter P. E., (1985) "Strength and Deformation Properties of Pipelines in Deepwater", Final Report of the Third Stage of MaTS Project, TNO-IBBC Report B-85-459/63.6.0585

Wolford D. S., and Rebholz M. J., (1958) "Beam and Column Tests of Welded Steel Tubing with Design Recommendations", American Society of Testing Material Bulletin 233, pp45-51

Wolfram, W.R., Getz, J.R., and Verly, R.L.P., (1987) " PIPESTAB Project: Improved Design Basis for Submarine Pipeline Stability", Proceedings of Offshore Technology Conference, OTC 5501, Society of Petroleum Engineers, Richardson, TX

Woodson, R.D., and Bea, R.G., (1990) "Offshore Pipeline Failures", Report to the National Research Council, National Academy of Engineering, Marine Board, Washington, DC., Marine Technology and Management Group, Dept. of Civil and Environmental Engineering, University of California at Berkeley

Yeh, M. K., and Kyriakides, S., (1986) "On the Collapse of Inelastic Thickn-Walled Tubes under External Pressure", ASME Journal of Energy Resource Technology, Vol. 108, pp 35-47

Yeh, M. K., and Kyriakides, S., (1988) " Collapse of Deepwater Pipelines", ASME Journal of Energy Resource Technology, Vol. 110, pp 1-11

Zhou, Z., and Murray, D.W., (1993) "Numerical Structural Analysis of Buried Pipelines", Structural Engineering Report No. 181, Dept. of Civil Engineering, University of Alberta